ELECTROSPUN SULFONATED SILICA-BASED PROTON EXCHANGE MEMBRANES FOR PEM FUEL CELLS

by

NAEIMEH RAJABALIZADEH MOJARRAD

Submitted to the Graduate School of Engineering and Natural Sciences

in partial fulfillment of

the requirements for the degree of Doctor of Philosophy

Sabanci University
JULY 2022

ELECTROSPUN SULFONATED SILICA-BASED PROTON EXCHANGE MEMBRANES FOR PEM FUEL CELLS

Naeimeh Rajabalizadeh Mojarrad

Ph.D. Dissertation, July 2022

Supervisor: Prof. Dr. Selmiye Alkan Gürsel

Co-advisor: Dr. Begüm Yarar Kaplan

ABSTRACT

Keywords: PEMFC, Fuel cells, Electrospinning, Sulfonated silica, Sol-gel, poly (vinylidene fluoride-co trifluoroethylene)

Proton exchange membrane fuel cells (PEMFCs) are considered as the most promising alternative systems for fossil fuel-based devices due to their outstanding characteristics such as high efficiency and applicability in a wide range of sectors. Nevertheless, the materials characteristics and system designs with promising performance, durability, and cost-effectiveness still need to be improved for their commercialization. In this regard, a growing amount of research has been conducted to enhance the properties of their various parts, particularly the membrane as the heart of a PEMFC which serves numerous vital functions. Nafion® membranes are commonly used as the membrane material in PEMFCs due to their several advantages but they suffer mainly from insufficient proton conductivity at low relative humidity (RH) and elevated temperatures as well as high-cost production cost. To overcome the disadvantages of Nafion® membranes, in the present thesis two different strategies were used to synthesis and fabrication of proton conductive membranes with a promising performance at low humidity operation conditions. In the first approach, for substitution of Nafion® membranes sulfonated silica/ poly (vinylidene fluoride-co trifluoroethylene)-based (P(VDF-TrFE)) and sulfonated silica/ poly (vinylidene fluoride)-based (PVDF) hybrid membranes were prepared via single electrospinning method where sulfonated silica (S-SiO_2) nanoparticles were used as proton conductive additives and PVDF or P(VDF-TrFE) as the carrier polymers. Hybrid S-SiO_2/P(VDF-TrFE) membranes showed a superior proton conductivity (102 mS/cm) at 80°C and 100% RH than the S-SiO_2/ PVDF membranes (43 mS/cm) at the same conditions. These

superior results are due to the P(VDF-TrFE) polymer in the hybrid membrane structure that creates larger micro-channels for proton conduction. In the second approach, modification of Nafion® membranes were investigated by incorporation of sulfonated silica (S-SiO_2) network into the Nafion®/PVDF or Nafion®/P(VDF-TrFE) fibrous mats. For this purpose, a single-step dual-electrospinning and sol-gel method were combined for the preparation of composite membranes as a fast and scalable technique. In this part of the thesis, the P(VDF-TrFE)-based membranes showed higher proton conductivity than PVDF-based ones (132 vs. 79 mS/cm at 80°C and 100% RH). Moreover, composite membranes exhibit superior cell performance especially at lower applied humidity conditions. The maximum power density is at 344 mW/cm^2 60% RH, and this value is higher than the PVDF-based membranes which are 190 mW/cm^2 at the same conditions. These observations suggest that P(VDF-TrFE)-based membranes can be considered as promising alternative membranes for PEMFC applications operating at low humidity conditions.

PEM YAKIT PİLLERİ İÇİN SÜLFONLANMIŞ SİLİK-ESASLI ELEKTRODOKUNMUŞ PROTON DEĞİŞİM MEMBRANLARI

Naeimeh Rajabalizadeh Mojarrad

Doktora Tezi, Temmuz 2022

Tez Danışmanı: Prof. Dr. Selmiye Alkan Gürsel

Tez Yardımcı Danışmanı: Dr. Begüm Yarar Kaplan

Özet

Anahtar kelimeler: PEMFC, Yakıt pilleri, Elektro-eğirme, Sülfonlanmış silika, Sol-jel, Poli (viniliden florür-trifloroetilen)

Proton değişim membranlı yakıt pilleri (PEMFC), bir çok alanda kullanıma uygunluğu ve yüksek verim sağlayabilme gibi öne çıkan özelliklerinden dolayı fosil yakıtlardan enerji üreten cihazlara en önemli alternatif olarak görülmektedir. Ancak yakıt pillerinin ticarileşebilmesi için yüksek performans, uzun ömürlülük, ve daha ucuza imalatı konularında geliştirmeler gerekmektedir. Bundan dolayı, PEMFC'ler performansını arttırmak için, özellikle membran alanında, gün geçtikçe artan sayıda araştırma yapılmaktır. Günümüzde PEMFC'ler için Nafion® membranları tercih edilmektedir. Ancak bu membranların yüksek sıcaklıkta ve düşük bağıl nem oranlarındaki (%RH) düşük proton iletkenliği ve yüksek üretim maliyeti öne çıkan en önemli dezavantajlarıdır. Bu dezavantajları ortadan kaldırmak için bu tez çalışmasında iki farklı yöntem ile düşük bağıl nem koşullarında yüksek performans gösterebilecek membranlar üretilmiştir. Yöntemlerin ilki, Nafion® yerine sülfonlanmış silika ve poli(viniliden florür-trifloroetilen) (P(VDF–TrFE)) bazlı veya sülfonlanmış silika ve PVDF bazlı hibrit membranları tekli elektro-eğirme ile hazırlanmasıdır. Bu yöntemde, sülfonlanmış silika (S-SiO_2) nanoparçacıkları proton iletimini arttıracak katkı malzemesi olarak, P(VDF-TrFE) veya P(VDF) ise taşıyıcı polimerler olarak kullanılmıştır. %100 RH ve 80°C'de yapılan ölçümlerde hibrit S-SiO_2/P(VDF-TrFE) membranlar (102 mS/cm), S-SiO_2/PVDF membranlara (43 mS/cm) kıyasla iki kattan fazla proton iletkenliği göstermiştir. Bu üstünlük, hibrit P(VDF-TrFE) yapısının proton iletimini kolaylaştıran daha geniş mikrokanallar oluşturabilmesinden kaynaklanmaktadır. İkinci yöntemde ise, S-SiO_2 ağı ile desteklenmiş fiber Nafion®/PVDF ve Nafion®/P(VDF-TrFE) esaslı hibrit membranlar

incelenmiştir. Bu amaçla, hızlı ve ölçeklenebilir bir kompozit membran üretimi için tek basamakta dual-fiber yapılı mat üretimi ve sol-jel yöntemleri birleştirilerek kullanılmıştır. Tezin bu kısmında, P(VDF-TrFE) bazlı membranlar sadece P(VDF) bazlı olanlara kıyasla daha yüksek proton iletkenliği göstermiştir (%100 RH ve 80°C'de 132 mS/cm ve 79 mS/cm). Ek olarak, kompozit membranların yakıt pili performans testleri, özellikle düşük bağıl nem oranlarında daha iyi sonuçlar göstermiştir. Kompozit membranlardan elde edilen maksimum gün yoğunluğu 344 mW/cm^2 (%60 RH) olup aynı koşullardaki P(VDF) bazlı membranlardan (%60 RH'de 190 mW/cm^2) daha iyi sonuçlar göstermiştir. Elde edilen bu sonuçlar, hibrit P(VDF–TrFE) bazlı membranların PEMFC uygulamaları için umut veren bir alternatif olarak düşünülebileceğini işaret etmektedir.

To my Lovely Family

AKNOWLEDGMENTS

I would like to express my appreciation to my kind supervisor, Prof. Dr. Selmiye Alkan Gürsel, for her academic and emotional support and encouragement during my Ph.D. I extend my especial gratefulness and thanks to my supportive co-advisor, Dr. Begüm Yarar Kaplan. I would like to give very special thanks to Dr. Alp Yürüm for his guidance and academic support. I would like to give my great thanks to my committee members: Prof. Dr. Gözde İnce, Assoc. Prof. Önder Metin, Asst. Prof. Enver Güler, and Asst. Prof. Alp Yürüm.

I must thank the faculty members of department of Materials Science and Nanoengineering for their valuable and educative lectures throughout my Ph.D. which helps me shape my profession in materials science.

In addition, my sincere thanks to Dr. Navid Haghmoradi, Dr. Adnan Tasdemir, Dr. Buse Bulut Köpüklü, Dr. Aysu Yurduşen Öztürk and Dr. Mohammed Zabara.

I would like to thank my supportive groupmates Bilal Sayyed Said Iskandarani, Ahmet Can Kırlıoğlu, Vahid Charkhesht, Esaam Jamil, Mohammad Alinezhadfar, Emre Burak Boz.

I will never forget the joyful memories from my friends: Faraz Tehranizadeh, Nasim Barzegar, Pegah Zahedimaram, Navid Haghmoradi, Deniz Mortazavi, Sina Rastani, Amin Ahmadi, Ali Asgharpour, Meysam Rafiei, Mahsa Nourani, Mehri Ahmadian, Ali Azizi, Ali Barzegar, Amin Ahmadi, Sirous Khabbaz Araz Sheibani, Ehsan Khoshniat, Negar Farhadi, Zoher Aliabadi, Mohammad Dabbagh, Kaveh Rahimzadeh, Amin Bagherzadeh. I am grateful to them for all joyful memories they made for me.

Finally, I would like to thank my lovely family and all their support they gave me. My parents and kind brothers. Getting old knowing there are lovely people out there who are always hope your success gives you an endless motivation.

I would like to show my appreciation for all the support received from Sabanci University Nanotechnology Research and Application Center (SUNUM) and Faculty of Engineering and Natural Science in Sabanci University.

Table of Contents

Table of Figures

List of Tables

1. INTRODUCTION

1.1 History of the Fuel Cells

Research and growth of the functional fuel cells dates back to the early 1800s. Based on some resources the German scientist, Christian Friedrich Schoenbein discovered the principle of fuel cell for the first time in 1838 [1]–[3]. However, the hydrogen fuel cell is generally credited to Sir William Robert Grove, who discovered that the process of decomposing water to its elements was practically reversible. Grove realized that hydrogen and oxygen gasses could undergo a chemical reaction in presence of two platinum electrodes as catalysts, which were immersed in dilute sulfuric acid, to form water. As the subsequent step, he recognized that linking pairs of electrodes in series produced a greater voltage drop, thereby creating the first fuel cell, which he called gas battery [2]. A schematic of the primary experimental apparatus of Sir William Robert Grove was depicted in Figure 1, which consisted of two Pt electrodes and two sealed gas containers. He immersed one end of each Pt electrode in a sulfuric acid bath, and the other end into the oxygen and hydrogen containers. As the first step he passed an electric current through two Pt electrodes which led to decomposition of water to oxygen and hydrogen gas and accumulated these gasses into the two separate tubes. Then he used the right hand one in which he replaced the power source with an ampere meter. He noticed a small electric current flow and an increasing water level over time in gas tubes. The recombination of oxygen and hydrogen gasses as the reverse electrochemical reaction of the water electrolysis accounted for these observations [1].

However, the first hydrogen/ oxygen fuel cell with practical use was developed more than a century later by Thomas Bacon in 1932 for the American manned space program. By 1955, Thomas Grubb, a chemist at General Electric (GE), made the first Proton Exchange Membrane Fuel cell (PEMFC) by further modifications to the fuel cell design via introducing polystyrene sulphated as an ion exchange membrane, and continued by Leonard Niedrach via depositing of platinum on the membrane which acts as catalyst for HOR and ORR reactions [3].

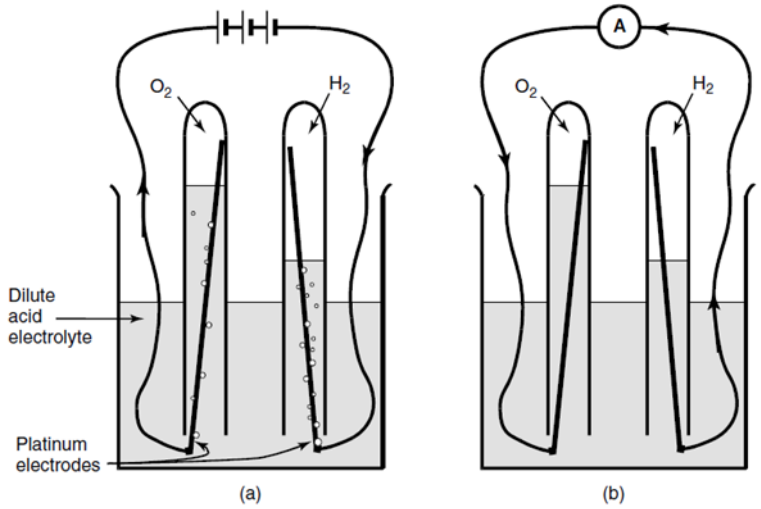

Figure 1. Schematic representation of Sir William Robert Grove for a) water electrolysis and b) recombination of H_2 and O_2 gases [1]

Consequently, in 1962 GE fabricated the 1 k-W Gemini space mission based on their works as the first applicable fuel cell with Pt loading of 35 mg/cm^2 and 37 mA/cm^2 performance at 0.78 V. Each stack was composed of 31 cells in series, and porous nickel, lithiated NiO and potassium hydroxide solution were used as anode electrode, cathode electrode and electrolyte respectively [4]. A combination of the above-mentioned success and a strategy of commercializing space technology resulted in significant research programs in America and Japan between the 1970s and 1980s, as well as later in European countries [1]. The milestones in the history of fuel cells are summarized in **Table 1**.

Table 1. The milestones in the history of fuel cells [5]

Year(s)	Milestone
1839	W.R. Grove and C.F. Schönbein separately demonstrate the principals of a hydrogen fuel cell
1889	L. Mond and C. Langer develop porous electrodes, identify carbon monoxide poisoning, and generate hydrogen from coal
1893	F.W. Ostwald describes the functions of different components and explains the fundamental electrochemistry of fuel cells
1896	W.W. Jacques builds the first fuel cell with a practical application
1933–1959	F.T. Bacon develops AFC technology
1937–1939	E. Baur and H. Preis develop SOFC technology
1950	Teflon is used with platinum/acid and carbon/alkaline fuel cells
1955–1958	T. Grubb and L. Niedrach develop PEMFC technology at General Electric
1958–1961	G.H.J. Broers and J.A.A. Ketelaar develop MCFC technology
1960	NASA uses AFC technology based on Bacon's work in its Apollo space program
1961	G.V. Elmore and H.A. Tanner experiment with and develop PAFC technology
1962–1966	The PEMFC developed by General Electric is used in NASA's Gemini space program
1968	DuPont introduces Nafion®
1992	Jet Propulsion Laboratory develops DMFC technology
1990s	Worldwide extensive research on all fuel cell types with a focus on PEMFCs
2000s	Early commercialization of fuel cells

1.2 Principles of Fuel Cells

Fuel cells are electrochemical devices whereby the stored chemical energy of the reactants is converted into the electrical energy in a continuous manner as long as the reactants are fed into the system [5], [6]. Regardless of their type, they are all composed of three main parts: a gas or liquid permeable anode (negative terminal) and cathode (positive terminal) electrodes as well as a non-gas permeable, ion exchange electrolyte which is sandwiched between these two electrodes. The electrodes connect to each other via an external circuit. Hydrogen or hydrogen-containing gasses such as methanol and ethanol are continuously fed into these systems from the anode side. From the cathode, an oxidant such as pure oxygen, air, or a halogen is supplied. The oxidation and reduction reactions occur at the interfaces between these components, resulting in the consumption of fuel and the generation of water and/or carbon dioxide as the product based on the type of fuel cell [6]–[8]. The overall reaction and operation temperature of each type are listed in **Table 2**.

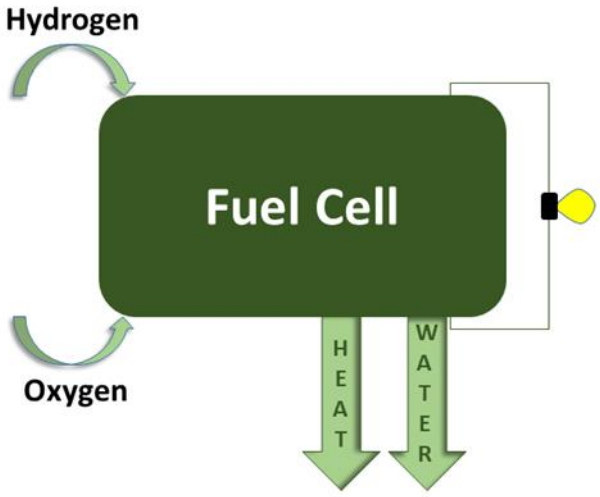

Figure 2. Fuel Cell converts chemical energy to electrical energy via a single step process.

The produced voltage as the result of this reactions can be related to the change of Gibbs free energy via the following equation:

$$\Delta G = \pm n\, F\, \Delta U_0 \qquad (1)$$

where n, F and ΔU_0 ($U_{0,\text{cathode}}$ - $U_{0,\text{anode}}$) stands for electrons involved in each reaction, Friday constant and the difference of equilibrium potential of cathode and anode electrode at zero current (equilibrium cell voltage), respectively. These equilibrium potentials can be described via the Nernst equation. Due to the electrical work performed by the cell, a deviation occurs from the open circuit voltage when current flows. Overpotential (η) refers to this deviation from equilibrium value [6].

1.2.1 Main Irreversible Losses in Fuel Cells

As we discussed in the previous section, the cell voltage is always lower than its equilibrium value due to the several losses mechanisms [6], [9]. The voltage drop in these systems is caused by four main irreversible loss mechanisms (polarizations) that can be distinguished easily by polarization curves as shown in **Figure 3** (I-V curves).

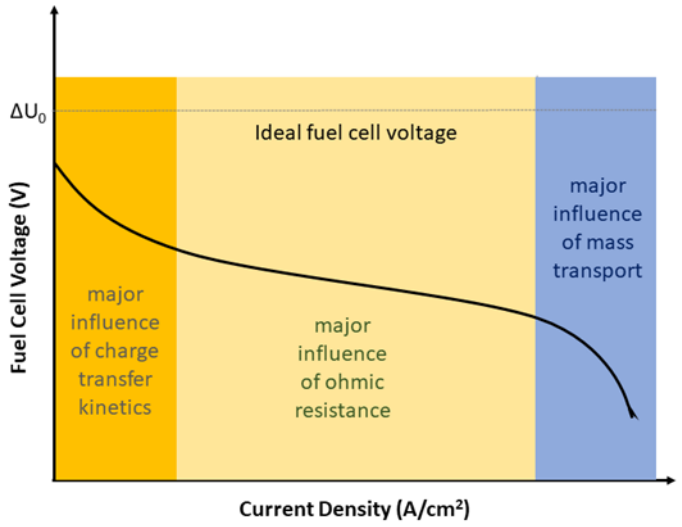

Figure 3. Voltage of fuel cell vs. current density

Activation overpotential (η_{ac}): This originates from the activation potential of the electrochemical reactions that take place on the surface of the anode and the cathode electrodes. Sluggish kinetic reactions, particularly at the cathode, is the main reason for this type of loss, which leads to the voltage drop in fuel cells [1], [5], [9].

Ohmic resistance (R_e): This type of loss is attributed to the electrolyte resistance for ion transfer and electrical resistance of electrodes as well as contact resistance between various components. The ohmic losses, or resistive losses, result in voltage drop which is directly proportional to the current density [3], [6].

Mass transportation or concentration overpotential (η_{con}): This sort of loss results from the limitation of reactant rates in reaching the interface surface between electrode and electrolyte by utilizing the fuel [6], [9].

Crossover of fuel and short circuit: This energy loss is caused by the improper use of fuel in contact with the electrolyte, and, to a smaller extent, conduction of electrons via the electrolyte [1], [3].

Considering the above-mentioned losses, the overall cell voltage can be calculated via following equation [6]:

$$\Delta U_{fc} = \Delta U_0 - (|\eta_{act}| - |\eta_{con}| - R_e) \qquad (2)$$

1.2.2 Efficiency of Fuel Cells

Different types of fuel cells have been developed with various principles and features since Sir William Grove invented the first fuel cell. Regardless of their type and operational temperature most fuel cells generate electrical energy with an efficiency of between 40% and 60%. Energy conversion efficiency in these devices is higher than that of internal combustion engines due to direct conversion of chemical energy to electrical energy [7], [8], [10]. A comparison between theoretical and real efficiency of these devices is shown in Table 2, which reveals that their actual efficiency is significantly lower than maximum theoretical efficiency values. This evidence is attributed to the partial conversion of the stored chemical

energy of the reactants to electrical energy and the rest of this energy is released as waste heat into the environment. It is possible to partially utilize this heat energy by a heat engine [10]. The efficiency of the fuel cell is calculated via the Gibbs free energy (ΔG) of the reactions and the change of enthalpy. For an ideal system, the reaction's free energy completely converts into electrical energy, and its efficiency can be calculated by the following equation [6]:

$$\varepsilon_r = \frac{We}{-\Delta H} = \frac{\Delta G}{\Delta H} = 1 - \frac{T\Delta S}{\Delta H} \qquad (3)$$

Where the ε, W_e, ΔH and ΔS stand for thermodynamic efficiency of system, electrical work, enthalpy change and the change of entropy of reaction. The efficiency of a real fuel cell is less than 1 due to the various loss mechanisms which are discussed in the previous section.

In addition to thermodynamic efficiency, electrochemical efficiency of the fuel cells can be calculated via the following equation [6]:

$$\varepsilon_v = \frac{\Delta Ufc}{\Delta U0} = 1 - (|\eta_{act}| - |\eta_{con}| - R_e) / \Delta U_0 \qquad (4)$$

This parameter is more informative in case of fuel cells. The efficiency of fuel cells must be considered in the context of practical operation as well in order to provide a complete picture. Moreover, the released heat as the waste in fuel cells can be partially used by a heat engine. Tehrefore, to benefit from a higher overall efficiency, high temperature fuel cells are becoming increasingly popular for Combined Heat and Power (CHP) systems [11].

Table 2. Characteristics and reactions of the various fuel cell types [10]

Fuel cell type	Fuel	Overall reaction	Operating temperature (°C)	Theoretical efficiency (%)	Actual system efficiency (%)	
				Electric	Electric	CHP
PEMFC	H_2	$H_{2(g)} + {}^1/_2O_{2(g)} = H_2O_{(l)}$	60–80	83	45–50	80–90
PEMFC	NG	$CH_{4(g)} + 2O_{2(g)} = CO_{2(g)} + 2H_2O_{(l)}$	60–80	–	35–40	80–90
DMFC	CH_3OH	$CH_3OH_{(l)} + 1{}^1/_2O_{2(g)} = CO_{2(g)} + 2H_2O_{(l)}$	20–60	97	20–25	n/a
AFC	H_2	$H_{2(g)} + {}^1/_2O_{2(g)} = H_2O_{(l)}$	70	83	45–60	n/a
PAFC	NG	$CH_{4(g)} + 2O_{2(g)} = CO_{2(g)} + 2H_2O_{(g)}$	200	–	40	90
SOFC	NG	$CH_{4(g)} + 2O_{2(g)} = CO_{2(g)} + 2H_2O_{(g)}$	600–1000	92	45–60	90
MCFC	NG	$CH_{4(g)} + 2O_{2(g)} = CO_{2(g)} + 2H_2O_{(g)}$	650	92	45–55	90
DCFC	Carbon	$C_{(s)} + O_{2(g)} = CO_{2(g)}$	500–1000	100	70–80	90

PEMFC, Polymer Electrolyte Membrane Fuel Cell; DMFC, Direct Methanol Fuel Cell; AFC, Alkaline Fuel Cell; PAFC, Phosphoric Acid Fuel Cell; SOFC, Solid Oxide Fuel Cell; MCFC, Molten Carbonate Fuel Cell; DCFC, Direct Carbon Fuel Cell.

1.3 Advantages of the Fuel Cells

A brief comparison between fuel cells, batteries, and heat engines as the three main energy converting systems as listed in **Table 3**. Fuel cells and batteries are electrochemical systems based on oxidation-reduction reactions, in contrast to the heat engines in which a combustion reaction takes place as a multi-step energy conversion procedure. The greenhouse gas emissions and low efficiency in case of the heat engines as well as limited lifetime of the batteries due to their electrode depletion as the most important drawbacks of these systems, suggests fuel cells as the most promising candidate for next hydrogen-based power generation technology.

Table 3. A brief comparison between fuel cells, batteries and heat engines [5]

Comparison	Fuel cell	Battery	Heat engine
Function	Energy conversion	Energy storage & conversion	Energy conversion
Technology	Electrochemical reactions	Electrochemical reactions	Combustion
Typical fuel	Usually pure hydrogen	Stored chemicals	Gasoline, diesel
Useful output	DC electricity	DC electricity	Mechanical power
Main advantages	High efficiency	High efficiency	High maturity
	Reduced harmful emissions	High maturity	Low cost
Main disadvantages	High cost	Low operational cycles	Significant harmful emissions
	Low durability	Low durability	Low efficiency

The most significant advantages of the fuel cells can be summarized as follows [5], [8], [9]:

- High efficiency
- Zero emission
- Fuel flexibility
- Static nature (no noise or vibration),
- Simple and compact construction
- Applicable in a wide range of applications
- Ability to run as long as the fuel fed in the cell

1.4 Applications of Fuel Cells

Various scales of these devices ranging from W to MW are now commercially available for a wide range of applications as depicted in

Figure 4. Thanks to the flexibility of this technology, all fields can be covered from small portable electronics to the energy grids as well as vehicles with various size such as airplanes, boats, trucks, and buses. Among other types PEMFCs are used as the main category for transportation sector by Toyota, Hyundai and General Motors companies due to their zero emission and high power density [4].

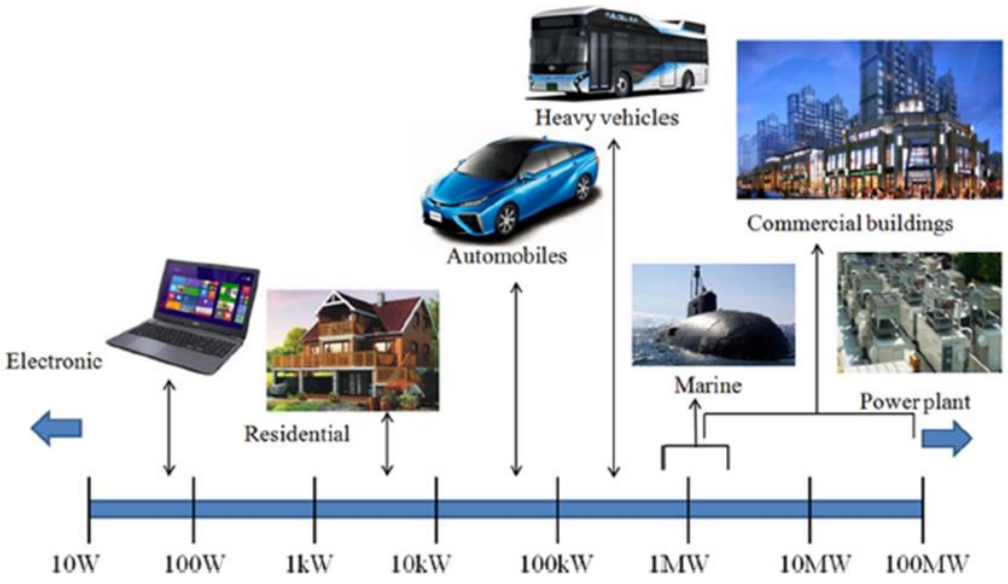

Figure 4. Various applications of fuel cells [8]

1.5 Types of Fuel Cells

There are two fundamental technical problems associated with fuel cells: Slow reaction rate which results in low currents and power output and the difficulties in hydrogen production and storage for hydrogen fuel cells. Various fuel cell types have been tested in order to resolve these problems.

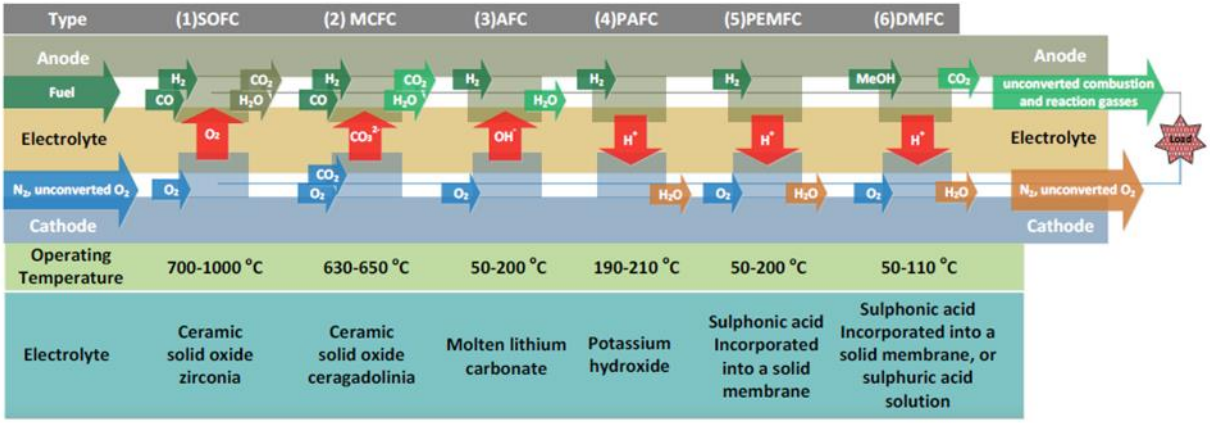

Figure 5. Types of fuel cells [12]

As shown in **Figure 5**, fuel cells are available in a variety of forms. In general, they are classified based on their electrolyte type. However, DMFC (Direct Methanol Fuel cell) is the exception to this classification in which the fuel type is used for naming. Moreover, the operation temperature range could be also used for classification of fuel cells into two distinct categories:

- Low-temperature fuel cells: Alkaline Fuel Cells (AFCs), Polymer Electrolyte Membrane Fuel Cells (PEMFCs), Direct Methanol Fuel Cells (DMFCs), Phosphoric Acid Fuel Cells (PAFCs)

- High-temperature fuel cells: Molten Carbonate Fuel Cells (MOFCs) and Solid Oxide Fuel Cells (SOFCs) [6], [10].

The characteristics, advantages and disadvantages of each type are summarized in **Table 4.**

Table 4. Fuel types and characteristics [13]

	PEMFC	AFC	PAFC	DMFC	MCFC	SOFC
Catalyst layer	Pt	Pt or Ni	Pt	Pt and Ru (1:1)	Ni	Ni
Electrolyte	Nafion™	KOH	H_3PO_4	Nafion™	Molten Carbonate	YSZ
Anodic Reactant	H_2	H_2	H_2/CH_3OH	CH_3OH/H_2	H_2/CO	H_2/CO
Cell temperature (°C)	60–85	20–80	Greater than 170	Less than 70	500–750	650–1100
Merits	1- Wider range of power operation. 2- Scaling is simple. 3- Starting it can be done within a limited period of time. 4- Increased power density compared to other types of fuel cells	1- Pt can be substituted with other materials. 2- Cost effective 3- Faster rate of reaction. 4- Can be started quickly.	1- Lesser impact of carbon monoxide on the cell. 2- Cost effective because less pt is required. 3- Can be utilised with combine heat and power systems 4- Very stable	1- Not toxic emissions. 2- Energy density from cell high. 3- Storage of methanol can be done easily. 4- Methanol is less expensive.	1- Higher cell performance 2- Different type of fuel can be used. 3- Can be integrated on gas turbines. 4- Less expensive.	1- Less expensive 2- Less expensive. 3- Different type of fuel can be used.
Demerits	1- Reduction reaction can be slow. 2- Management of heat in cell. 3- Excess water in cell. 4- Carbon monoxide poisoning. 5- The purity of the fuel used must be high.	1- Cell performance reduce in the presence of carbon dioxide. 2- The purity of the oxidant at the cathode region must also be very high.	1- Takes longer time to start. 2- Materials used in the manufacture of the cells are limited. 3- Ionic conductivity in the cell is low. 4- Power density is lower compared to that obtained from other cell.	1- Possibility of the reactants mixing. 2- The concentration of the fuel has direct effect on the cell performance. 3- Catalyst used is expensive. 4- Cathodic electrode can easily be poisoned.	1- Some of the materials used in building the cell are susceptible to corrosion. 2- Power density is lower. 3- Takes quite sometime for it to start. 4- Materials suitable for the cell development are few.	1- Takes time for it to start. 2- Materials suitable for the cell development are few 3- Electrolytes are susceptible to high resistance. 4- Application is limited.
Electrical Efficiency (%)	40–80	50–75	50	20–40	50%	55–60
Range of power operation	Less than 550 kW	5W–250 kW	45 kW–1.5 MW	80 MW–1.5 kW	Less than 1 kW–1.5 mW	4 kW–3.5 MW
Uses	1- Power backup like UPS. 2- Portable applications like charging laptops 3- Automotive industry	1- Unmanned vehicles. 2- Automotive applications. 3- Portable applications	1- Distributed generation	1- Portable applications	1- Portable applications 2- Distributed generation	1- Back up power 2- Distributed generation
Price ($/W)	40–150	-	3–5	130	-	-

1.5.1 Low-Temperature Fuel Cells (LT-FCs)

Low-temperature fuel cells (LT-FCs) are referred to the fuel cells that operate below 100°C and they can be classified into two main categories based on their electrolyte type: Proton exchange membrane fuel cells (PEMFCs) and Anion exchange membrane fuel cells (AEMFCs). In the first type, a proton-conductive polymer membrane transfers positively charged cations from anode to cathode, while in the second type, an anion-conductive polymer membrane transfers negatively charged anions from cathode to anode [13], [14]. Moreover, PEMFCs can be classified according to the fuel used: Direct methanol fuel cells (DMFCs) use methanol as fuel at the anode side, while in hydrogen fuel cells hydrogen is used as fuel at the anode side [8].

Alkaline Fuel Cells (AFCs)

The first type of fuel cell which was used in aircraft were AFCs during the early 20th century. AFC systems were first used by NASA's Apollo space program in the 1950s, and this technology is counting to use in shuttle missions today. In AFCs, potassium hydroxide (KOH) is used as an electrolyte solution since it is the best conductor of all alkaline hydroxides. Hydrogen reacts with hydroxyl at the anode side and generates water and electrons. Then, the produced electrons transfer via an external circuit towards the cathode, where the water and oxygen react with each other to form hydroxyl ions [15], [16]. In comparison with other fuel cell types, the AFCs display the highest electrical efficiency among all fuel cell types, and their lower catalyst cost, superior corrosion resistance, and significantly faster oxygen reduction kinetics than PEMFCs make them an attractive option for a wide range of applications. However, the main drawback of this type is their liquid electrolyte which is very sensitive to the presence of CO_2. As a result, highly pure gasses are required to be fed in these systems as the fuel. The AEMFCs (Anion exchange Membrane Fuel cells) referred to the new generation of AFCs in which a solid anion exchange polymer electrolyte replaced conventional liquid electrolyte. Developing this category of AFCs opens up a new era for further development and commercialization of AFCs via overcoming the electrolyte poisoning issue [16], [17]. The anode and cathode reactions and different components of an AEMFCs is illustrated in [17].

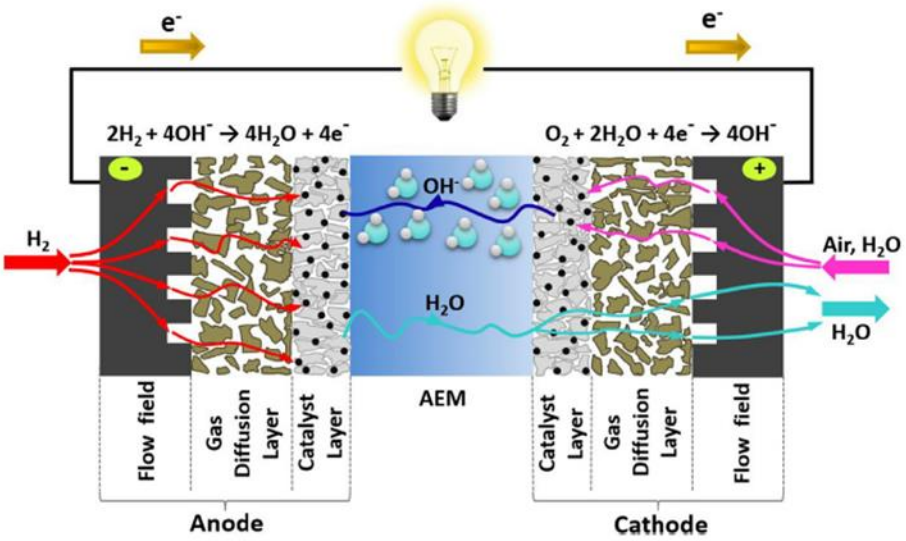

Figure 6. Schematic of an Anion exchange membranes fuel cell components and transportation of various species [17]

Proton Exchange Fuel Cells (PEMFCs)

Proton exchange membrane fuel cells (PEMFCs), also known as polymer electrolyte fuel cells (PEFCs) were the first type of fuel cells that used for space application in the Gemini space program where a 1kW fuel cell stack served as an auxiliary power source [2], [6], [18]. A proton conductive membrane used as the electrolyte in these systems which is interposed between two porous, electrically conductive electrodes. Commercially available Nafion® is used as the most relevant membrane material in PEMFCs. The invention of Nafion® membranes by DuPont was a significant milestone in the history of PEMFCs as they exhibit high acidity and high ionic conductivity as well as being far more stable than conventional polystyrene sulfonate membranes [19]. The electrodes are typically porous carbon supported platinum-based materials. In contrast to the membranes used in AEMFCs, which are only permeable to hydroxide ions due to their basic functionality, the membranes in PEMFCs are only permeable to protons **Figure 7**. This feature is provided by addition of acidic functionality to these membranes [18], [20].

The produced protons are transferred to the cathode side via the membrane and react with oxygen or air to generate water. Despite the numerous advantages of PEMFCs there are several shortcomings that need to be overcome by improving the properties of the materials used in various components of these devices, as well as modification of the system designs to fulfill the main requirements for achieving the desired performance and efficiency. The working principles, functions of each component and characteristics of PEMFCs will be discussed in the following sections.

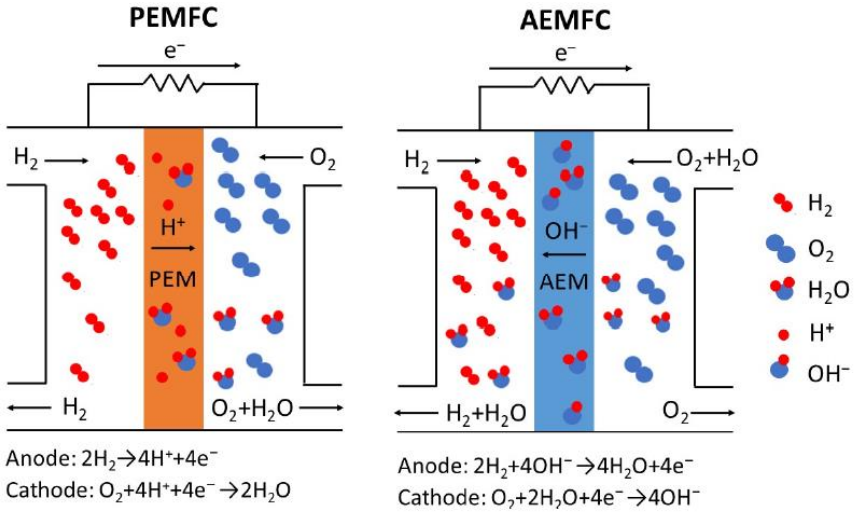

Figure 7. Schematic representation of PEMFCs and AEMFCs reactions and differences in their principles [21]

Phosphoric acid Fuel Cells (PAFCs)

One of the first commercially available fuel cells are phosphoric acid fuel cells (PAFC) that operate at temperatures ranging 150 to 200 °C. By operating at these temperatures, it is not only possible to mitigate catalyst poisoning issues, but also the efficiency up to 85% can be achieved for these devices when combined with heat engines [20], [22]. Phosphoric acid (PA) is used as a liquid electrolyte in these systems which stabilizes in a silicon carbide (SiC) matrix. In state-of-the-art PAFCs the SiC-based membranes are replaced by PA-imbibed systems such as polybenzimidazole (PBI) based membranes [22].

One of the first commercially available fuel cells are phosphoric acid fuel cells (PAFC) that operate at temperatures ranging 150 to 200 °C. By operating at these temperatures, it is not only possible to mitigate catalyst poisoning issues, but also the efficiency up to 85% can be achieved for these devices when combined with heat engines [20], [22]. Phosphoric acid (PA) is used as a liquid electrolyte in these systems which stabilizes in a silicon carbide (SiC) matrix. In state-of-the-art PAFCs the SiC-based membranes are replaced by PA-imbibed systems such as polybenzimidazole (PBI) based membranes [22]. Similar to PEMFCs, in this case also Pt-based catalysts with carbon support are typically used as electrode materials. Compared to LT-PEMFCs, PAFCs offer several advantages, including simple construction, chemical stability, and improved heat and water management problems [6], [23].

1.5.2 High Temperature Fuel cells (HT-FCs)

Molten Carbonate Fuel Cells (MCFCs)

Another type of fuel cells that operate at temperatures ranging from 600 to 700 °C, are molten carbonate fuel cells (MCFCs). Such operational temperatures not only allow for internal reforming and utilizing a variety of fuels but also the waste heat can be used in a combined cycle power plant which enhances their electrical efficiency up to 70% [6], [24]. They are typically composed of a binary or ternary eutectics of molten alkali metal carbonates (Li_2CO_3, Na_2CO_3 and K_2CO_3) stabilized in the alumina (Al_2O_3) matrix as electrolyte, Ni-based alloys as anode electrode and NiO as cathode material [25]. Compared to LT-FCs, the improved kinetic rate at elevated temperatures, mitigates the need for costly precious metals as the catalyst in this type. Therefore, the cost is reduced by both replacing inexpensive Ni-based electrodes and elimination of the external fuel reformer. Furthermore, they can be considered as CO_2 capture technologies due to their ability to separate and consume the CO_2 at the cathode reaction in an effective manner [24]. In the case of MCFC materials, the most commonly encountered problems are the leakage of electrolyte, dissolution of Ni-based electrodes, thermal stability and degradation due to corrosion of various components [26], [27].

Solid Oxide Fuel Cells (SOFCs)

Solid oxide fuel cells (SOFCs) have been explored and scientifically reported as a sustainable energy source since the late 1990s [7]. These systems typically operate at temperatures ranging between 400-1000°C. The electrode reaction kinetics is significantly accelerated at such elevated operational temperatures, therefore the need for precious metals as catalyst material is mitigated as for MOFCs. Furthermore, such high operating temperatures offers the advantage of being able to utilize a variety of fuels. SOFCs are composed of a solid oxide ceramic electrolyte that is interposed between two porous electrodes. In SOFCs generally, Yttrium-stabilized zirconium (YSZ) or Cerria-based material is used as electrolyte, NiO-based materials as the anode electrode, and $LaSrMnO_3$ (LSM) as the cathode electrode materials [6], [26]. SOFCs can be classified into three different categories as: oxygen ion-conducting SOFCs (O-SOFC), proton-conducting SOFCs (P-SOFC) and dual ion-conducting SOFCs (D-SOFC), due to the type of the species which are transported during the cell operation [26]. Compared to MCFCs, SOFCs are more stable due to the presence of a solid electrolyte, which eliminates electrolyte leakage problems. However, it is difficult to find thermally stable materials that can withstand such high operational temperatures. The main technical issues associated with SOFCs include the long startup time, safety problems, utilizing high-cost materials, complexity of the system and system failure due to the thermal stress. Therefore, development of adapted materials and designs must be carried out to fulfill the requirements for practical applications [28].

1.6 Principles of PEM Fuel Cells

In a PEMFC hydrogen (hydrogen containing fuel) is supplied from anode side and the oxidant (oxygen or air) from the cathode side. Hydrogen is oxidized to hydrogen ions and electrons through the anode reaction which is called hydrogen oxidation reaction (HOR). The electrolyte allows positively charged ions to move towards the cathode, but not the electrons. Afterwards, the generated electrons pass through an external electric circuit and cause an electric current. As the ions reach to the cathode side, electrons are coupled with the positively charged ions, and react with the cathode fuel to form water, electricity, and heat.

This reaction is called oxygen reduction reaction (ORR) [5], [18]. A schematic of a proton exchange membrane (PEMFC) is shown in **Figure 8** that represents the above-mentioned phenomena.

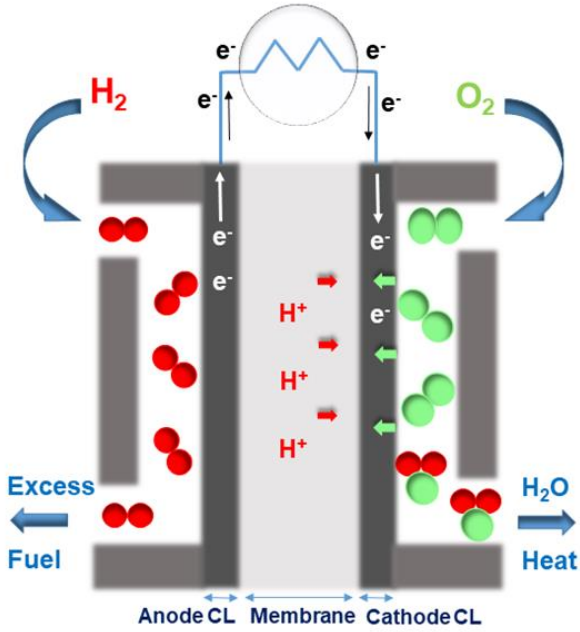

Figure 8. Schematic of a Proton exchange membrane fuel cell

The half-cell reactions as well as the overall reaction in a H_2/O_2 fuel cell are:

Anode reaction: $2H_2 \rightarrow 4H^+ + 4e^-$ (5)

Cathode reaction: $O_2 + 4H^+ + 4e^- \rightarrow 2H_2O$ (6)

Overall reaction: $2H_2 + O_2 \rightarrow 2H_2O + heat$ (7)

$(\Delta G = -237\ kJ/mol, \Delta U = 1.23\ V)$

1.7 Components of PEM Fuel Cells

In general, PEMFCs consist of different components each performing a variety of functions (**Figure 9**). The Membrane is interposed between two catalyst layers which are called membrane electrode assembly (MEA).

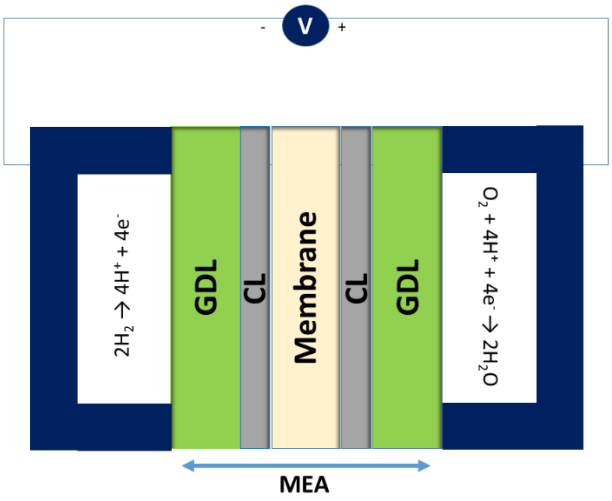

Figure 9. Schematic of various MEA components

Membrane

The membrane is referred to a solid electrolyte that interposed between two catalyst layers with a typical thickness in range of 10-100 µm. Various types of membranes are used for PEMFC applications based on their operational conditions such as temperature. The most significant characteristics and functions of membranes are discussed in the following sections.

Catalyst Layer

CLs are porous, carbon-based materials containing platinum (Pt) nanoparticles as catalysts for HOR and ORR reactions. CL plays a vital role in electrochemical reactions by providing pathways for transportation of the reactants and conduction of electrons and protons between anode and cathode.

Gas diffusion Layer (GDL)

GDLs are porous gas diffusion components that are made from carbon cloth or carbon paper. Their typical thickness is in the range of 100-300 μm. Transferring the reactant gasses towards the catalyst layer, conduction of electrons to and from the catalyst layer as well as heat and water management can be named as the main functions of GDLs in PEMFCs [29].

1.7.1 Membrane

Membranes is generally a solid proton conductive material which is used as the electrolyte in PEMFCs. It is responsible for several key functions such as transferring the protons from anode to cathode side, acting as a barrier to prevent direct mixing up the reactant gasses and insulating electrons. Proton exchange membranes can be divided into three different categories according to their chemical structure: ceramic, polymeric and inorganic-organic composite membranes. A PEM fuel cell's efficiency and lifetime is generally determined by its membrane electrode assembly (MEA), which is made up of a proton conducting membrane placed between two catalyst layers (**Figure 9**). To ensure high cell performance and adequate durability in harsh operating conditions of the fuel cell, high ionic conductivity, minimum ohmic losses, as well as good mechanical, chemical, and thermal stability are the main requirements for a membrane. Moreover, the hydration level and membrane thickness are two factors that significantly affect a proton exchange membrane performance [30], [31].

1.7.1.1 Proton Exchange Membrane Types

There are five different types of solid membranes for PEMFCs namely (**Table 5**):

- **Perfluorinated membranes (PFSA membranes):** This type is composed of a fluorinated backbone and sulfonic acid groups as proton conducting side chains. High proton conductivity as well as excellent chemical stability and durability are their main advantages. However, they suffer from intense performance drop at elevated temperatures and anhydrous environments. Additionally, their production costs are high [31]–[33].

- **Partially fluorinated membranes:** An aromatic or hydrocarbon side chain is attached to a fluorocarbon backbone in this category. One of the major advantages of these membranes is their lower cost and the ability to enhance proton conductivity via grafting of proton conductive side chains. But their overall cell performance and durability are lower than those of perfluorinated membranes [34], [35].
- **Non-fluorinated hydrocarbon:** These membranes contain a hydrocarbon backbone with proton conductive functional groups. They exhibit excellent mechanical properties but poor thermal and chemical characteristics as well as low proton conductivity values [36], [37].
- **Acid-base blend membranes:** These membranes are made from alkaline base polymers grafted by acidic functional groups. In addition to their excellent proton conductivity, they possess good chemical and thermal properties. However, they showed lower durability values then the above-mentioned categories [38], [39].
- **Ionic Liquids:** They are fabricated from an organic cation with an organic/inorganic anion. Good thermal and chemical durability and high proton conductivity are the main benefits of these membranes. Nevertheless, fabrication of solid membranes from these components is challenging [40].

Table 5. Various types of polymeric membranes for PEMFCs [35]

Perfluorinated	Partially fluorinated	Non-fluorinated	Acid-base blends	Others
• PFSA • PFCA • PFSI • Gore-select	• PTFE-g-TFS • PVDF-g-PSSA	• NPI • BAM3G • SPEEK • SPPBP • MBS-PBI	• SPEEK/PBI/P4VP • SPEEK/PEI . SPEEK/PSU(NH_2)$_2$ • SPSU/PBI/P4VP • SPSU/PEI . SPSU/PSU(NH_2)$_2$. PVA/H_3PO_4	• Supported composite membrane • Poly-AMPS

Perfluorinated Membranes

Perfluorosulfonic acid (PSFA) membranes with long side chains are the most commonly used membranes in PEM fuel cells, such as Nafion®, Flemion®, Aciplex®, and Gore-Select®. Recently, several alternative PSFA membranes including Dow®, Aquivion® and Hyflon® with shorter side chains have been developed [41]. Among these membranes Nafion® is the most widely used category in PEM fuel cells due to its outstanding characteristics. The development of Nafion® membranes by Dupont company dates to the 1970s [42]. This ionomer is composed of a hydrophobic polytetrafluoroethylene (PTFE) backbone and hydrophilic sulfonic acid groups as the side chains. The chemical structure of Nafion® is shown in **Figure 10.**

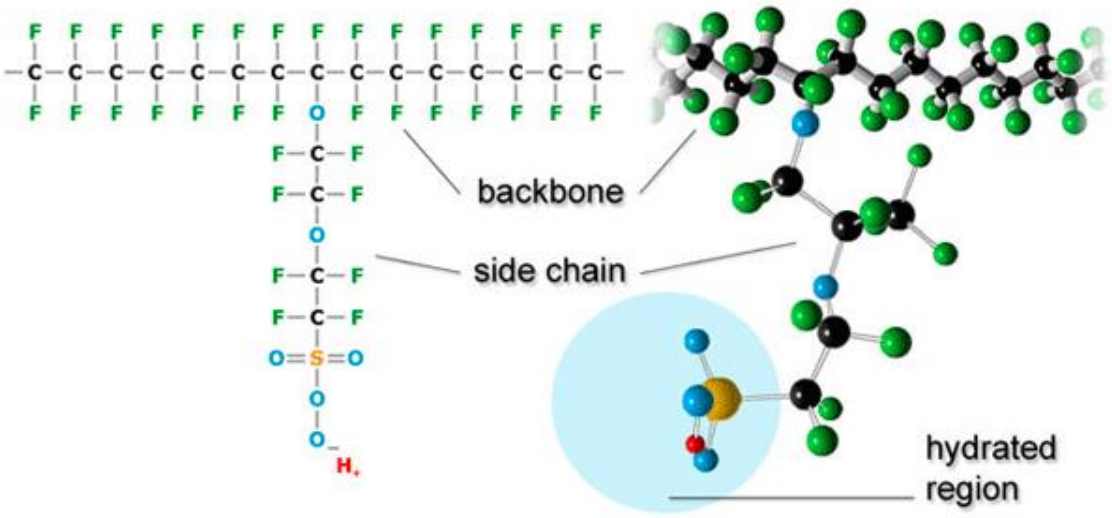

Figure 10. Nafion® Structure [43]

The PTFE backbone supports this structure and gives membranes a hydrophobic nature. However a large amount of water has been absorbed by the ionic groups that results in the hydration of the polymer.Zawodzinski et al reported that at room temperature and a fully hydrated condition the water content (absorbed water molecules/ sulfonic acid group) of these membranes are equal to 22 which gives rise to achieve a protonic conductivity of 0.1 S/cm [42]. But this value decreses to 0.06 S/cm when the water content is reduced to 14.

In addition the conductivity increase to up to 0.18 S/cm at fully humidified condition and 80 ˚C [44]. These two evidence shows that the conductivity of Nafion® membranes are highly depend hydration level of membrane and the cell temperature. Compared to other membranes they show excellent characteristics such as desirable proton conductivity (130 mS/cm at 75°C at 100% RH), favorable chemical stability at temperature below 80°C, superior thermal as well as mechanical properties, and relatively extended lifetime (over 60,000 hours) [32]. However, their practical application is faced with some limitations [45], [46]. One significant disadvantage of Nafion® membrane is that they are subject to significant mechanical degradation over prolonged operation of PEMFCs, particularly through repeated hydration/dehydration cycles or alternating temperature conditions. Moreover, the electrochemical reactions as well as the water management procedures that take place at the catalyst layer significantly affects the overall performance and results in a variety of membrane degradation mechanisms in a fuel cell. Additionally, the upper operating temperature limit of Nafion® is very low (only 80–100°C). Normally, Nafion® loses proton conductivity when the temperature increases above 80 °C, while a significant decline occurs at 120 °C [42].

1.7.2 Challenging Issues in Membranes

Despite the extensive studies and developments in the field of membranes for PEMFC application they still suffer from several problems such as short lifetime and cost as mentioned in previous section. Insufficient proton conductivity, excess water swelling, and inadequate mechanical robustness are the main drawbacks of homopolymer membranes such as Nafion®. In addition to inherit chemical composition of the membrane material several physical parameters and environmental factors also have various impacts on the membrane performance. For example in general a thicker membrane offers better electrical insulation as well as greater mechanical strength, chemical strength but higher protonic resistance [41]. Therefore, to balance the performance and durability requirements, the membrane characteristics must be optimized accordingly in real applications by investigating the mechanisms and reasons for such problems.

1.7.2.1 Water Management

The protonic conductivity of the membrane is usually affected by the amount of water present inside the membrane, since water ionizes the acid groups and facilitates the proton conduction through the membrane due to reduction in protonic resistance. But it can be noted that excessive water results in liquid water flooding issues such preventing reactants reaching the reaction sites due to the blockage of the reactant gas channels. Consequently, water management is another major technical challenge, and it is necessary to optimize the water amount in PEM fuel cells in a way that the sufficient humidification of membrane is provided at the same time preventing water flooding problems [47], [48].

1.7.2.2 Membrane Degradation

The other issue is related to the lifetime of the membrane which is affected by various degradation modes that occur in membranes. Generally, membranes can undergo three different degradation types including: thermal, mechanical, and chemical degradation.

Mechanical degradation: Cracks, pinholes and delamination of the MEA components can be considered as various mechanical degradation modes **Figure 11**. Presence of cracks and pinholes gives rise to the gas crossover which in turn leads to thermal and water management issues as well as direct reaction of reactants and safety concerns. Theses defects can be originated due to severe pressure difference and repeated swelling and shrinkage during hydration and dehydration process. For example Nafion® membranes exhibits 10% shrinkage when the humidity drops from 100 to 50% [41], [49].

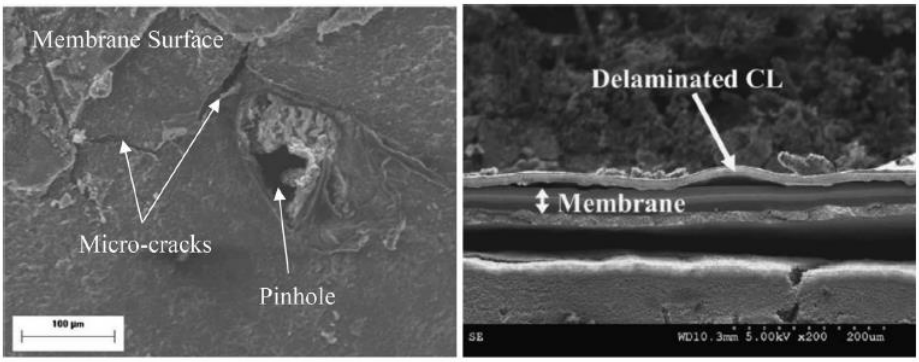

Figure 11. Mechanical degradation mechanisms in membrane [41]

Thermal degradation: Thermal degradation caused by material decomposition at high temperatures. For example, the glass transition temperature for PFSA membranes is around 80°C therefore at this point softening stars to happen and further increase in temperature leads to chemical decomposition of these membranes via two different mechanisms: unzipping of the main chain or dissociation of the side-chain [50], [51]. Electrochemical/chemical degradation: chemical decomposition of membrane results in reduction of membranes thickness (membranes thinning) that can cause gas crossover issues and thermal deterioration via exothermic combustion of reactants. This direct, extensively exothermic, combustion reaction leads to destroying the MEA and generation of pinholes and microcracks. Additionally, further decomposition may take place through the attack of active peroxide (HO*) and hydroperoxide (HOO*) radicals produced during the half-cell reaction [52], [53]. Another source for this kind of membrane deterioration is presence of foreign cations in membrane. These impurities mainly result from corrosion of stack's metallic components or incorporate to system via the fed fuel. Generally, PFSA membranes exhibit greater affinity between their sulfonic acid group and theses metallic cations than proton, as a consequence, during cell operation more active sites are utilized by these cations resulting in dramatic reduction in cell performance [53]. In order to mitigate the above-mentioned limitations, various strategies have been applied to modify the properties of Nafion® membranes or entirely replace them with alternative proton conductive membranes. As of now, membranes have been divided into three groups:

i) modified PFSA membranes with using nonvolatile solvents, incorporated hydrophilic oxides or proton conducting inorganic agent, ii) an alternative sulfonated polymer or its composite membranes, such as SPEEK or SPSF, iii) acid–base polymeric membranes like Nafion®–PBI membranes [53].

1.7.3 Composite Membranes

Among other strategies synthesizing composite or hybrid membranes have captured the interest of researchers due to their ability to combine dissimilar properties of both inorganic and organic components, while exhibiting the favorable properties of both materials. Using this approach to mitigate the characteristics of Nafion® membranes are extensively investigated. These membranes can be classified as:

i. Nafion®-based composite membranes: Direct blending of polymers with Nafion® or incorporation of inorganic additives

ii. Non- Nafion® composite membranes

These membranes can be considered as promising candidates for PEMFC applications due to their improved characteristics such as high ionic conductivity, superior dimensional stability and good mechanical, chemical and thermal properties compare to that of pristine Nafion® membranes.

Nafion®-based Composite Membranes

Numerous research groups have been investigated the effect of addition of some metal oxides such as TiO_2 [54]–[56], ZrO_2 [57]–[59] and SiO_2 [60]–[62] additives as inorganic fillers on the final characteristics of Nafion® membranes. Inorganic fillers can fall into three categories based on the property that they give to the membrane. They can use as inert fillers to reduce the fuel crossover or increasing dimensional stability, or for improving their mechanical strength and/or the proton conductivity.

1.7.3.1 Preparation Methods of Composite membranes

In addition to chemical composition modifications via incorporation of fillers and additives, structural modifications of membranes, by using various fabrication methods is reported in literature. These methods can be classified to three different types as [63].

1.7.3.1.1 Infiltration

Infiltration involves swelling of a prefabricated ionomer membrane in a solution of dispersed inorganic particles that are attracted to its hydrophilic domains. The particles need to be stabilized by annealing. In this method the problem is leaching off the particles due to the lack of a strong interaction of particles with polymers. This challenge can be overcome by using a combination of the infiltration of organically modified particles and subsequently polycondensation in order to obtain strong covalently bonded particles to polymer phase.

1.7.3.1.2 Recasting or Blending

Recasting method provides unique advantages of preparing thin membranes and allows simple process parameters optimizations. The essential requirement for this technique is proper dissolution of the starting materials in the solvent to achieve the initial dispersion of inorganic particles. Surface incompatibility or polymer chain mobility can result in particle agglomeration, which can be prevented by combination of blending and sol-gel processes. Using this method, make it possible to incorporate inorganic phase into the both hydrophilic domains of the polymer matrix and the hydrophobic backbone to increase the thermal and mechanical stability of the membrane.

1.7.3.1.2 Electrospinning

Recently, electrospinning is considered as one the most attractive techniques for fabrication of fibrous materials with diameter size in range of hundred nanometers to few micrometers for verity of applications including membranes for fuel cells [64]. In this technique, charged strands of a polymer solutions are drawn by electric force between the tip of a spinneret and a fixed or a rotating collector [65]. This electric force is created via utilizing a high voltage power source. A pump with ability to adjust the flow rate is used to push the polymer solution to eject from spinneret. A Taylor cone forms from the solution when the surface charge built up on the solution at the tip of the spinneret surpasses its surface tension and leads to generation of a liquid jet. As the jet is directed towards the collector, the solvent evaporates.

The properties of the resultant fibers depend on electrospinning parameters and can be tune via altering them such as applied voltage, the distance between tip of spinneret and the collector, concentration of the polymer solution [21], [66], [67]. A schematic of an electrospinning set-up and produced fiber mat are depicted in **Figure 12.**

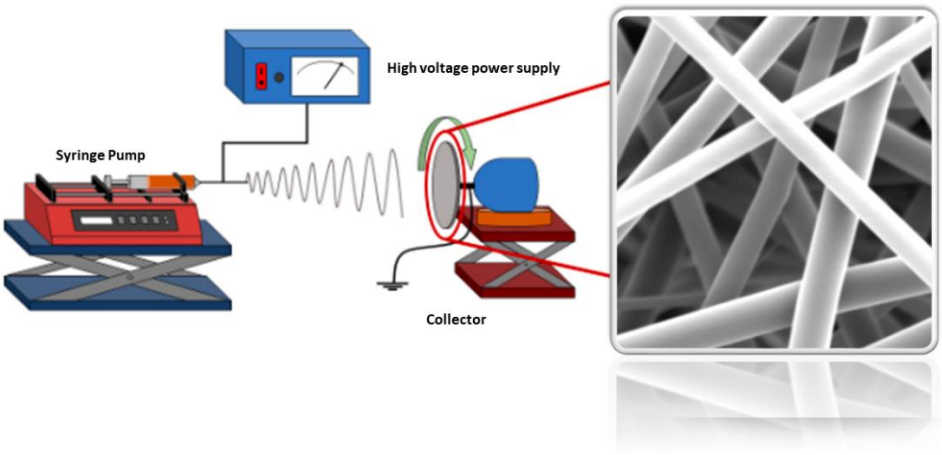

Figure 12. Schematic of an electrospinning set-up [68]

This method can be classified into three different types based on the number and type of the nozzles used for fabrication of the fibers. As shown in **Figure 13** the variety of designs gives rise to obtain different morphologies. This method is not only fast, cheap and scalable but also it gives the opportunity of using a combination of wide range of materials such as carrier polymers and additives simultaneously to achieve the desired characteristics. Furthermore, tuning of the various properties of the resultant fibrous networks is possible via optimization of the electrospinning parameters in a simple manner [70].

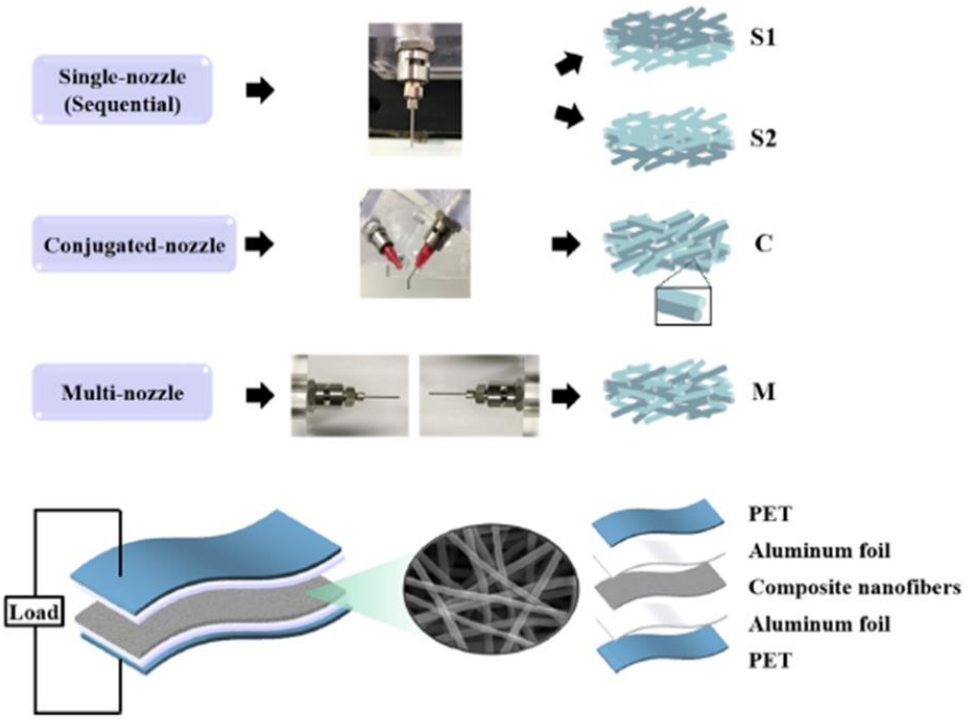

Figure 13. Different types of electrospinning [69]

1.7.3.2 Electrospun Composite Membranes for PEM Fuel Cells

As mentioned, fabrication of composite membranes as alternatives to pristine Nafion® membranes are studied extensively over the years. These membranes are generally prepared via melt-extrusion and solution-cast techniques. However, the prepared membranes via these conventional methods suffer from several issues including inhomogeneity of the membrane composition, difficulty in preparation of well-dispersed and homogenous cast solutions and limitations in preparation of thin membranes with promising mechanical properties [71]. Therefore, in recent years electrospinning is commonly used as preferred method for preparation of membranes thanks to their numerous advantages such as the possibility of fabricating high-quality reinforcing nanofiber 3D networks with tailored porosity from a wide range of chemically and mechanically stable polymers. Furthermore, electrospinning can be used to produce multicomponent membranes with homogeneous composition from polymer blends which is not possible via other methods.

Generally, four different approaches can be used for preparation of electrospun membranes:

- The nanoparticles with desired functional groups are added to electrospun composite mats during the membrane fabrication to improve their water retention ability and provide a fast and quick proton conductivity. Furthermore, the fibrous structure exhibits enhanced mechanical characteristics in comparison to solution-casting of the same compositions [73]-[76].

- The porous of the electrospun nanofiber is fabricated using an ionomer or uncharged polymer. Subsequently, the pores are filled either with the ionomer or the uncharged polymer solution by impregnation or welding. The impregnation process may need to repeat several times for proper filling of the existent pores. Generally a carrier polymer is used for electrospinning of the ionomer such as poly(ethylene oxide) or poly(acrylic acid). An alternate method of fabricating the composite membranes involves dual fiber electrospinning [59], [61].
- In the approach an ionomer solution and a reinforcing polymer solution (uncharged polymer solution) are used to electrospun simultaneously onto a single collector. The compact membranes can be obtained after densification of the produced mats by subsequent treatments such as hot-pressing which results in the formation of a densified two-component composite membrane. Based on the inherent nature of the components the retaining fibers can be either the ionomer fibers in a reinforcing polymer matrix or vice versa. In the other type a blend of ionomer solution and uncharged polymer is mixed prior to electrospinning. Then this mixed solution is used for preparation of fibrous mats via single electrospinning method. As the next step these porous mats are converted to densify membranes via mechanical pretreatments [71], [72].
- In the other type a blend of ionomer solution and uncharged polymer is mixed prior to electrospinning. Then this mixed solution is used for preparation of fibrous mats via single electrospinning method. As the next step these porous mats are converted to densify membranes via mechanical pretreatments [79].

1.8 Significant Bulk Properties of a Membrane

There are several parameters need to be considered to obtain a high performance PEMFCs. Among them the mechanical robustness, water uptake and proton conductivity can be considered as the most significant characteristics of the membranes which determines the membrane performance as well as overall cell performance.

1.8.1 Water Uptake

Water uptake refers to the ability of a membrane to absorb water, this affects several properties of the membrane such as its proton conductivity. Water content (λ) can be considered as a measure of water uptake that can be calculated as the mass ratio of water to dry polymer, or the ratio of the number of water molecules to the number of sulfonic acid groups. A membrane's maximum water content is greatly affected by the water state used to equilibrate it [72]. For example, for the Nafion® membrane that equilibrates in liquid water the λ is reported as 22, while this value is reduced to 14 when the Nafion® membrane equilibrates in water vapor instead [73], [74]. Furthermore, the uptake of water is determined by the membrane's chemical structure as well as the pretreatment procedures, such as the drying temperature. This evidence attributes to the morphological change at elevated temperatures, for example, this effect is significantly pronounced for Nafion® membranes at temperatures higher than 80°C. It is important to note that in PEMFCs, humidified gasses are fed into the system, so water is present in vapor form. Water adsorption from the vapor phase can take place via a two-step mechanism: i) via solvation in membranes' ions, ii) filling the pores which results in membrane swelling [72].

1.8.2 Proton Conductivity

Proton conductivity can be considered as the membrane ability to transfer the protons which is highly influenced by the structure of membrane and the water content. Springer et al. developed the following equation for calculating the proton conductivity of the Nafion® 117 membranes that can be applied for membranes in PEMFCs [31], [72]:

$$\sigma_p = (0.005139\,\lambda - 0.00326)\exp\left[1268\left(\frac{1}{303} - \frac{1}{T}\right)\right] \quad (8)$$

where σ_p, λ and T stand for ionic conductivity (S/cm), water content and temperature respectively. Based on this formula proton conductivity is directly proportional to water uptake and operational temperature of the cell. Increasing the water content in the medium facilitates ion transport through the membrane via reduction of ohmic resistance. In addition to water content value the operational temperature can also affect the proton conductivity [73]. By increasing the temperature while maintaining a sufficient level of humidity, proton conductivity is enhanced via improving ion mobility [75].

Besides the above-mentioned mathematical equation, other experimental methods such as direct current measurement and alternating current impedance are also employed to estimate the proton conductivity of membranes. To calculate the ionic conductivity, the measured total resistance via these methods plugs into the following equation:

$$\sigma = \frac{l}{RS} \tag{9}$$

where $\sigma\ (S/m)$ stands for ionic conductivity and $l\ (m)$, $R\ (\Omega)$, $S\ (m^2)$ represent the distance between two electrodes, resistance and the active surface of the membrane, respectively [31], [76]. Proton conductivity is governed by two different mechanisms in proton exchange membranes: Grotthuss or hopping mechanism and vehicle mechanism. The Grotthuss mechanism explains the ion transfer at lower water levels. This mechanism is based on formation and breakage of a hydrogen bonding between the proton and the hopping sites. Therefore, the conduction of protons takes place through the membrane by hopping of protons from one site to adjacent sites. Protons are subject to potential barriers based on the distance between these hopping sites. Thus, strength of H-bonding, the distance between sulfonate groups and their homogeneous distribution in the membrane are the critical parameters for this type of ionic conduction mechanism [77], [78]. In contrast, for proton conduction via vehicle mechanism higher water content in aqueous environment (or any other acid environments) is necessary. Because the charges needs a connected water channel network as carrier medium for transferring the hydrated ions such as H_3O^+, $H_5O_2^+$ which are formed by solvation of protons in aqueous solution [31], [77], [78].

This dissertation focuses on the preparation of sulfonated silica-based proton conducting membranes for PEM fuel cells operating at lower humidity operation of PEM fuel cells. The following chapters are focused on the sulfonated silica based electrospun membranes synthesized and fabricated with different approaches.

Electrospun Sulfonated Silica-based Proton Exchange Membranes for PEM fuel Cells

1.9 Nanofiber-based Hybrid Sulfonated Silica/PVDF-TrFE Membranes for PEM Fuel Cells

1.9.1 Objective

Invention of Nafion® membranes by DuPont was a breakthrough in the field PEMFCs and they can be considered as the most widely used membranes in hydrogen fuel cells due to their numerous outstanding merits. However, there are two major shortcomings for these membranes including: high production costs and reduced ionic conductivity at low humidity conditions. Therefore, searching for new inexpensive alternative membranes with desired characteristics is an interesting area of research. The goal of this study is to develop novel hybrid proton exchange membranes for low humidity PEMFCs applications. For this purpose, sulfonated silica nanoparticles as an inexpensive proton conducting additive with high water retention ability, and polyvinylidene fluoride-co-trifluoroethylene (PVDF-TrFE) as the reinforcing polymer were used to prepare these hybrid membranes via electrospinning.

1.9.2 Introduction

With the decline of fossil fuel reserves worldwide and the rising need for cleaner sources of energy, alternative energy sources are of crucial need. Many clean energy production and conversion devices have been developed to date. However, polymer electrolyte membrane (PEM) fuel cells are among the fastest emerging alternative sources for energy production used currently for various applications [4]. PEM fuel cells are generally composed of two electrodes (the cathode and the anode) sandwiching an electrolyte membrane, together they form the membrane electrolyte assembly (MEA) [79]. Membrane is regarded as the heart of a fuel cell since it permits the passage of protons between the two electrodes while blocking the passage of gasses and electrons between the electrodes. Nowadays, due to their superior proton conductivity, commercial Nafion® membranes; sulfonated tetrafluoroethylene-based fluoropolymer-copolymer; reside at the top of the pyramid of the most widely used ionomer electrolyte in commercialized recent PEM fuel cells. However, Nafion® membranes exhibit some drawbacks hindering the wide utilization of PEM fuel cells, especially with the fierce

competition in other energy storage and conversion devices namely Li-ion batteries and electrochemical supercapacitors [80], [81]. For instance, proton conductivity of Nafion® membranes are dependent on the water content of the system; in other words, they can function optimally only when the system is fully humidified. However, the PEM fuel cell system shows an efficiency drop at non or low-humid conditions due to the failure of Nafion® membranes to adapt within scarce water conditions limiting the mode of operation of PEM fuel cells to certain conditions. Furthermore, the high cost of Nafion® membranes possess a financial burden added to the already expensive PEM fuel cell [82]. In order to overcome those limitations exhibited by the usage of Nafion® membranes, extensive research has been done. In this regard, solutions have been proposed ranging between modifying Nafion® to completely substituting Nafion® membranes for a cheaper alternative possessing similar conductivity within a range of operating conditions. Some studies suggested the use Nafion® membranes along with an additive such as titanium oxide (TiO_2) [54]–[56], zirconium derivatives [58], and silica [60], [61], [71] enabling it to work at relatively higher temperatures and less humid atmospheres. Generally, the proton conductivity of a membrane relies on several parameters such as the nature of the material and its water uptake ability. In addition, due to the various problems occurring due to excessive amounts of water produced at the cathode, water intake is a crucial property that a membrane needs to be attributed to permitting water management within the fuel cell stack. In this sense, composite membranes presented advantageous water uptake properties over Nafion® membranes where TiO_2/Nafion® showed 51% more water uptake compared to that of Nafion® membranes leading to high PEM fuel cell performance even at high temperatures [54]. Similarly, SiO_2 particle additives have shown better water uptake leading to better fuel cell performance at a higher temperature and lower humidified media [58], [60], [62]. Since proton conduction is greatly correlated to the existence of functional groups facilitating its passage, many ionomers with functionalized surfaces were developed [83]. In this regard, further materials with promising performances were produced with surface functionalities such as acid-functionalized silica nanoparticle ionomers. Surface functionalized silica nanoparticles have shown remarkable water uptake and proton conductivity properties in which 0.05 S/cm was obtained for SPEEK/sulfonated silica (S-SiO_2) composite at 80% and 75% relative humidity [84], and a conductivity exceeding that of Nafion® for S-SiO_2/

Nafion® composite with 133.8 mS/cm 0.6 wt% S-SiO_2 loading [85]. Yet, excessive swelling accompanied with mechanical stress leading to cracks within the membrane greatly affects the durability of sulfonic acid containing membranes [86].

Electrospinning previously known as a versatile and simple, yet powerful tool has been used in favor of producing fiber-based membranes [87], [88]. Fiber structure with controlled diameters down to the nanometer range resulting in high surface area material can be produced with this technique. Due to this fact, this technique has been extensively used for membrane fabrication for fuel cell applications. A further enhanced water retention ability of the electrospun membranes has made them promising candidates for PEM fuel cells especially at lower humidified media. For instance, TiO_2 reinforced Nafion® membrane exhibited promising fuel cell performance at 90 °C and 50% relative humidity (93% of that in fully humidified condition) with good durability in comparison with pristine Nafion® membranes [56]. In another study, bio-functionalized silica with amino acids and a composite was made along with Nafion® via electrospinning. The composite has shown superiority in terms of conductivity for cysteine functionalized SiO_2/ Nafion® composite of 0.24 S/cm at 80 °C. The presence of proton acceptor/donor species, the connected conduction pathways along the fibers produced via electrospinning and the intersection of the fibers further increasing the pathways have permitted the better passage of protons [89], [90]. Therefore, bringing the pieces together via acid functionalizing silica, producing fibers and impregnating Nafion® within might become a great advance in the field eliminating a lot of drawbacks that Nafion® shows. Despite that major, minimal research has been conducted on Nafion® impregnated-acid functionalized silica nanofibers. With the scope summarized above, in this study, S-SiO_2 particles that are cheap, stable at low humidity were synthesized, characterized, and used as an additive/ionomer in membrane structures. Moreover, these synthesized, characterized S-SiO_2 particles were integrated into the membrane by using a one-step electrospinning technique.

Additionally, hydrophobic polymers (PVDF and (P(VDF-TrFE)) were used as carrier polymers in electrospinning and obtained electrospun mats impregnated with Nafion® solution. The effect of carrier polymer on the water uptake, mechanical behaviors and ionic conductivity at room temperature and different relative humidity levels of hybrid membranes were studied. There is no study related to membrane fabrication for PEM fuel cells with the

P(VDF-TrFE) copolymer and polymer/particle electrospinning technique. To the best of our knowledge, proton conducting electrospun membranes based on PVDF-TrFE and S-SiO2 particles were shown for the first time in literature.

1.9.3 Experimental

Materials

Aqueous solution of sodium silicate and cetyltrimethylammonium Bromide (CTAB) were purchased from AppliChem. Polyvinylidene fluoride (PVDF) (Solef®, Mw = 380,000) powder and polyvinylidene fluoride-co-trifluoroethylene (PVDF-TrFE) powder were purchased from Solvay, PolyK technologies and Aldrich companies respectively. Tetrahydrofuran (THF), N, N-dimethylacetamide (DMAc), hydrochloric acid (HCl), sulfuric acid (H_2SO_4) and 5 wt % Nafion® solution all was obtained from Sigma Aldrich.

Synthesis of sulfonated silica particles

Sulfonated silica was prepared via a three-step procedure. Firstly, mesoporous Si particles were prepared through the hydrothermal hydrolysis method reported elsewhere [91]. In summary, 11.7 g of CTAB surfactant was dissolved in 78 mL of distilled water, and 34 mL of sodium silicate solution was added dropwise into the water/surfactant mixture while stirring continuously in an oil bath with a temperature of 40 °C for 1 hour. Subsequently, 1 M HCl acid solution was added slowly to adjust the pH of the solution to 11. Then, the solution was stirred for an additional hour. The prepared silicate solution was transferred into a Teflon-lined stainless-steel autoclave. The autoclave was sealed then heated up to 120 °C for 48 hours in an oven. The resultant product was washed thoroughly with water then filtered to remove the surfactant. The remaining solid product was dried in an oven at 60 °C for 24 h. Then, the obtained product was calcined at 550 °C for 14 hours in a tube furnace under an air atmosphere with a heating rate of 10 °C/min [91], [92]. Finally, sulfonation was performed by adding 2.6 g of the as-prepared Si powder into 50 mL concentrated sulfuric acid (H_2SO_4) followed by stirring for 30 min. The mixture was then transferred into an autoclave and placed in an oven at 120 °C for 48 hours. Afterward, the resultant sample was washed with distilled water, filtered, and dried overnight at 60 °C.

Preparation of electrospinning solutions

Electrospinning solutions are composed of a carrier polymer solution and an S-SiO_2 dispersion. A 15% polymer/solvent (wt %) solution was prepared by stirring PVDF (P) or P(VDF-TrFE) (T) in a 7:3 wt ratio mixture of DMAc:THF overnight. S-SiO_2 dispersions were prepared with DMAc solvent (1:2 wt ratio of solid: solvent). The dispersion was probe sonicated for 40 min and stirred for 24 h. Finally, S-SiO_2 dispersion was added into the polymer solution and mixed 24 h to obtain a homogenous solution. The composition of electrospinning solutions are shown in **Table 6.**

Table 6. Composition of electrospinning solutions [93]

Sample	P/S-SiO_2-50	P/S-SiO_2-60	P/S-SiO_2-70	T/S-SiO_2-50	T/S-SiO_2-60	T/S-SiO_2-70
Carrier Polymer	PVDF	PVDF	PVDF	P(VDF-TrFE)	P(VDF-TrFE)	P(VDF-TrFE)
Polymer/ S-SiO_2 (wt:wt %)	50:50	40:60	30:70	50:50	40:60	30:70

* PVDF:P, P(VDF-TrFE):T

Electrospinning of PVDF/S-SiO_2 and P(VDF-TrFE)/S-SiO_2

The electrospinning of the prepared solutions was carried out by a syringe pump and high voltage source in a controlled relative humidity (RH) home-made designed chamber with adjustable a rotating drum collector as shown in **Figure 14**. All experiments were performed with a flow rate of 0.8 mL/h, applied voltage of 14 kV, RH% of 60% for PVDF and 50% for P(VDF-TrFE), collector speed of 300 rpm, a distance of 10 cm.

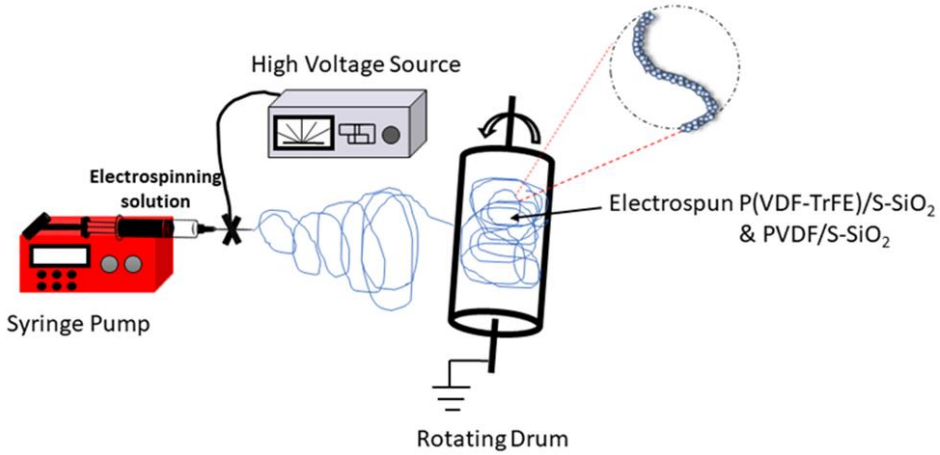

Figure 14. Schematic of electrospinning set-up [93]

Preparation of hybrid membranes

The prepared electrospun mats were densified by hot-pressing at 110 °C and under 2000 psi, followed by Nafion® impregnation which was done by placing the membrane on a glass surface already brushed with 3 mL of 5wt% Nafion® solution. Then the upper surface of the membrane was brushed again with another 3 mL of the 5wt% Nafion® solution. The obtained membrane was left to dry at 60 °C for 24 h. After repeating the procedure twice for each sample to achieve a homogenous surface coverage. Final compact membrane annealed in a vacuum oven for 2 h at 100 °C.

Characterization of SiO_2 and S-SiO_2

FTIR spectroscopy measurements were carried out using Bruker Equinox 55 equipment in the range of 500 to 4000 cm^{-1}. SPECS XP Flexmod (Germany) model XPS equipped with a PHOIBOS hemispherical energy analyzer, and a monochromatic Al Kα X-ray excitation ($h\nu = 15\,kV,\ 400\,W$) was used. The morphology of synthesized SiO_2 particles was investigated by a JEOL JEM 2000FX TEM model transmission electron microscope (TEM).

Characterization of hybrid electrospun membranes

The membranes were immersed in DI water for 24 hours at room temperature, dried in an oven and weighed for water uptake measurements [94].

Eq. **(10)** was used to calculate the water uptake:

$$\text{water uptake } \% = (M_W - M_D)/M_D \times 100 \quad \textbf{(10)}$$

in which M_W and M_D stand for the wet and dry membrane's mass, respectively. The mechanical properties of the resultant membranes were measured using a Universal Tensile Machine (Zwick/Roell Z100). The tensile tests were performed at room temperature and according to ASTM D882 standard test method conditions, elongation rate was set to 100 mm/min [95]. The average of three specimens for each membrane was used. The morphology of the electrospun mats was investigated via scanning electron microscope (SEM) using Supra 35VP Leo, Germany equipment.

The ionic conductivities of the membranes were measured via an in-plane 4-probe conductivity method where BekkTech conductivity cell equipped with Gamry Reference 3000 Potentiostat/Galvanostat device (Gamry Instruments, USA) was used. A sample of 2 cm×2.5 cm was placed in a cell and the test was performed at various relative humidity values (RH%) at 80 °C. The following equation was used to calculate the ionic conductivity of the samples:

$$\sigma = \frac{L}{R\,T} \quad \textbf{(11)}$$

by which, R (Ω) stands for the resistance of the sample measured via electrochemical impedance spectroscopy (EIS), w is the width (cm) of the sample, t is the sample thickness (cm), and L is the distance between inner electrodes of the cell (0.425 cm).

1.9.4 Results and Discussions

The morphology and particle size of SiO_2 particles were investigated by TEM, as depicted in **Figure 15**, almost spherical SiO_2 particles with relatively homogeneous particle size distribution around 50 nm (specific surface area of SiO_2 powder is 1.031 m^2/g) were achieved.

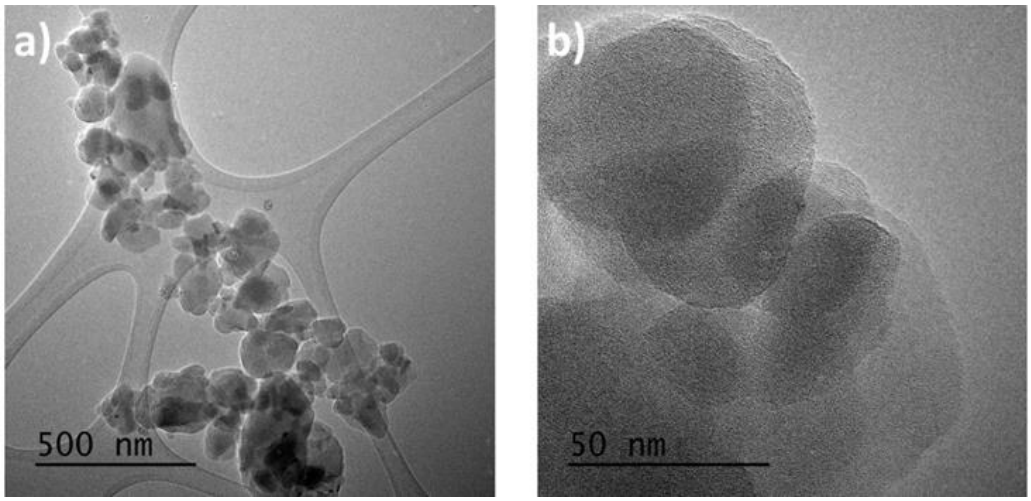

Figure 15. TEM image of SiO_2 particles at a) low, b) high magnification [93]

The chemical composition of S-SiO_2 was further investigated with x-ray photoelectron spectroscopy (XPS) (**Figure 16**). Peaks at 535.0, 284.0, 103.5 eV were attributed to silica's Si2p, C1s and O1s, respectively. Overlapping Si2s and S2p peaks were observed. Therefore, deconvolution of the related peaks and calculation were performed to prove the incorporation of sulfone groups as mentioned in the literature [96]. The peaks at 154.1 to156.6 and 166.6 to 172.1 eV are shown in **Figure 16a** and **Figure 16b** represent the Si2s and S2p peaks. The existence of carbon C1s is probably due to residual carbon after the calcination process which has a higher intensity after the sulfonation. Integrating the area under the graph shows an increase in O/Si ratio for S-SiO_2 sample in comparison with the silica sample indicating successful sulfonation of Si particles and the incorporation of $–SO_3$ functional groups [91].

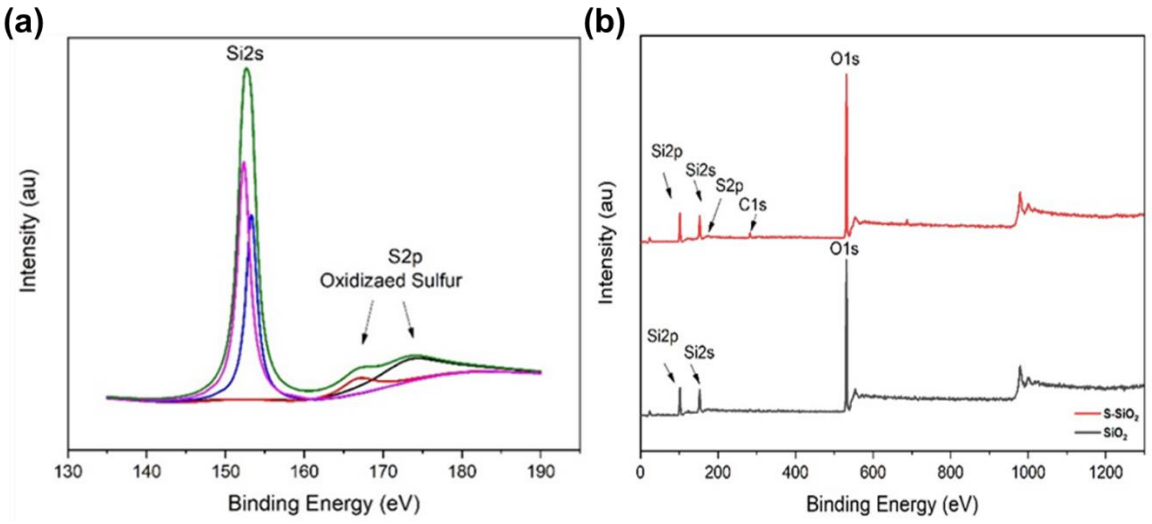

Figure 16. XPS of SiO_2 and S-SiO_2 [93]

Figure 17 shows the FTIR spectra of SiO_2 NPs and S-SiO_2 NP. The characteristic peaks at 3430 and 1632 cm^{-1} were attributed to the Si-OH band and absorbed water molecules, respectively [91], [97]. The bands at 1100 and 800 cm^{-1} can be assigned to the symmetric and asymmetric vibrations of Si-O-Si bonds. However, after sulfonation the existence of broad peaks related to Si-O-Si vibrations in the range of 1000 to 1250 cm^{-1} overlaps with characteristic peaks for the $–SO_3$ band at 1060, 1168 and 1210 cm^{-1} [97]. Due to this fact, no significant change was observed after sulfonation.

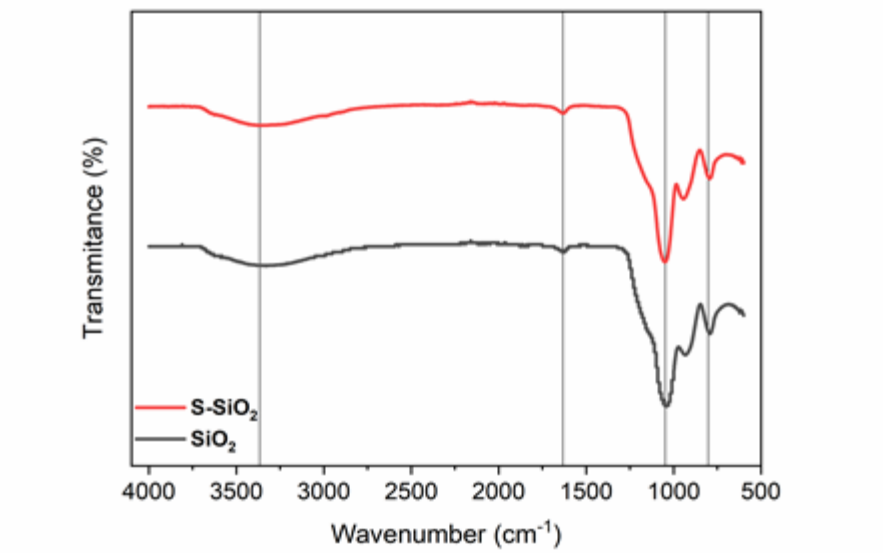

Figure 17. FTIR spectra of the SiO_2 and S-SiO_2 [93]

Figure 18 and **Figure 19** show the SEM images and average fiber diameter diagrams of P/S-SiO_2 and T/S-SiO_2 mats with various polymer/S-SiO_2 weight ratios. Almost bead-free, uniform, and nano-sized fiber mats from both carrier polymers were achieved. It needs to be noted that not all polymer/S-SiO_2 mixture produce nanofibers and significant effort must be made for the electrospinning polymer/particle mixtures. For instance, the electrospinning solution with 80% S-SiO_2 wt.% ratio or lower total solid ratio produced electrosprayed droplets due to the inadequate number of polymer chain entanglements. Furthermore, electrospun mats from P(VDF-TrFE) carrier polymer have lower fiber diameter (average fiber diameter in range of 210-330 nm) (Fig. 6g, h, i) compared to fibers mats prepared using P(VDF) carrier polymer (average fiber diameter of 580-610 nm) (Fig. 5g, h, i).

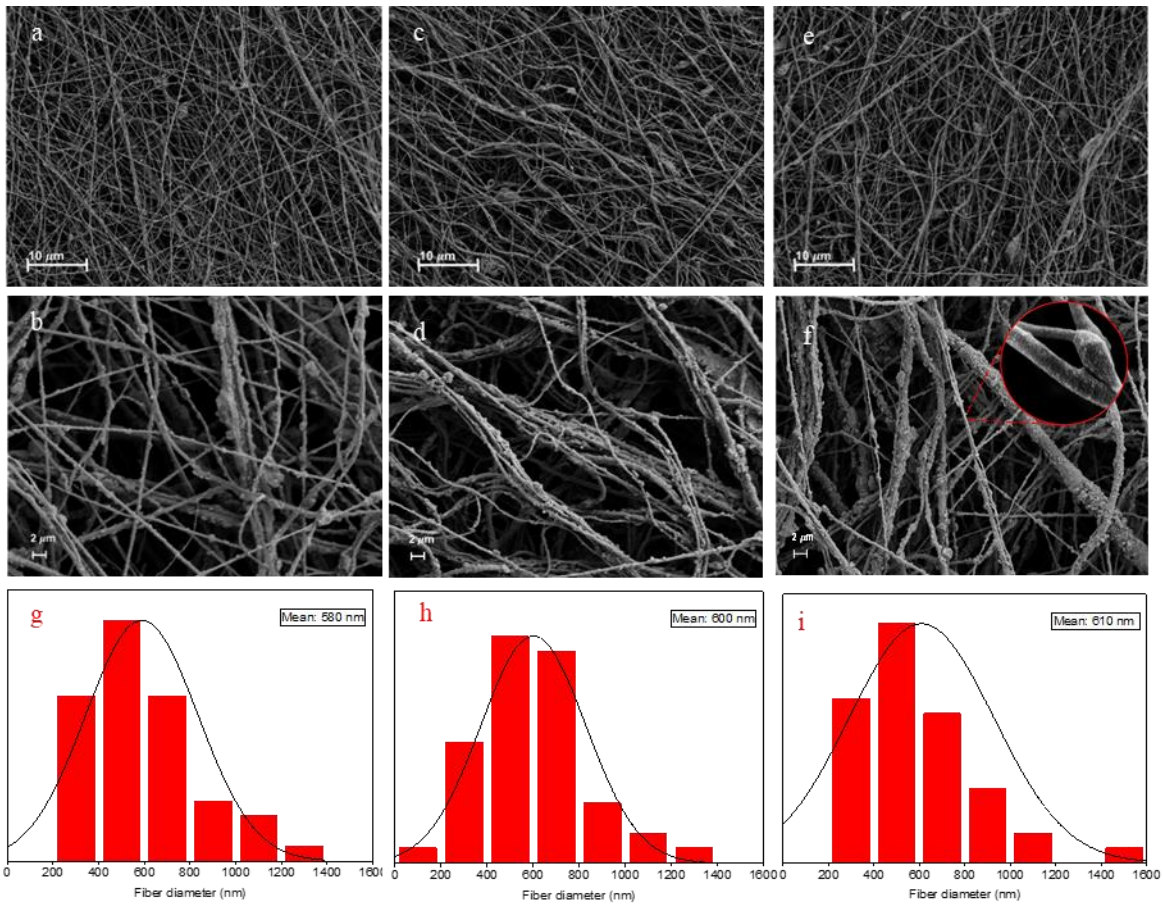

Figure 18. SEM micrographs of electrospun PVDF/S-SiO_2 mats and corresponding size distribution histograms (a, b, g) P/S-SiO_2-50, (c, d, h) P/S-SiO_2-60, (e, f, i) P/S-SiO_2-70 [93]

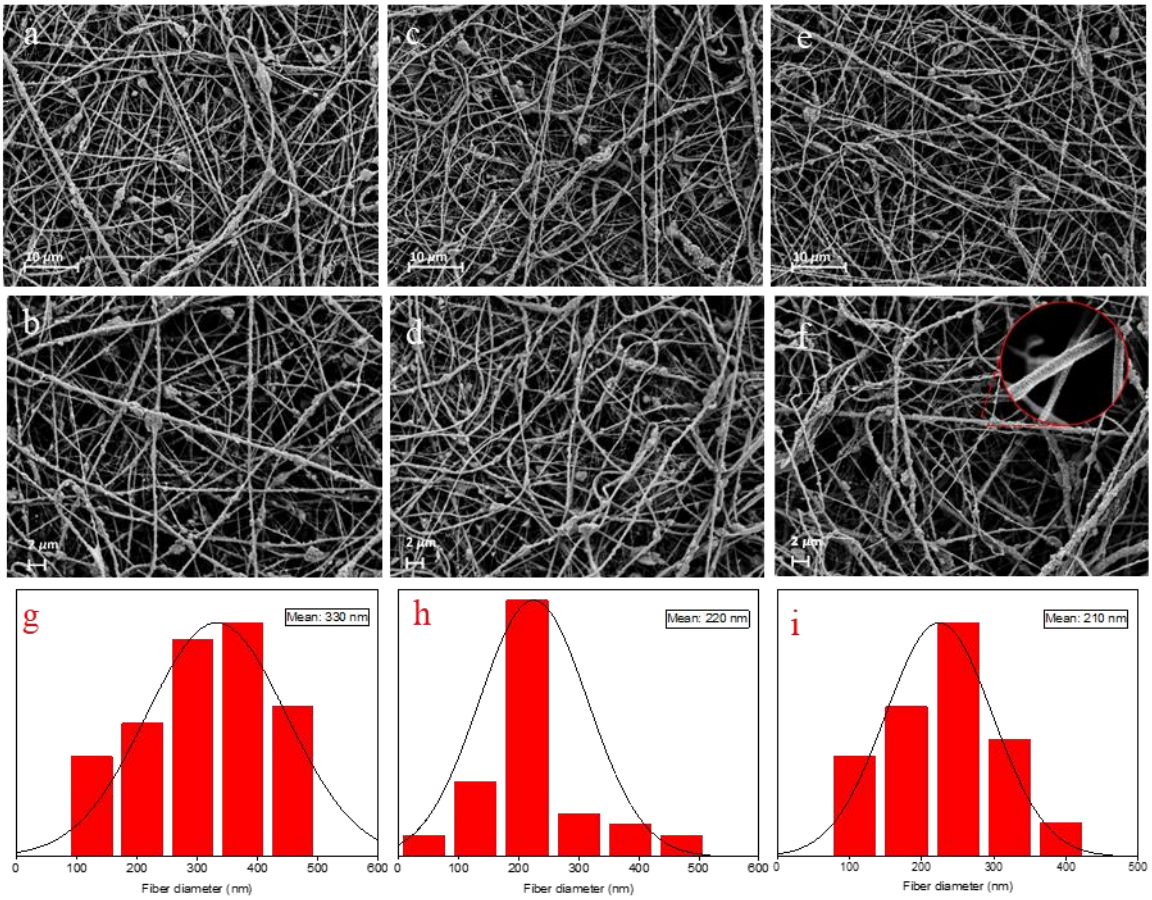

Figure 19. SEM micrographs of electrospun P(VDF-TrFE)/S-SiO_2 mats and corresponding size distribution histograms (a, b, g) for T/S-SiO_2-50, (c, d, h) T/S-SiO_2-60, (e, f, i) T/S-SiO_2-70 [93]

The membranes with the same areal dimensions (2 cm x 2.5 cm) were used to calculate water uptake measurements. The water uptakes (%) given in **Table 7** indicate a similar increasing trend of water uptake by the enhancement of S-SiO2/carrier polymer wt% that verifies the existence of more hydrophilic S-SiO_2 NPs. The PVDF based membranes possessed the water uptake values in the range of 26-31% which are comparable with previous work using the same polymer [30]. Furthermore, the higher water uptake of T/ S-SiO_2 membranes than that of P/ S-SiO_2 and Nafion® 212 (24%) [70], leads to providing a higher ionic conductivity due to the presence of more connected pathway for protons.

Table 7. Characteristics of the membranes

Sample	P/S-SiO_2-50	P/S-SiO_2-60	P/S-SiO_2-70	T/S-SiO_2-50	T/S-SiO_2-60	P/S-SiO_2-70
Thickness (µm)	102	98	100	110	112	108
Proton conductivity (mS/cm) at *RT	32.7	39.2	57.4	42.5	55.8	69.2
Water uptake (%)	26	28	31	30	31	34
Young's modulus (MPa)	280	148	126	250	156	135

* RT: Room temperature

The proton conductivities of the membranes were measured at two different conditions: firstly, in the water at room temperature (RT) as reported in Error! Reference source not f ound.**,** and then at various humidity values (40, 60, 80, and 100 %) and the corresponding temperatures as shown in **Figure 20**. In the first set of measurements, the highest ionic conductivity of 69 mS/cm was obtained for T/S-SiO_2-70 sample where it is comparable with ionic conductivity of the Nafion® membrane prepared by solution casting (95 mS/cm) at same condition [25], [74]. Moreover, all the prepared membranes showed higher ionic conductivity (Error! Reference source not found.**)** than that of reported cast Nafion® /PVDF composite membrane (containing 80 wt% Nafion®) scoring 12 mS/cm in previous studies [98]. When the ionic conductivities of the membranes with both carrier polymers are compared, an increasing trend by enhancement of the weight ratio of S-SiO_2 NPs to carrier polymer, which was expected since the presence of the higher amount of S-SiO_2 leads to provide further proton-conducting agents in the medium. However, T/S-SiO_2 membranes showed superior ionic conductivity at all humidity levels than those of the P/S-SiO_2 membranes. This trend in proton conductivity can be attributed to higher hydrophobicity of P(VDF-TrFE) polymer and thinner fiber diameter (200 nm) than PVDF (600 nm) [99]. Furthermore, the proton conductivity does not differ significantly between 80% and 100% RH, and 40% and 60% RH for both PVDF and P(VDF-TrFE) carrier included membranes. However, the dramatic change in proton conductivity between 60% and 80% RH was observed.

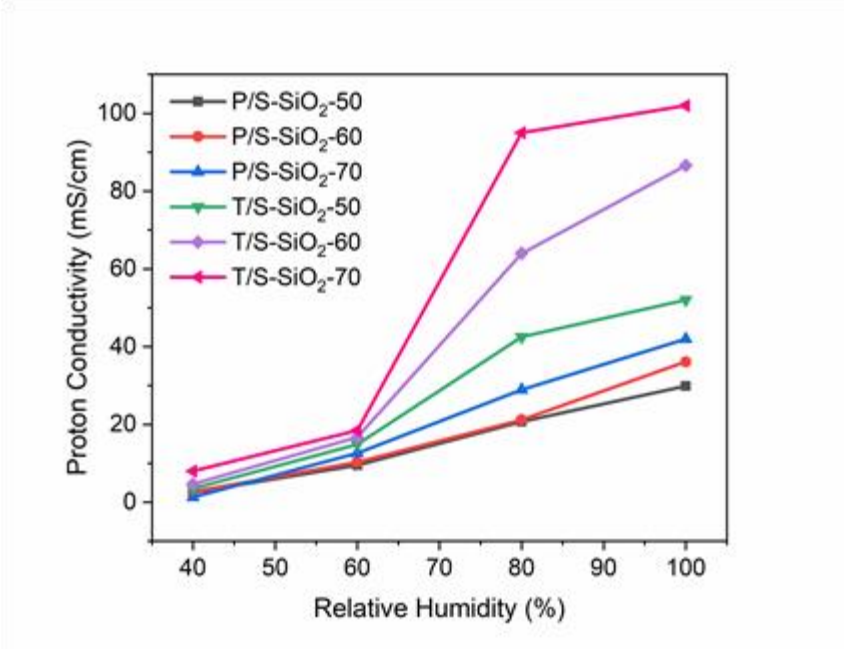

Figure 20. Proton conductivity at various RH (%) and temperatures for the membranes [93]

The mechanical properties of the P/S-SiO_2 and T/S-SiO_2 membranes were investigated via stress-strain measurements and summarized in Table 2. The obtained stiffness values are comparable with that of Nafion® 212 but the elongation values are relatively lower [94]. The stress-strain curves of the samples are shown in **Figure 21** and were used to calculate their Young's modulus [98]. T/S-SiO_2 membranes exhibit higher tensile strength yet slightly lower elongation than P/S-SiO_2 membranes due to their smaller average fiber diameter. Increasing the S-SiO_2 NPs loading in the case of both carrier polymers not only adversely affected their stiffness but also decreased the elongation of samples by diminishing the fiber content in membrane structure.

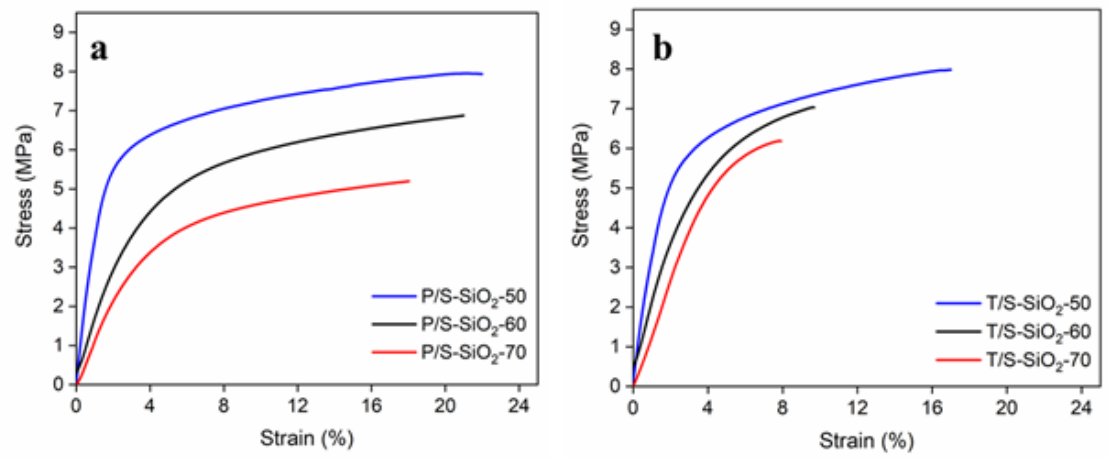

Figure 21. Stress-strain curves for a) P/S-SiO_2, b) T/S-SiO_2 [93]

1.10 P(VDF-TrFE) Reinforced Composite Membranes Fabricated via Sol-gel and Dual- Fiber Electrospinning for Low Relative Humidity Operation of PEM Fuel Cells

1.10.1 Objective

In the previous section of this study the effect of carrier polymer type and various polymer to S-SiO_2 ratios on the obtained properties of the electrospun P(VDF-TrFE)/S-SiO_2 and PVDF/S-SiO_2 membranes were studied. Despite the promising proton conductivity results that was obtained for resultant membranes, S-SiO_2 nanoparticle preparation procedure was time-consuming and complicated. In addition, the highly homogenous and stable dispersion of these particles in the electrospinning solution was difficult during this process. Therefore, in this section a single step dual-electrospinning and sol-gel method were used for preparation of high-performance sulfonated silica/Nafion®-based composite membranes for low humidity operation conditions. The effect of reinforcing polymer type (P(VDF-TrFE) and PVDF) as well as polymer/ Nafion® ratio on final characteristics on theses membranes such mechanical properties, proton conductivity and fuel cell performance were investigated.

1.10.2 Introduction

Climate change is the most urgent environmental crisis that can be solved or at least slowed down by switching from fossil fuels to renewable energy as the main energy source [13], [100]. Switching to renewable energy production and more prevalent usage of H_2 as the energy reinforcing would alleviate the greenhouse effect of excessive carbon dioxide in the atmosphere that is emitted mainly by fossil fuels. One way to use H_2 as the energy carrier is the fuel cell technologies that are energy conversion devices in which, generally, H_2 and air (or O_2) are used as fuels to provide cleaner and greener electricity and can replace fossil fuel engines especially for mobile vehicle applications. Proton exchange membrane (PEM) fuel cells are shining through the other energy conversion devices and other fuel cell designs by their high efficiency, mild operating temperatures, and fast start-up [4].

The Nafion®-based membranes, or similar sulfonated tetrafluoroethylene-based fluoropolymer-copolymers, have enabled the PEM fuel cells to compete with other fuel cell technologies in the commercialization process thanks to their high proton conductivity as well as desirable chemical and mechanical properties [101]. Although the development of Nafion® was a significant breakthrough in the field of the PEM fuel cells, it possesses some shortcomings such as insufficient proton conductivity at low humidity and high additional cost to the already expensive Pt-based electrodes existing in these systems [101].

The water management is another crucial factor in the PEM fuel cells since excess water leads to the blockage of species' transport pathways; on the other hand, water deficiency results in insufficient moisturizing of the membrane causing decreased proton conductivity and irreversible membrane degradation issues [93], [102]. Due to this fact, developing new membrane material is necessary to achieve enhanced proton conductivity and fuel cell performance in partially humid conditions [103].

Recently, to overcome the drawbacks of the widely used homopolymer-based membranes, researchers have focused on the incorporation of hygroscopic inorganic fillers such as silica [93], [104], [105], ZrO_2 [54], [106], TiO_2 [107], heteropolyacid [108], [109] or some combinations of them [58]. Amjadi et al. showed that TiO_2 incorporation to Nafion® increased the water uptake by 51%, which is close to the commercially available Nafion®, and enhanced the cell performance even with a diminished proton conductivity [54]. Similarly, Jiang et al. reported higher water uptake and better cell performance with silica incorporation in spite of a decreased conductivity[60]. Alternatively, some researchers have functionalized the surface of fillers to get even more water uptake [110]. For example, perfluorosulfonic acid functionalized-silica incorporation increased the conductivity of Nafion® membranes more than twice at 120 ^oC with an improved water uptake [90].

Incorporation of hygroscopic inorganic fillers is generally done by a couple of methods: impregnating fine powder of the filler into the pores of the solid Nafion® membrane, and filling a precursor solution, then converting them into the desired additives within the membrane by hydrolyzing. These methods, however, lead to inhomogeneous filler distributions, sedimentation of heavier fillers, and thus the inefficient use of fillers and the other parts of the membrane, which results in a suboptimal cell performance [90].

In recent years the sol-gel technique has been used as a cheap, rapid, and versatile approach for preparation of S-SiO_2 for the PEM fuel cell application by many groups to use these fillers more efficiently [111]. This technique provides a rapid way to incorporate the surface-functionalized silica fillers with a more homogenous distribution and minimized agglomeration [112]. For instance, G. Liu et al. used the sol-gel method for surface functionalization of PVDF electrospun mats by S-SiO_2 to obtain a proton conducting membrane [110]. Moreover, some groups have used the electrospinning and in-situ sol-gel methods for fabrication of hybrid organic/inorganic membranes which gives rise to obtaining a very homogeneous distribution of the hydrophilic and hydrophobic constituents in the entire membrane [104], [113].

In order to prepare the membranes for PEM fuel cells, electrospinning has emerged as a versatile approach for fabrication of nanoscale fibrous materials [70], [114], [115]. Through the electrospinning process, polymer fibers drawn from a polymer solution in a spinneret tip via an applied high voltage, can create mechanically robust and phase-separated fibrous architectures [115]. Using this technique not only offers fabrication of porous electrospun mats with desired characteristics like high surface area, tunable fiber, and porosity size, but also it gives the opportunity to fine-tune the chemical composition of the final product [70]. For instance, Park et al. claimed that the electrospun Nafion®/PVDF-based membranes showed superior water uptake, ion exchange capacity (IEC) and proton conductivity compared to the solution-casted membranes with the same composition [116].

Besides the conventional electrospinning method, a dual fiber (multi-nozzle) electrospinning method in which two different polymer solutions are concurrently spun onto a collector can be used to obtain a mixed fiber mat. Once the fibers from the two nozzles reach the collector, they become entangled [117]. Generally, an ionomer as an ion exchange component and a mechanically strong inert polymer as reinforcing component are selected for dual-fiber electrospinning. Subsequent hot pressing of the dual electrospun membrane eliminates the pores while preserving the two-component structure. Dual-fiber electrospinning provides a way to control the final membrane's various properties by adjusting the volume ratios of the polymer solutions [70]. Despite the above-mentioned advantages, the scientific literature for dual-fiber electrospinning is limited. Ballengee et al. prepared two dual-fiber membrane structures: a Nafion® reinforced polyphenylsulfone fiber system and a polyphenylsulfone reinforced Nafion® fiber system. They reported that the conductivity linearly increased with Nafion® volume ratio, and the dual fiber-based membranes showed better mechanical properties [98]. Another way to prepare dual fiber-based membrane is using polymers with the same backbone and different functional groups. This way allows one to control the overall functionalization, swelling degree, and related mechanical properties of the final membrane. Oroujzadeh et al. used sulfonated and non-sulfonated poly(ether ketone) to create hydrophobic/hydrophilic regions and compared them with membranes prepared by the conventional solution-casted method. They showed that dual fiber-based membranes are more thermally stable even at high temperatures and better in terms of conductivity even with the even with the same IECs [118].

Using dual-fiber electrospinning, Dos Santos et al. created composite membranes for PEM fuel cells by incorporating sulfonated-silica into the Nafion® and PVDF fibrous mats. The components were switched to create two different structures, one serving as the matrix and the other as the reinforcing fibrous network. The authors concluded that incorporation of sulfonated silica into a perfluorosulfonic acid matrix (PFSA) performed better than those incorporated into PVDF fibers [104]. Thanks to exercising greater control over membrane properties with a simple preparation procedure, the dual fiber electrospinning method was selected for this work.

In our previous study, the sulfonated-silica nanoparticles were synthesized through a multi-step hydrothermal method, and electrospun PVDF/S-SiO_2 or P(VDF-TrFE)/S-SiO_2 hybrid membranes were fabricated via a single electrospinning process. The resultant membranes showed promising ionic conductivity at low humidity levels due to the incorporation of hygroscopic sulfonated silica nanoparticles [93]. However, the time-consuming multi-step nanoparticle synthesis and difficulties in keeping homogeneous dispersion of nanoparticles within the solution during the several hours of electrospinning were of the major drawbacks.

Therefore, in the present study, we synthesized a chemically stable S-SiO_2 precursor via a single step sol-gel method. Then, the dual electrospinning method was used to prepare a mix-fiber membrane. One of the fibers is drawn from a Nafion®/PVDF or Nafion®/P(VDF-TrFE) solution and the other fiber is drawn from S-SiO_2/polyethylene oxide (PEO) precursor solution. The combination of dual-fiber electrospinning and sol-gel synthesis provides some advantages such as scalability, simplicity and cost effectiveness of the process. To our best knowledge, P(VDF-TrFE) as the reinforcing polymer and 3-(Trihydroxysilyl)-1-propanesulfonic acid (TPS) as the precursor for sulfonation of silica were used for the first time for the PEM fuel cells in the literature.

We aimed to investigate the impact of the reinforcing polymer selection and ratio of reinforcing polymer to Nafion® on the final characteristics of the obtained membranes. For this purpose, microstructure, chemical composition, mechanical properties, water uptake, ion exchange capacity (IEC), ionic conductivity and fuel cell performance were characterized and discussed. Although Young's moduli of PVDF-based membranes (324 MPa) are higher compared to the P(VDF-TrFE)-based membranes (228 MPa), the later showed greater proton conductivity (132 mS/cm at 80°C, 100% RH) and fuel cell performance , particularly at low

relative humidity conditions. Furthermore, P(VDF-TrFE)-based membranes provided a maximum power density of 344 mW/cm^2 which is almost 2-times higher than that of PVDF-based membranes.

1.10.3 Experimental

Materials

Polyvinylidene fluoride (PVDF) (SoleF®, M_w=380,000 g/mol) and polyvinylidene fluoride-co-trifluoroethylene 70/30 (P(VDF-TrFE)) powders were acquired from Solvay, PolyK technologies and Sigma-Aldrich respectively. 3-(Trihydroxysilyl) -1-propanesulfonic acid, 30–35 wt% in water (TPS) was purchased from abcr Gute Chemie. PEO (M_w=1,000,000 g/mol), Tetraethyl orthosilicate (TEOS, ≥ 99%), N,N-dimethylacetamide (DMAc, 99%), Tetrahydrofuran (THF), N,N-dimethylformamide (DMF, 99%), Acetone, hydrochloric acid (HCl, 37%), sulfuric acid (H_2SO_4, 95-97%) and 20 wt % Nafion® solution all were purchased from Sigma-Aldrich. The precursors used in sol-gel preparation, and final sulfonated silica chemical structure are shown in **Figure 22**.

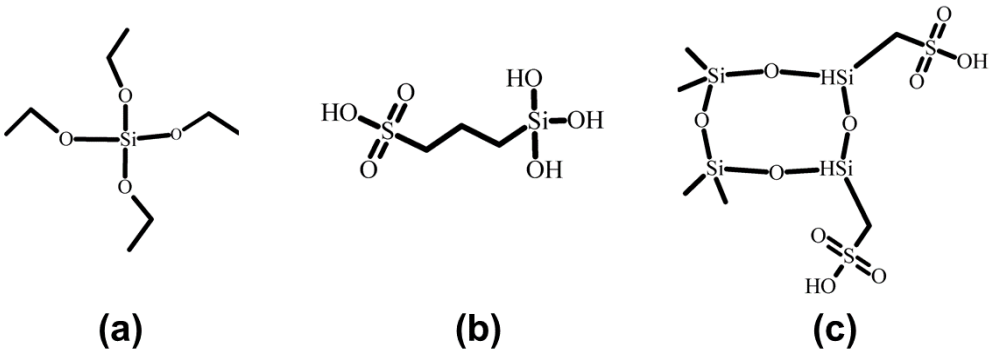

Figure 22. Chemical structures of sulfonated silica (S-SiO_2) precursors: (a) tetraethyl orthosilicate (TEOS), (b) 3-(Trihydroxysilyl)-1-propanesulfonic acid (TPS), and product of sol-gel reaction (c) sulfonated silica network.

Preparation of sulfonated silica via sol-gel method

TEOS as a silica precursor was added to the mixture of 50 µL of 0.2M HCl, DMAC and THF mixture and mixed on a magnet stirrer for 1 hour. The PEO solution of 10 wt% concentration was prepared separately and mixed with TEOS mixture for 2 hours at 70 °C. Then TPS was added to the PEO/TEOS solution and reaction continued for 1 hour at the same temperature. For preparation of the PVDF/Nafion® or P(VDF-TrFE)/Nafion® solution, a mixture of DMAc/THF solvents with 7/3 weight ratio was added to the PVDF or P(VDF-TrFE) powders and mixed overnight. 20 wt% Nafion® solution was dried and a mixture of DMF/Acetone with a weight ratio of 2/1 was added to the dried Nafion®, mixed overnight to become a homogeneous solution. Then the prepared Nafion® solution was added to PVDF or P(VDF-TrFE) solutions and stirred for 3 hours prior to electrospinning. Finally, PVDF-Nafion® or P(VDF-TrFE)-Nafion® as the right-side solution and PEO/S-SiO_2 as the left side solution were loaded into the two individual 5 mL syringes.

Preparation of solutions for electrospinning

Dual electrospinning method was used for fabrication of electrospun mats with two different solutions using a homemade electrospinning chamber with controllable temperature and humidity: 1) PVDF-Nafion® or P(VDF-TrFE)-Nafion® mixture from one side, 2) PEO/S-SiO_2 solution from the other side. The distance between the tips of the needles and rotating drum was kept 10 cm and relative humidity of the system was set to 60%. Applied voltage and flow rates for the right-side solution were set to 20 kV, 0.6 mL/h, and left-hand side solution were set to 15 kV, 0.25 mL/h, respectively. The electrospinning solution compositions are listed in **Table 8**.

Table 8. Materials and composition of solutions

Sample composition	Nafion® (wt.%)	TEOS-TPS/PEO (wt.%)	Reinforcing Polymer (wt.%)
PN40 (PVDF-Nafion®/S-SiO_2)	40	28/2	30
TN40 (P(VDF-TrFE)-Nafion®/S-SiO_2)	40	28/2	30
PN50 (PVDF-Nafion®/S-SiO_2)	50	28/2	20
TN50 (P(VDF-TrFE)-Nafion®/S-SiO_2)	50	28/2	20
PN60 (PVDF-Nafion®/S-SiO_2)	60	28/2	10
TN60 (P(VDF-TrFE)-Nafion®/S-SiO_2)	60	28/2	10

Preparation of Compact Membranes

The prepared mats were left to dry at 60°C overnight, then PVDF-Nafion®/S-SiO_2 (PN50, PN60) and P(VDF-TrFE)-Nafion®/S-SiO_2 (TN50, TN60) mats were hot-pressed at 140°C and 130°C respectively, both at 8 MPa for 10 min. Afterwards the condensed PN50, PN60 samples were annealed at 200°C and TN50, TN60 at 150°C for 30 min. Followed by boiling in 1M H_2SO_4 at 80°C for reactivation of sulfonic acid groups for 1 hour and then in DI water at 80°C for an additional hour. The prepared composite membranes were dried and kept in plastic bags prior to characterizations. **Figure 23** shows the electrospun membrane preparation steps; including solution preparation, dual fiber electrospinning, obtained fiber mat, and final compact membrane, respectively.

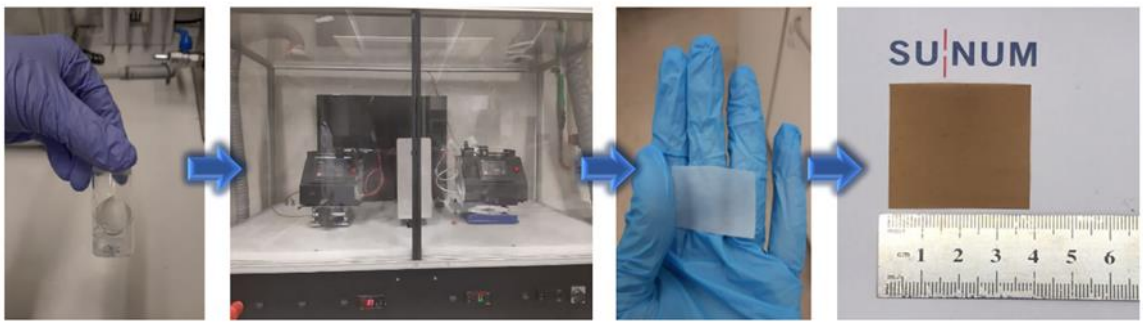

Figure 23. Electrospinning set-up and membrane preparation steps.

Characterization of Electrospun Mats and Membranes

SEM images were used to track the morphology of synthesized membranes in the sense of homogeneity of fibrous structure and fibers diameters before hot-pressing and further processing as well as their compactness after hot pressing. FTIR spectroscopy was performed for detection of chemical composition by Bruker Equinox 55 equipment in a range of 500 to 4000 cm^{-1}.

Static water contact angle method was used to measure the wettability of the membranes at room temperature. For this purpose, dry membranes were placed on the holder and a drop of water was used for these measurements.

Thermogravimetric analysis (TGA) was performed using Shimadzu DTG-60 under N_2 atmosphere using 10°C/min up heating rate up to 850°C.

Using **Eq. (10)**, the gravimetric water up-take was measured; therefore, the membranes were immersed in DI water for 24h, then they were weighed after removing the excess water from their surface. Afterwards they weighed after drying overnight at 60 °C.

The ion exchange capacity (IEC) of the membranes were measured via titration of dried membranes and using the **Eq. (12)**. The membranes were soaked in 1 M HCl solution 24 hours and then rinsed thoroughly with DI water to remove the excess HCl. Afterwards, the membranes were soaked in 2 M NaCl overnight to convert H^+ to Na^+. The soaked solution was titrated using 0.1 M NaOH after removing the membrane [119]. The following equation was used to calculate the IEC:

$$IEC\ [mmol/g] = (V_{NaOH} \times C_{NaOH}) / M_D \quad \textbf{(12)}$$

where V_{NaOH} [mL] stands for volume of NaOH used for neutralization of the soaked solution, C_{NaOH} [M] is the concentration of NaOH solution and M_D is the dry mass of the membrane.

Proton conductivity of membranes were measured at room temperature in water to provide fully humidified condition as well as at 80 °C applying various relative humidities (40, 60, 80 and 100%) using in-plane 4-point probe method by BekkTech conductivity cell equipped with Gamry Reference 3000 Potentiostat/Galvanostat device (Gamry Instruments, USA). For this pupose samples of $2\,cm \times 2.5\,cm$ were placed in the cell. For room temperature measurments samples were immersed in DI water overnight prior to test. **Eq. (11)** was used to calculate the conductivity.

The stress-strain mechanical tests of the obtained membranes were carried out using Universal Tensile Machine (Zwick/Roell Z100) at room temperature with a static 200N load cell. ASTM D882 standard test method was used to measure the tensile properties. Elongation rate was set to 100 mm/min.

Fuel Cell Testing

The dual fiber-based membranes which have promising ionic conductivity, water up-take, IEC and mechanical strength, were selected, and the performance tests were conducted in Scribner 850e fuel cell test station. The membrane-electrode-assemblies (MEAs) were prepared before starting the tests using fabricated fiber-based membranes and sprayed electrodes with 0.3 g/cm^2 catalyst loading. The catalyst ink solution was prepared by mixing 30 wt% Pt/C with 20 wt% Nafion® and isopropyl alcohol as solvent. Then the catalyst ink was ultrasonicated for 1 hour and followed by stirring for 2 hours. Afterwards, obtained ink was sprayed on the surface of the Sigracet 39BC gas diffusion layers from the Fuel Cell Store. Prior to fuel cell tests, cells connected to potentiostat/galvanostat (Reference 3000, Gamry Instruments) to measure the hydrogen crossover by means of linear sweep voltammetry (LSV) technique. LSV measurements were conducted using H_2 gas with anode (reference electrode), on the opposite side N_2 gas fed to the cathode (working electrode). The H_2 and N_2 flow rate was kept 1:4 ratio during LSV measurements. Furthermore, the fuel cell performance tests were performed at varying humidity levels (in the 60-100% RH) at 80 °C applying 25 psi back pressure.

1.10.4 Results and Discussions

SEM

The morphology of the obtained membranes was investigated via scanning electron microscopy. For optimization of hot-press procedure various forces was applied to find the sufficient force that need to be applied for pore free membranes as shown in **Figure 24.**

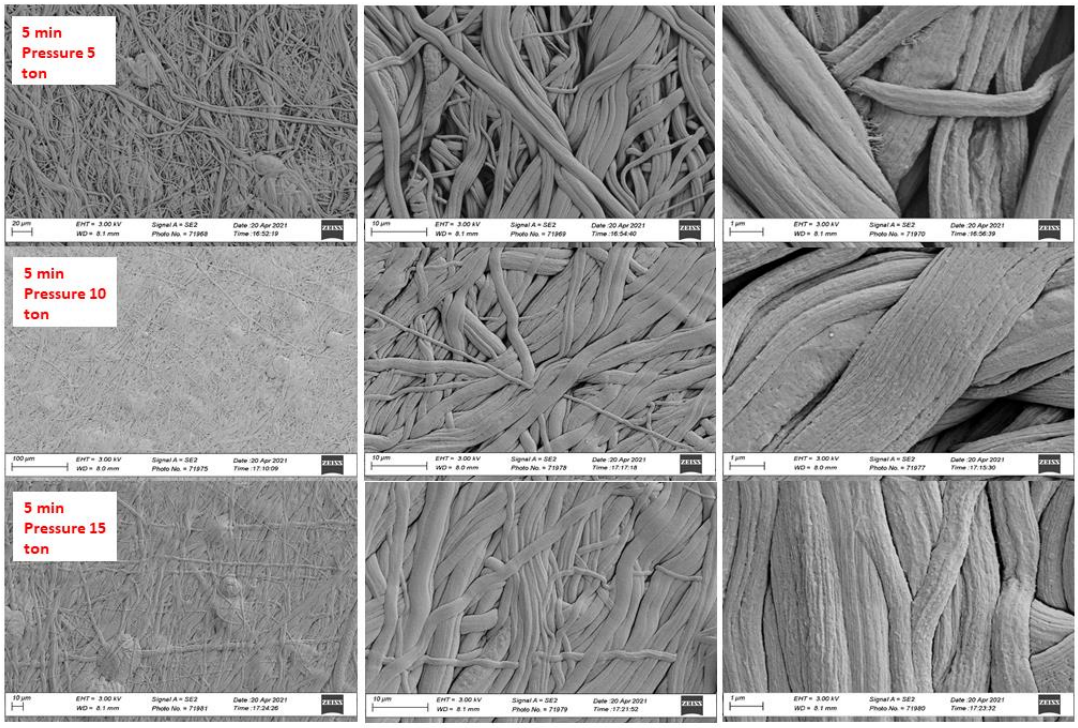

Figure 24. Effect of various applied pressures on compactness of electrospun mats.

A homogeneous and bead-free fibrous structure for all prepared fibrous mats were achieved as indicated in **Figure 25**a-c-e-g for PN50, PN60, TN50 and TN60 samples respectively. After hot-pressing, a compact, smooth, and defect free top surface was achieved (**Figure 25**b-d-f-h stands for TN50, TN60, PN50 and PN60 respectively). It is worth mentioning that to obtain such homogeneous fibrous mats, the reinforcing polymer to Nafion® ratio needs to be optimized properly [97]. As depicted in the SEM micrographs of PEO/S-SiO_2, fibers are equivalently spread in either the PVDF-Nafion® or P(VDF-TrFE)-Nafion® fibrous web. In contrast to the solution cast membranes, no macroscopic phase separation or agglomeration was observed between the two hydrophobic and hydrophilic constituents in the dual electrospun membranes [120]. Moreover, the fibers' trace under the top surface shows the almost defect-free and dense hot-pressed mats. These traces could be attributed to the presence of PVDF or P(VDF-TrFE) reinforcing fibers embedded in the softened Nafion® matrix after hot-pressing and annealing without significant phase-separation.

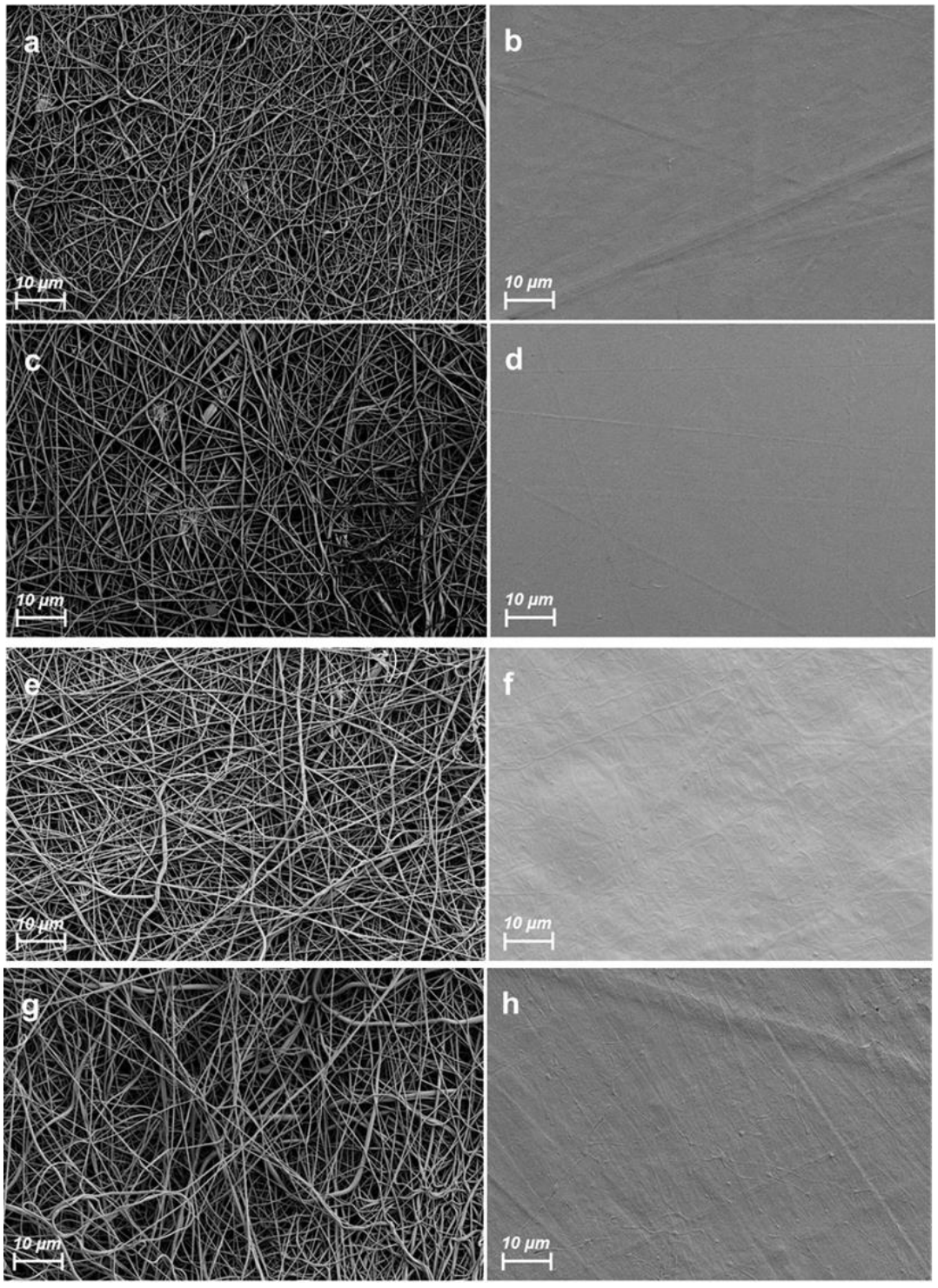

Figure 25. SEM micrographs of electrospun mats before and after hot-pressing a,b) TN60, c,d) TN50, e,f) PN60 and g,h) PN50.

FTIR

FTIR was used to determine the chemical composition of the membranes. **Figure 26,** a and b compare the FTIR spectra of pristine PVDF and PVDF-TrFE powders with the related PN50, P60, TN50, and TN60 composite membranes. Compared to the pristine powders, composite membranes showed lower peak intensities. A new broad peak was observed in the range of 3500 to 3300 cm^{-1} for all composite membranes corresponding to the stretching of the -OH band [110], [111]. An additional peak in the range of 1780 to 1630 cm^{-1} can be ascribed to H_3O^+ [121]. The absorption of peaks in the range of 1250 cm^{-1} to 1000 cm^{-1} were associated with the asymmetric vibration of Si-O-Si bonds, and less intense peaks around 800 cm^{-1} were related to the Si-O-Si symmetric stretching [111]. The characteristic peaks at 1050 and 1200 cm^{-1} in spectra of the composite membranes associated with the $-SO_3H$ bond overlap with Si-O-Si band at the same wavelength range [122], [123]. Furthermore, the peaks at 1200 cm^{-1} and 1140 cm^{-1} correspond to the symmetric and asymmetric vibrations of $-CF_2$ bonds in Nafion®, respectively [124]**.**

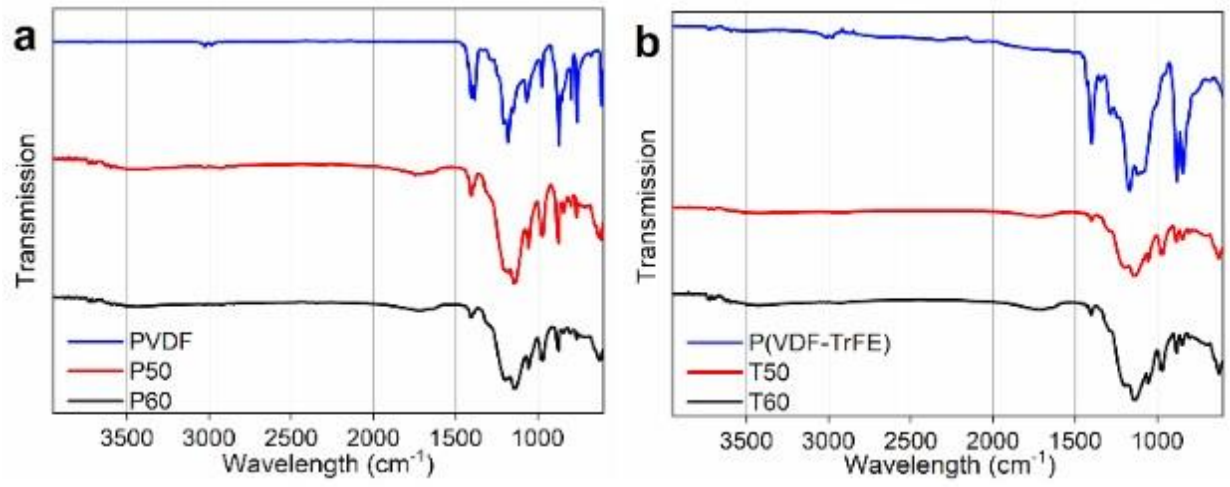

Figure 26. FTIR spectra of a) PVDF, b) P(VDF-TrFE) fiber mats and fabricated dual-fiber based membranes; PN50, PN60, TN50 and TN60.

Thermal Gravimetric Analysis

TGA thermograms of the composite PN60 and TN60 membranes in comparison with the pristine PVDF and P(VDF-TrFE) are shown in **Figure 27a** and **b** respectively. The pristine PVDF and P(VDF-TrFE) showed almost zero and single step mass loss up to 450 °C that indicates their highly hydrophobic nature of these polymers as well as their high thermal stability. A rapid weight loss at temperatures over 450 °C was observed for both pristine polymers is an indication of their thermal decomposition [125]. TN60 and PN60 were exhibited similar thermal three step profiles, with thermal stability up to around 200 °C. The initial small mass loss at below 200 °C temperatures of composite membranes is attributed to the loss of absorbed water due to the hydrophilicity of these membranes. The weight loss at around 220 °C and above 400 °C were related to sulfonated groups decomposition and fluorocarbon backbone of Nafion® as well as reinforcing polymers respectively. The final residual mass observed for composite membranes are expected and can be attributed to the silica.

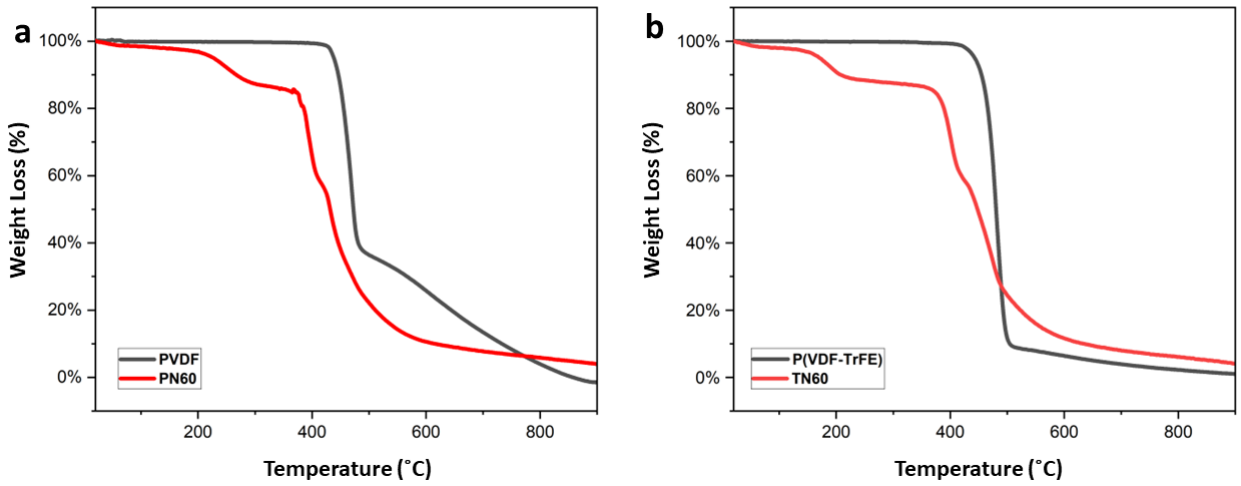

Figure 27. TGA curves of a) PVDF and PN60 and b) P(VDF-TrFE) and TN60

Wettability

To investigate the surface properties of the membranes contact angle measurmets were conducted. Figure 28a, b, c and d show the contact angle of PN50 (~87˚), PN60 (~85˚), TN50 (91˚~) and TN60 (~90˚) membranes, respectively. All composite membranes showed lower contact angles than than those of pristine PVDF and P(VDF-TrFE) with contact angles around 94° and 105°respectively [126]. This evidence attributes to existance of polar groups such –OH and $–SO_3H$ that are present in chemical structure of Nafion® and S-SiO_2 components [127]. The observation of slighty higher contact angle in case of P(VDF-TrFE)-based membranes than PVDF-based ones can be ascribed to the higher hydrophobic nature of them compare to PVDF-based ones due to the presence of more fluorine atoms in their chemical structure.

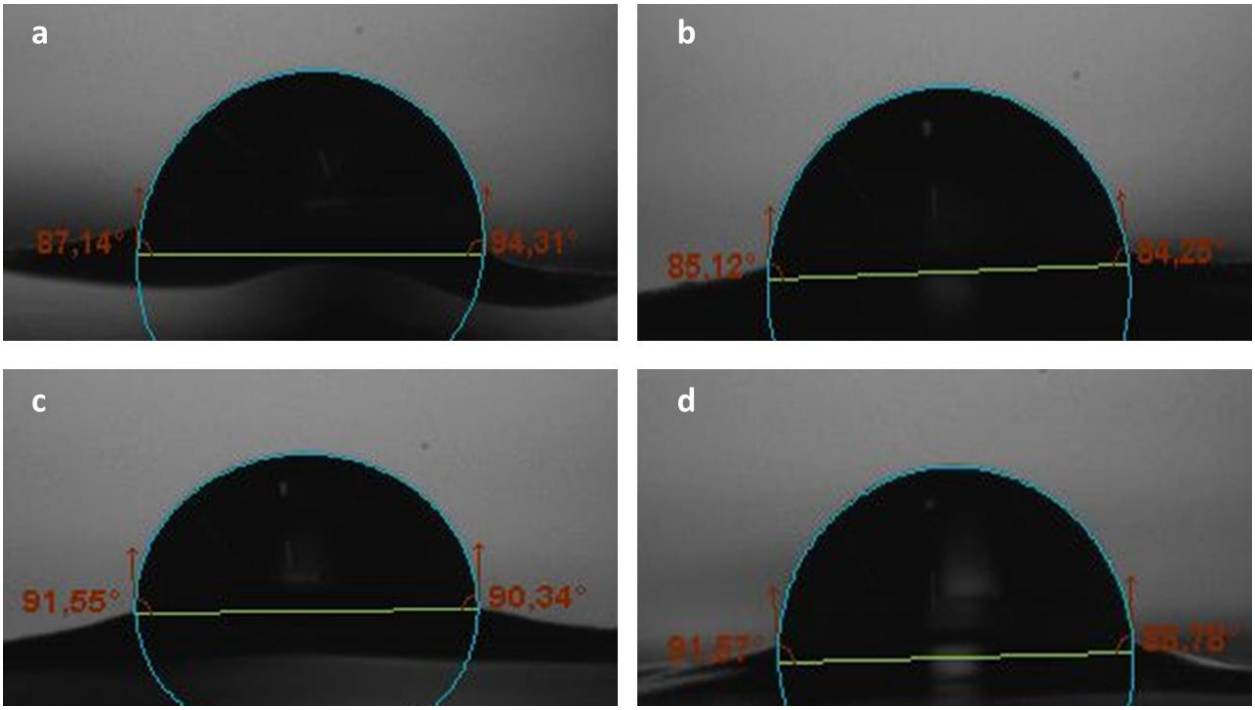

Figure 28. Contact angle measurements of a) PN50, b) PN60, c) TN50 and d) TN60

Water uptake

Water uptake is a very significant factor for the proton exchange membranes. Presence of sufficient amounts of water in the medium is vital for the creation of continuous water channels which promote protons transport through the membrane from the anode side to cathode side. Nevertheless, the excess water uptake causes excessive swelling which inversely affects the mechanical properties of the membrane [110]. As depicted in Table 9. TN60 exhibits the highest water uptake (55%) that is 1.4 times higher than the TN50 (39%) membrane. On the other hand, water uptake of the PN60 membrane (42%) is 1.2 times higher than that of PN50 membrane (35%). As the concentration of sulfonated silica is kept constant in these membranes, the observed differences in water uptake values were due to the difference in the weight percentage and type of reinforcing polymer in their composition.

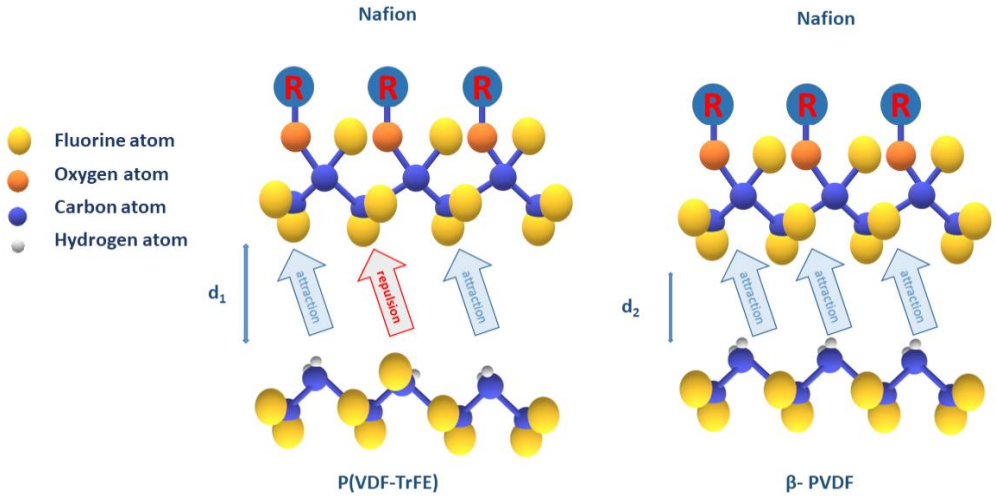

Figure 29. Interaction between Nafion® and carrier polymers

The highly hydrophobic nature of both types of the reinforcing polymers as well as their strong dipole-dipole interaction with the PTFE backbone of Nafion® lead to a dramatic decrease in water uptake [125]. Therefore, the ratio of hydrophilic to hydrophobic constituents has a direct effect on this characteristic of the prepared membranes. Consequently, as expected, samples with lower reinforcing polymer amounts (TN60 and PN60) demonstrated a greater water uptake compared to those with a higher reinforcing polymer amount (TN50 and PN50) [120], [128]. Comparing the impact of the P(VDF-TrFE) vs. PVDF illustrates that the membranes containing P(VDF-TrFE) copolymer exhibit higher water uptake with the same content of hydrophilic components. It can be attributed to the higher surface area as well as larger average pore size in case of P(VDF-TrFE) fibers than PVDF fibers [126]. Moreover, the difference in chemical and structural nature of these two reinforcing polymers leads to exhibit dissimilar properties such as degree of miscibility in Nafion® before and after electrospinning, strength of the dipole-dipole interaction between Nafion® backbone and reinforcing polymer as well as fiber characteristics (morphology and size) **Figure 29**. Each factor can affect the final characteristics of these composite membranes [129], [130]. It is worth noting that there is a relatively stronger dipole-dipole interaction of the hydrogen atoms of PVDF with F atoms of PTFE backbone of Nafion® [125] due to the presence of an additional F atom in the chemical structure of P(VDF-TRFE) copolymer. Therefore, creation of wider water channels and resulting higher water uptake of P(VDF-TRFE)-based membranes compared to the PDVF-based membranes are also expected.

Ion exchange capacity (IEC)

IEC is an indicator of the density of the ionisable proton exchange groups of these membranes which are S-SiO_2 and Nafion® groups as both components contain sulfonic acid groups [131].

The IEC values of the four fabricated composite membranes as well as Nafion® 212 for comparison was listed in **Table 9.** As was the case for water uptake, incorporation of S-SiO_2 results in a greater IEC value of composite membranes compared to the recast Nafion® membrane (0.98 mEq/g) [132] and the commercial Nafion® 212 (0.9 mmol/g) [110], [133].

Moreover, the TN60 (1.4 mmol/g) and PN60 (1.31 mmol/g) membranes exhibit higher IECs in comparison with TN50 (1.26 mmol/g) and PN50 (1.15 mmol/g) respectively, which attributes to the higher Nafion® /hydrophobic carrier ratio in their composition. Furthermore, the observed difference between the IEC values of the membranes with the same amount of Nafion® and sulfonated silica (TN60 and PN60) relies on their different chemical nature as discussed in the previous section. The P(VDF-TrFE)-based membranes showed a superior IEC compared to PVDF-based ones that can be ascribed to the higher miscibility of P(VDF-TrFE) copolymer in Nafion® solution compared to PVDF [129], [130].

Proton conductivity

The proton conductivity results of the composite membranes and Nafion® 212 measured at room temperature under fully hydrated condition were listed in **Table 9.** On the basis of the proton conductivity data, the following conclusions can be drawn: firstly, the PN60 (64 mS/cm) and TN60 (82 mS/cm) membranes, possessing higher Nafion® concentration, showed greater proton conductivities compared to the PN50 (48 mS/cm) and TN50 (59 mS/cm) membranes, respectively [93]. Secondly, among the membranes with the same Nafion® concentrations, P(VDF-TrFE)-containing samples (82,6 mS/cm) displayed a superior proton conductivity compared to the PVDF-based ones (64, 48 mS/cm). These results are in parallel with the water uptake and IEC results of the related membranes. Proton conductivity in proton exchange membranes works in two main mechanisms. First is the vehicle mechanism in which protons form a complex ($H_5O_2^+$, $H_9O_4^+$) with the water molecules to diffuse through the membrane. Second is the proton hopping mechanism (Grotthuss mechanism) in which protons hop from a functional group or a water molecule to another one by forming and breaking hydrogen bonds throughout [134]. Our results are in line with these proposed mechanisms for proton transportation. Higher water uptake would increase the conductivity by easing the vehicle mechanism by increasing the available amount of water molecules to form a complex [94], [122], [134], [135].

The second evidence originates from the difference in the strength of intermolecular interactions between Nafion® backbone with the hydrophobic constituent (dipole-dipole forces) specially in low humidity conditions and distinct morphological characteristics of P(VDF-TrFE) and PVDF fibers. Higher porosity and smaller average fiber diameter of P(VDF-TrFE)-based membranes not only ensures a larger surface area and more water channels throughout the medium but also it reduces the distance between the proton hopping sites facilitating the Grotthuss mechanism [126].

In order to investigate the proton conductivity as the function of relative humidity, the PN60 and TN60 membranes were selected to test at 80 °C under 40, 60, 80 and 100% relative humidities. Conductivity is dependent on the relative humidity as both proton conduction mechanisms need water molecules. **Figure 30** shows this dependence; higher relative humidity provides higher conductivity as expected. Also, the dependence is becoming more prominent at higher relative humidity. This is an indication of the predominant role of sulfonated silica in controlling the conductivity at lower relative humidity. Since two membranes have the same amount of sulfonated silica, their conductivities are relatively close within a low humidity range. However, a more significant variation between their conductivities was observed by switching to a water-reliable conductivity mechanism when the relative humidity was increased. The TN60 membrane exhibited a superior proton conductivity over whole applied humidity levels compared to the PN60 membrane, which is consistent with the room temperature conductivity measurements and water uptake results. Furthermore, comparing the proton conductivities of the both TN60 (132 mS/cm) and PN60 (79 mS/cm) membranes in 100% RH at 80°C with their room temperature values at the same humidity reveals a significant increase in their proton conductivities. Hence, an elevated temperature provides the required activation energy for proton transportation and results in their fast movement [103], [127]. The higher respective IEC of TN50 and TN60 compared to that of PN50 and PN60 also were in parallel with obtained proton conductivity of these membranes.

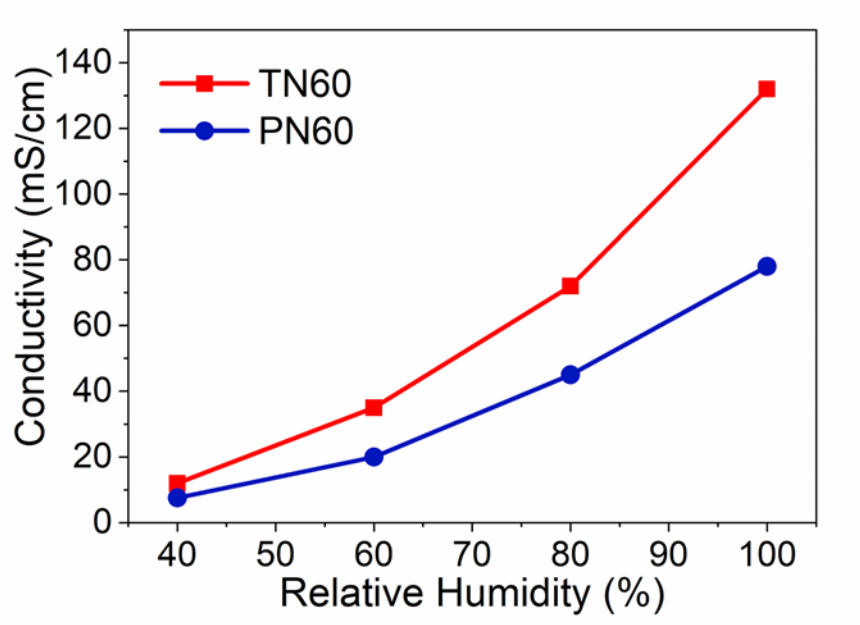

Figure 30. Proton conductivity at 80°C vs. relative humidity for TN60 and PN60 membranes.

Mechanical properties

As shown in **Figure 31**, the PVDF-based membranes (PN50, PN60) showed greater stiffness and elongation compared to the P(VDF-TrFE)-based ones (TN50, TN60). This is attributed to the differences in their fiber morphology, diameter of fibers, and the strength of the intermolecular bonds. Moreover, stiffness of the both PVDF- and P(VDF-TrFE)-based membranes were improved (~ 1.3 and ~1.5 times higher respectively) with increasing reinforcing polymer volume fraction [93], [115] (from 10 wt% to 20 wt%) in the composition. The better mechanical performance of the membranes with lower Nafion® (higher carrier polymer) content is correlated to the increased average fiber diameter by enhancing reinforcing polymer content in the composition [120]. Comparing the Young's Modulus of resultant composite membranes to that of Nafion 212®, P(VDF-TrFE)- and PVDF-based membranes reveal almost 2.5 and 4-times higher stiffness than Nafion 212®, respectively.

However, they possessed relatively lower elongations. Additionally, the homogeneous incorporation of long order sulfonated-silica network into the polymer/Nafion® fibers via simultaneous sol-gel reaction and dual-electrospinning process results in an enhancement of mechanical properties of these membranes due to the formation of new hydrogen bonds between sulfonated-silica and Nafion®. This observation is also valid at wet conditions, where the inorganic network prevents the composite membranes from their excess swelling [104].

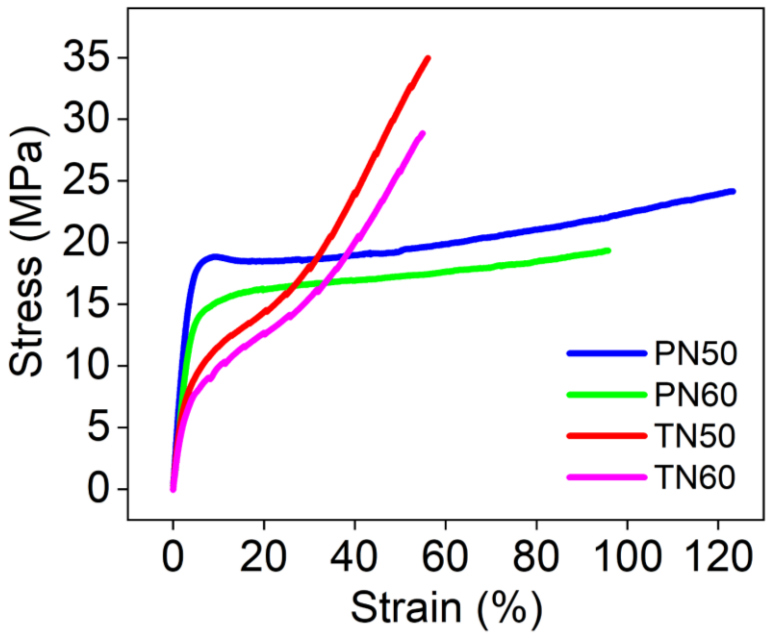

Figure 31. Stress strain curves of PN50, PN60, TN50 and TN60 membranes.

Table 9. Characteristics of the composite membranes.

Sample	Water uptake (%)	IEC (mmol/g)	Conductivity at RT (mS/cm)	Young's Modulus (MPa)	Yield strength (MPa)	Strain at break (%)
PN50	35	1.15	48	495±1.5	18.2	123
PN60	42	1.31	64	342±1.3	13.9	95
TN50	39	1.26	59	286±1.7	10	56
TN60	55	1.40	82	228±1.3	8.5	54.5
Nafion® 212	24 [70]	0.9 [70]	71	112±8.4 [70]	9 [70]	185 [71]

Single Cell Performance and In-situ LSV Analyses

Fuel cell performance and durability are adversely affected by hydrogen crossover, as it accelerates the degradation of the MEA, particularly at the membrane and cathode catalyst materials. Among various techniques to evaluate the hydrogen crossover in fuel cells, Linear sweep voltammetry (LSV) is the most common one [132]. In this study, the LSV measurements were performed to investigate the compactness of the prepared MEAs prior to the fuel cell tests. The LSV tests for the PN60 and TN60 membranes were carried out at 60, 80 and 100% relative humidity at the open circuit voltage (OCV) condition. Both membranes with different reinforcement polymers showed a similar hydrogen impermeability, but the H_2 limiting crossover current density of PVDF-TrFE-based membrane is slightly higher than that of PVDF-based one **(Figure 32**). This result should be attributed to the greater water uptake and swelling as well as a lower mechanical strength of the TN60 membranes compared to PN60 [136], [137]. Besides, the TN60 membrane exhibited a very stable hydrogen crossover performance for all three relative humidity levels that indicates dimensional stability of these membranes under various applied humidity (**Figure 32b**).

On the other hand, the hydrogen limiting crossover density of the composite membrane reinforced with PVDF differs at different relative humidity (**Figure 32a**). Maximum H_2 crossover current is observed at 100% RH which shows a higher degree of swelling compared to the lower applied humidity. This result is considered as a proof showing P(VDF-TrFE) is more reliable under operating conditions at different relative humidity. These results are consistent with the fuel cell performance of the TN60 membrane (**Figure 33)**.

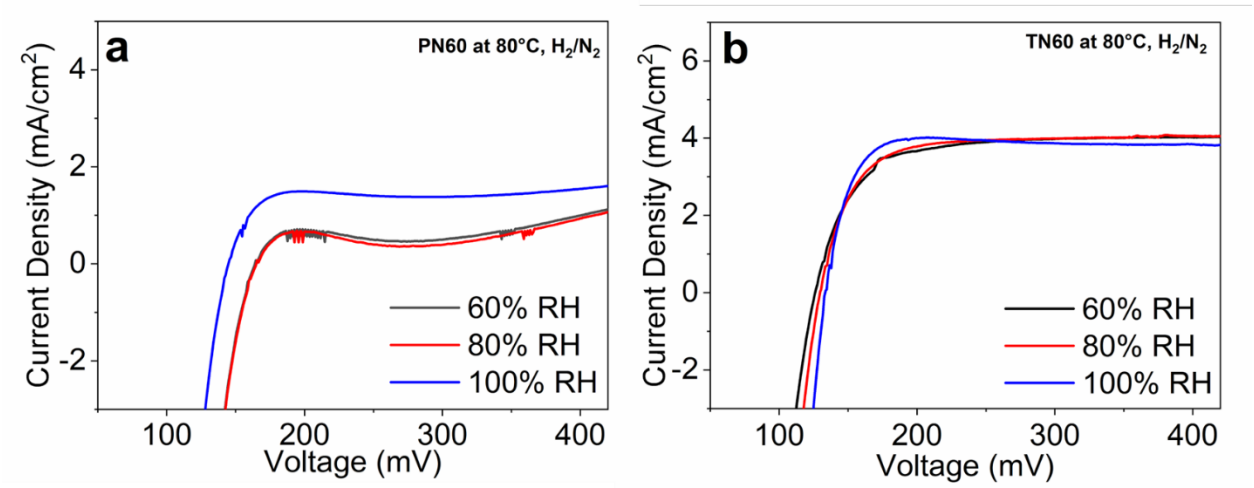

Figure 32. Linear sweep voltammetry H_2 limiting current density graphs of a) PN60, and b) TN60 membranes.

The single-cell fuel cell performance of fabricated composite membranes was performed at 80°C and varying relative humidity levels. The promising fuel cell performances obtained from the P(VDF-TrFE)-based membranes. It is also clear that the relative humidity dependence of these composite membranes is neglectable, especially for the TN60 membranes, compared to the commercial Nafion® 212 membranes [138]. Additionally, the PN60 membrane showed a superior fuel cell performance at 80 %RH, and there is no significant performance loss between 60% RH and fully humidified condition **(Figure 33a**). Besides, the TN60 membrane showed a stable performance under different relative humidity operations, particularly at 60% RH compared to 80 and 100% RH (**Figure 33b**).

The maximum power density values of each membrane at corresponding applied relative humidity are listed in **Table 10**. Here, the reported performance results of fabricated membranes are quite enhanced compared to the fuel cell performance results of reported SiO_2-based membranes in the literature [139].

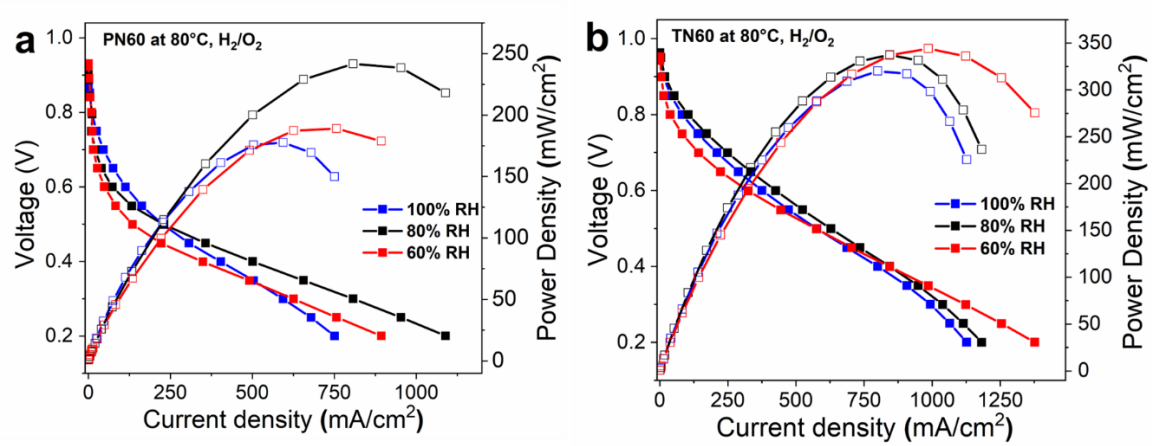

Figure 33. Polarization and power density curves of PN60 and TN60 membranes at varied RH%.

Table 10. Maximum power density values of PN60 and TN60 membranes at different RH%.

Sample	Relative Humidity (%)	Max. Power Density (mW/cm^2)
PN60	60	190
	80	241
	100	173
TN60	60	344
	80	337
	100	320

1.10.5 Conclusion

Electrospinning has been emerged as a versatile and scalable technique for fabrication of fibrous hybrid/composite membranes for fuel cells. This method has the advantage of use of various combinations of carrier polymers and inorganic nanoparticles or polymer blends. In this study, electrospun sulfonated silica-based membranes were studied. Two different routes were selected for incorporation of sulfonated silica into these electrospun proton conducting membranes:

i. Synthesizing sulfonated silica nanoparticles via sol-gel hydrothermal method and electrospinning with polyvinylidene fluoride or poly(vinylidene fluoride-*co*-trifluoroethylene) as reinforcing polymers: In this approach optimum electrospinning parameters (i.e. solvent, carrier polymer, electrospinning voltage, relative humidity, and flow rate) were determined to produce nanofibers with homogeneously distributed S-SiO_2. Furthermore, fiber mats were transformed into dense membranes by subsequent hot-pressing and Nafion® impregnation. Consequently, room temperature conductivity, proton conductivity at varying humidity levels, water uptake and mechanical strength of the densified hybrid membranes were examined in detail. The membranes prepared by PVDF carrier polymer exhibited higher elongation than P(VDF-TrFE) based membranes due to their higher average fiber diameter while there was no noticeable difference between their Young's modulus values. Hybrid membrane with P(VDF-TrFE) carrier showed a superior proton conductivity (102 mS/cm) compared with PVDF carrier polymer containing membrane (43 mS/cm) and solution casted Nafion® membrane (95 mS/cm) at the same condition. As a consequence of those encouraging results herein, P(VDF-TrFE)/ S-SiO_2 nanofiber-based membranes can be considered as potential membranes for PEM fuel cells at medium and high humidity levels.

ii. Dual-electrospinning of sulfonated silica and PVDF/ Nafion® or P(VDF-TrFE)/Nafion® solutions: In this part proton conductive composite membranes were fabricated successfully via combination of the dual electrospinning and sol-gel methods. With the proposed approach here, not only a uniform distribution of all constituents within the membranes was obtained but well-organized pathways for facile H^+ transport were achieved as well. Incorporation of sulfonated silica into the composite membranes resulted in improved water retention ability, ionic conductivity and dimensional stability. The fabricated P(VDF-TrFE)-based membranes exhibited superior proton conductivity at lower relative humidity compared to both the PVDF-based membranes and the pristine Nafion® membranes. To investigate the impact of reinforcing polymer (PVDF or P(VDF-TrFE)) and reinforcing polymer to Nafion® ratio on the final properties of the membranes, four different types of membranes were chosen in which the content of the sulfonated-silica precursors was kept constant, while the ratio of reinforcing polymers (PVDF or P(VDF-TrFE)) to Nafion® were examined. Addition of various amounts of the carrier polymers gives rise to an enhanced mechanical strength compared to the commercial Nafion® membranes. Increasing the Nafion® content results in higher proton conductivity with a moderate decrease in mechanical properties of theses membranes. The maximum proton conductivity was achieved for TN60 at 80°Cover the entire relative humidity range (132 mS/cm at 100% RH). Moreover, TN60 showed an enhanced fuel cell performance at 60% RH (344 mW/cm^2) compared to 80% (337 mW/cm^2) and 100% (320 mW/cm^2) suggesting a promising candidate for the PEM fuel cells at low humidity operation condition.

References

[1] J. Larminie and A. Dicks, *Fuel cell systems explained*, 2nd ed. Chichester, West Sussex: J. Wiley, 2003.

[2] J. M. Andújar and F. Segura, “Fuel cells: History and updating. A walk along two centuries,” *Renew. Sustain. Energy Rev.*, vol. 13, no. 9, pp. 2309–2322, Dec. 2009, doi: 10.1016/j.rser.2009.03.015.

[3] U. Lucia, “Overview on fuel cells,” *Renew. Sustain. Energy Rev.*, vol. 30, pp. 164–169, Feb. 2014, doi: 10.1016/j.rser.2013.09.025.

[4] Y. Wang, D. F. Ruiz Diaz, K. S. Chen, Z. Wang, and X. C. Adroher, “Materials, technological status, and fundamentals of PEM fuel cells – A review,” *Mater. Today*, vol. 32, pp. 178–203, Jan. 2020, doi: 10.1016/j.mattod.2019.06.005.

[5] O. Z. Sharaf and M. F. Orhan, “An overview of fuel cell technology: Fundamentals and applications,” *Renew. Sustain. Energy Rev.*, vol. 32, pp. 810–853, Apr. 2014, doi: 10.1016/j.rser.2014.01.012.

[6] L. Carrette, K. A. Friedrich, and U. Stimming, “Fuel Cells - Fundamentals and Applications,” *Fuel Cells*, vol. 1, no. 1, pp. 5–39, May 2001, doi: 10.1002/1615-6854(200105)1:1<5::AID-FUCE5>3.0.CO;2-G.

[7] N. Sazali, W. N. Wan Salleh, A. S. Jamaludin, and M. N. Mhd Razali, “New Perspectives on Fuel Cell Technology: A Brief Review,” *Membranes*, vol. 10, no. 5, p. 99, May 2020, doi: 10.3390/membranes10050099.

[8] L. Fan, Z. Tu, and S. H. Chan, “Recent development of hydrogen and fuel cell technologies: A review,” *Energy Rep.*, vol. 7, pp. 8421–8446, Nov. 2021, doi: 10.1016/j.egyr.2021.08.003.

[9] D. K. Madheswaran and A. Jayakumar, “Recent advancements on non-platinum based catalyst electrode material for polymer electrolyte membrane fuel cells: a mini techno-economic review,” *Bull. Mater. Sci.*, vol. 44, no. 4, p. 287, Dec. 2021, doi: 10.1007/s12034-021-02572-6.

[10] S. P. S. Badwal, S. S. Giddey, C. Munnings, A. I. Bhatt, and A. F. Hollenkamp, “Emerging electrochemical energy conversion and storage technologies,” *Front. Chem.*, vol. 2, Sep. 2014, doi: 10.3389/fchem.2014.00079.

[11] E. Pohl, P. Meier, M. Maximini, and J. vom Schloß, “Primary energy savings of a modular combined heat and power plant based on high temperature proton exchange membrane fuel cells,” *Appl. Therm. Eng.*, vol. 104, pp. 54–63, Jul. 2016, doi: 10.1016/j.applthermaleng.2016.05.055.

[12] Y.-S. Ye, J. Rick, and B.-J. Hwang, “Water Soluble Polymers as Proton Exchange Membranes for Fuel Cells,” *Polymers*, vol. 4, no. 2, pp. 913–963, Mar. 2012, doi: 10.3390/polym4020913.

[13] A. Alaswad *et al.*, “Technical and Commercial Challenges of Proton-Exchange Membrane (PEM) Fuel Cells,” *Energies*, vol. 14, no. 1, p. 144, Dec. 2020, doi: 10.3390/en14010144.

[14] S. Gottesfeld *et al.*, “Anion exchange membrane fuel cells: Current status and remaining challenges,” *J. Power Sources*, vol. 375, pp. 170–184, Jan. 2018, doi: 10.1016/j.jpowsour.2017.08.010.

[15] G. Merle, M. Wessling, and K. Nijmeijer, “Anion exchange membranes for alkaline fuel cells: A review,” *J. Membr. Sci.*, vol. 377, no. 1–2, pp. 1–35, Jul. 2011, doi: 10.1016/j.memsci.2011.04.043.

[16] M. Hren, M. Božič, D. Fakin, K. S. Kleinschek, and S. Gorgieva, “Alkaline membrane fuel cells: anion exchange membranes and fuels,” *Sustain. Energy Fuels*, vol. 5, no. 3, pp. 604–637, 2021, doi: 10.1039/D0SE01373K.

[17] W. E. Mustain, “Understanding how high-performance anion exchange membrane fuel cells were achieved: Component, interfacial, and cell-level factors,” *Curr. Opin. Electrochem.*, vol. 12, pp. 233–239, Dec. 2018, doi: 10.1016/j.coelec.2018.11.010.

[18] R.-A. Felseghi, E. Carcadea, M. S. Raboaca, C. N. Trufin, and C. Filote, “Hydrogen Fuel Cell Technology for the Sustainable Future of Stationary Applications,” *Energies*, vol. 12, no. 23, p. 4593, Dec. 2019, doi: 10.3390/en12234593.

[19] L.-Y. Zhu, Y.-C. Li, J. Liu, J. He, L.-Y. Wang, and J.-D. Lei, “Recent developments in high-performance Nafion membranes for hydrogen fuel cells applications,” *Pet. Sci.*, vol. 19, no. 3, pp. 1371–1381, Jun. 2022, doi: 10.1016/j.petsci.2021.11.004.

[20] J. R. Varcoe *et al.*, “Anion-exchange membranes in electrochemical energy systems,” *Energy Env. Sci*, vol. 7, no. 10, pp. 3135–3191, 2014, doi: 10.1039/C4EE01303D.

[21] Z. Shang, R. Wycisk, and P. Pintauro, “Electrospun Composite Proton-Exchange and Anion-Exchange Membranes for Fuel Cells,” *Energies*, vol. 14, no. 20, p. 6709, Oct. 2021, doi: 10.3390/en14206709.

[22] K. Strickland *et al.*, “Anion Resistant Oxygen Reduction Electrocatalyst in Phosphoric Acid Fuel Cell,” *ACS Catal.*, vol. 8, no. 5, pp. 3833–3843, May 2018, doi: 10.1021/acscatal.8b00390.

[23] S. S. Araya *et al.*, “A comprehensive review of PBI-based high temperature PEM fuel cells,” *Int. J. Hydrog. Energy*, vol. 41, no. 46, pp. 21310–21344, Dec. 2016, doi: 10.1016/j.ijhydene.2016.09.024.

[24] J.-H. Wee, “Carbon dioxide emission reduction using molten carbonate fuel cell systems,” *Renew. Sustain. Energy Rev.*, vol. 32, pp. 178–191, Apr. 2014, doi: 10.1016/j.rser.2014.01.034.

[25] A. C. Rady, S. Giddey, S. P. S. Badwal, B. P. Ladewig, and S. Bhattacharya, “Review of Fuels for Direct Carbon Fuel Cells,” *Energy Fuels*, vol. 26, no. 3, pp. 1471–1488, Mar. 2012, doi: 10.1021/ef201694y.

[26] H. Shi, C. Su, R. Ran, J. Cao, and Z. Shao, “Electrolyte materials for intermediate-temperature solid oxide fuel cells,” *Prog. Nat. Sci. Mater. Int.*, vol. 30, no. 6, pp. 764–774, Dec. 2020, doi: 10.1016/j.pnsc.2020.09.003.

[27] T. Wejrzanowski *et al.*, “Microstructure driven design of porous electrodes for molten carbonate fuel cell application: Recent progress,” *Int. J. Hydrog. Energy*, vol. 45, no. 47, pp. 25719–25732, Sep. 2020, doi: 10.1016/j.ijhydene.2019.12.038.

[28] N. Mahato, A. Banerjee, A. Gupta, S. Omar, and K. Balani, “Progress in material selection for solid oxide fuel cell technology: A review,” *Prog. Mater. Sci.*, vol. 72, pp. 141–337, Jul. 2015, doi: 10.1016/j.pmatsci.2015.01.001.

[29] S. Litster and G. McLean, “PEM fuel cell electrodes,” *J. Power Sources*, vol. 130, no. 1–2, pp. 61–76, May 2004, doi: 10.1016/j.jpowsour.2003.12.055.

[30] N. Cele and S. S. Ray, “Recent Progress on Nafion-Based Nanocomposite Membranes for Fuel Cell Applications: Recent Progress on Nafion-Based Nanocomposite Membranes …,” *Macromol. Mater. Eng.*, vol. 294, no. 11, pp. 719–738, Nov. 2009, doi: 10.1002/mame.200900143.

[31] M. Pan, C. Pan, C. Li, and J. Zhao, “A review of membranes in proton exchange membrane fuel cells: Transport phenomena, performance and durability,” *Renew. Sustain. Energy Rev.*, vol. 141, p. 110771, May 2021, doi: 10.1016/j.rser.2021.110771.

[32] Y. Prykhodko, K. Fatyeyeva, L. Hespel, and S. Marais, “Progress in hybrid composite Nafion®-based membranes for proton exchange fuel cell application,” *Chem. Eng. J.*, vol. 409, p. 127329, Apr. 2021, doi: 10.1016/j.cej.2020.127329.

[33] W. Vielstich, *Handbook of fuel cells: fundamentals, technology, and applications*. Hoboken, N.J.: John Wiley & Sons, 2010. Accessed: Aug. 07, 2022. [Online]. Available: https://doi.org/10.1002/9780470974001

[34] M. Mohammadi and S. Mehdipour-Ataei, “Durable sulfonated partially fluorinated polysulfones as membrane for PEM fuel cell,” *Renew. Energy*, vol. 158, pp. 421–430, Oct. 2020, doi: 10.1016/j.renene.2020.05.124.

[35] E. Ogungbemi *et al.*, “Fuel cell membranes – Pros and cons,” *Energy*, vol. 172, pp. 155–172, Apr. 2019, doi: 10.1016/j.energy.2019.01.034.

[36] N. Esmaeili, E. MacA. Gray, and C. J. Webb, “Non-Fluorinated Polymer Composite Proton Exchange Membranes for Fuel Cell Applications-A Review,” *ChemPhysChem*, p. cphc.201900191, Jul. 2019, doi: 10.1002/cphc.201900191.

[37] G. H. Byun, J. A. Kim, N. Y. Kim, Y. S. Cho, and C. R. Park, “Molecular engineering of hydrocarbon membrane to substitute perfluorinated sulfonic acid membrane for proton exchange membrane fuel cell operation,” *Mater. Today Energy*, vol. 17, p. 100483, Sep. 2020, doi: 10.1016/j.mtener.2020.100483.

[38] G. A. Giffin *et al.*, “Interplay between structure and properties in acid-base blend PBI-based membranes for HT-PEM fuel cells,” *J. Membr. Sci.*, vol. 535, pp. 122–131, Aug. 2017, doi: 10.1016/j.memsci.2017.04.019.

[39] T. K. Maiti *et al.*, “Advances in perfluorosulfonic acid-based proton exchange membranes for fuel cell applications: A review,” *Chem. Eng. J. Adv.*, vol. 12, p. 100372, Nov. 2022, doi: 10.1016/j.ceja.2022.100372.

[40] M. Díaz, A. Ortiz, and I. Ortiz, “Progress in the use of ionic liquids as electrolyte membranes in fuel cells,” *J. Membr. Sci.*, vol. 469, pp. 379–396, Nov. 2014, doi: 10.1016/j.memsci.2014.06.033.

[41] J. Zhao and X. Li, “A review of polymer electrolyte membrane fuel cell durability for vehicular applications: Degradation modes and experimental techniques,” *Energy Convers. Manag.*, vol. 199, p. 112022, Nov. 2019, doi: 10.1016/j.enconman.2019.112022.

[42] S. Shamim, K. Sudhakar, B. Choudhary, and J. Anwar, “A review on recent advances in proton exchange membrane fuel cells: Materials, technology and applications,” p. 13, 2015.

[43] “nafion structure,” *Nafion figure*. http://weblab.open.ac.uk/lab/fuelcells/nafion/index.php

[44] N. Sammes, *Fuel Cell Technology: Reaching Towards Commercialization*. Springer Science & Business Media, 2006.

[45] X. Ge, F. Zhang, L. Wu, Z. Yang, and T. Xu, “Current Challenges and Perspectives of Polymer Electrolyte Membranes,” *Macromolecules*, vol. 55, no. 10, pp. 3773–3787, May 2022, doi: 10.1021/acs.macromol.1c02053.

[46] L. Liu, Y. Xing, Y. Li, Z. Fu, Z. Li, and H. Li, “Enhanced mechanical durability of perfluorosulfonic acid proton-exchange membrane based on a double-layer ePTFE reinforcement strategy,” *Int. J. Hydrog. Energy*, p. S0360319922028348, Jul. 2022, doi: 10.1016/j.ijhydene.2022.06.199.

[47] P. Hong, L. Xu, J. Li, and M. Ouyang, “Modeling and analysis of internal water transfer behavior of PEM fuel cell of large surface area,” *Int. J. Hydrog. Energy*, vol. 42, no. 29, pp. 18540–18550, Jul. 2017, doi: 10.1016/j.ijhydene.2017.04.164.

[48] Q. Liu, F. Lan, J. Chen, C. Zeng, and J. Wang, “A review of proton exchange membrane fuel cell water management: Membrane electrode assembly,” *J. Power Sources*, vol. 517, p. 230723, Jan. 2022, doi: 10.1016/j.jpowsour.2021.230723.

[49] C. Lim *et al.*, “Membrane degradation during combined chemical and mechanical accelerated stress testing of polymer electrolyte fuel cells,” *J. Power Sources*, vol. 257, pp. 102–110, Jul. 2014, doi: 10.1016/j.jpowsour.2014.01.106.

[50] M. Bodner, B. Cermenek, M. Rami, and V. Hacker, “The Effect of Platinum Electrocatalyst on Membrane Degradation in Polymer Electrolyte Fuel Cells,” *Membranes*, vol. 5, no. 4, pp. 888–902, Dec. 2015, doi: 10.3390/membranes5040888.

[51] P. C. Okonkwo, I. Ben Belgacem, W. Emori, and P. C. Uzoma, “Nafion degradation mechanisms in proton exchange membrane fuel cell (PEMFC) system: A review,” *Int. J. Hydrog. Energy*, vol. 46, no. 55, pp. 27956–27973, Aug. 2021, doi: 10.1016/j.ijhydene.2021.06.032.

[52] X. Huang *et al.*, “Mechanical endurance of polymer electrolyte membrane and PEM fuel cell durability,” *J. Polym. Sci. Part B Polym. Phys.*, vol. 44, no. 16, pp. 2346–2357, Aug. 2006, doi: 10.1002/polb.20863.

[53] J. Wu *et al.*, “A review of PEM fuel cell durability: Degradation mechanisms and mitigation strategies,” *J. Power Sources*, vol. 184, no. 1, pp. 104–119, Sep. 2008, doi: 10.1016/j.jpowsour.2008.06.006.

[54] M. Amjadi, S. Rowshanzamir, S. J. Peighambardoust, M. G. Hosseini, and M. H. Eikani, “Investigation of physical properties and cell performance of Nafion/TiO2 nanocomposite membranes for high temperature PEM fuel cells,” *Int. J. Hydrog. Energy*, vol. 35, no. 17, pp. 9252–9260, Sep. 2010, doi: 10.1016/j.ijhydene.2010.01.005.

[55] F. Mura, R. F. Silva, and A. Pozio, “Study on the conductivity of recast Nafion®/montmorillonite and Nafion®/TiO2 composite membranes,” *Electrochimica Acta*, vol. 52, no. 19, pp. 5824–5828, May 2007, doi: 10.1016/j.electacta.2007.02.081.

[56] W. Zhengbang, H. Tang, and P. Mu, “Self-assembly of durable Nafion/TiO2 nanowire electrolyte membranes for elevated-temperature PEM fuel cells,” *J. Membr. Sci.*, vol. 369, no. 1–2, pp. 250–257, Mar. 2011, doi: 10.1016/j.memsci.2010.11.070.

[57] Y.-T. Kim, M.-K. Song, K.-H. Kim, S.-B. Park, S.-K. Min, and H.-W. Rhee, “Nafion/ZrSPP composite membrane for high temperature operation of PEMFCs,” *Electrochimica Acta*, vol. 50, no. 2–3, pp. 645–648, Nov. 2004, doi: 10.1016/j.electacta.2003.12.079.

[58] K. T. Park, U. H. Jung, D. W. Choi, K. Chun, H. M. Lee, and S. H. Kim, “ZrO2–SiO2/Nafion® composite membrane for polymer electrolyte membrane fuel cells operation at high temperature and low humidity,” *J. Power Sources*, vol. 177, no. 2, pp. 247–253, Mar. 2008, doi: 10.1016/j.jpowsour.2007.11.081.

[59] V. Di Noto, N. Boaretto, E. Negro, and G. Pace, “New inorganic–organic proton conducting membranes based on Nafion and hydrophobic fluoroalkylated silica nanoparticles,” *J. Power Sources*, vol. 195, no. 23, pp. 7734–7742, Dec. 2010, doi: 10.1016/j.jpowsour.2009.10.028.

[60] R. Jiang, H. R. Kunz, and J. M. Fenton, “Composite silica/Nafion® membranes prepared by tetraethylorthosilicate sol–gel reaction and solution casting for direct methanol fuel cells,” *J. Membr. Sci.*, vol. 272, no. 1–2, pp. 116–124, Mar. 2006, doi: 10.1016/j.memsci.2005.07.026.

[61] A. K. Sahu, G. Selvarani, S. Pitchumani, P. Sridhar, and A. K. Shukla, “A Sol-Gel Modified Alternative Nafion-Silica Composite Membrane for Polymer Electrolyte Fuel Cells,” *J. Electrochem. Soc.*, vol. 154, no. 2, p. B123, Dec. 2006, doi: 10.1149/1.2401031.

[62] C.-C. Ke, X.-J. Li, Q. Shen, S.-G. Qu, Z.-G. Shao, and B.-L. Yi, “Investigation on sulfuric acid sulfonation of in-situ sol–gel derived Nafion/SiO2 composite membrane,” *Int. J. Hydrog. Energy*, vol. 36, no. 5, pp. 3606–3613, Mar. 2011, doi: 10.1016/j.ijhydene.2010.12.030.

[63] E. Bakangura, L. Wu, L. Ge, Z. Yang, and T. Xu, “Mixed matrix proton exchange membranes for fuel cells: State of the art and perspectives,” *Prog. Polym. Sci.*, vol. 57, pp. 103–152, Jun. 2016, doi: 10.1016/j.progpolymsci.2015.11.004.

[64] K. Waldrop, R. Wycisk, and P. N. Pintauro, “Application of electrospinning for the fabrication of proton-exchange membrane fuel cell electrodes,” *Curr. Opin. Electrochem.*, vol. 21, pp. 257–264, Jun. 2020, doi: 10.1016/j.coelec.2020.03.007.

[65] Y.-Z. Long, X. Yan, X.-X. Wang, J. Zhang, and M. Yu, “Electrospinning,” in *Electrospinning: Nanofabrication and Applications*, Elsevier, 2019, pp. 21–52. doi: 10.1016/B978-0-323-51270-1.00002-9.

[66] V. Beachley and X. Wen, “Effect of electrospinning parameters on the nanofiber diameter and length,” *Mater. Sci. Eng. C*, vol. 29, no. 3, pp. 663–668, Apr. 2009, doi: 10.1016/j.msec.2008.10.037.

[67] Z. He, F. Rault, M. Lewandowski, E. Mohsenzadeh, and F. Salaün, “Electrospun PVDF Nanofibers for Piezoelectric Applications: A Review of the Influence of Electrospinning Parameters on the β Phase and Crystallinity Enhancement,” *Polymers*, vol. 13, no. 2, p. 174, Jan. 2021, doi: 10.3390/polym13020174.

[68] “Electrospining.” https://sites.tufts.edu/pcebe/electrospun-fibers/

[69] Y. Kim, X. Wu, C. Lee, and J. H. Oh, “Characterization of PI/PVDF-TrFE Composite Nanofiber-Based Triboelectric Nanogenerators Depending on the Type of the Electrospinning System,” *ACS Appl. Mater. Interfaces*, vol. 13, no. 31, pp. 36967–36975, Aug. 2021, doi: 10.1021/acsami.1c04450.

[70] W. E. Teo and S. Ramakrishna, “A review on electrospinning design and nanofibre assemblies,” *Nanotechnology*, vol. 17, no. 14, pp. R89–R106, Jul. 2006, doi: 10.1088/0957-4484/17/14/R01.

[71] V. Di Noto, N. Boaretto, E. Negro, G. A. Giffin, S. Lavina, and S. Polizzi, “Inorganic–organic membranes based on Nafion, [(ZrO2)·(HfO2)0.25] and [(SiO2)·(HfO2)0.28]. Part I: Synthesis, thermal stability and performance in a single PEMFC,” *Int. J. Hydrog. Energy*, vol. 37, no. 7, pp. 6199–6214, Apr. 2012, doi: 10.1016/j.ijhydene.2011.07.132.

[72] “PEM FUEL CELL.” https://books.google.com.tr/books?hl=en&lr=&id=elO7n4Z6uLoC&oi=fnd&pg=PP1&dq=%5B34%5D%09F.+Barbir,+PEM+Fuel+Cells:+Theory+and+Practice.+Academic+Press,+2012.&ots=LwclXDDJM3&sig=ckoJtYZnAxg90jfMC3_UPi9l7do&redir_esc=y#v=onepage&q=%5B34%5D%09F.%20Barbir%2C%20PEM%20Fuel%20Cells%3A%20Theory%20and%20Practice.%20Academic%20Press%2C%202012.&f=false

[73] E. Misran, N. S. M. Hassan, W. R. W. Daud, E. H. Majlan, and M. I. Rosli, “Water transport characteristics of a PEM fuel cell at various operating pressures and temperatures,” *Int. J. Hydrog. Energy*, vol. 38, no. 22, pp. 9401–9408, Jul. 2013, doi: 10.1016/j.ijhydene.2012.12.076.

[74] V. Freger, “Hydration of Ionomers and Schroeder’s Paradox in Nafion,” *J. Phys. Chem. B*, vol. 113, no. 1, pp. 24–36, Jan. 2009, doi: 10.1021/jp806326a.

[75] D. N. Ozen, B. Timurkutluk, and K. Altinisik, “Effects of operation temperature and reactant gas humidity levels on performance of PEM fuel cells,” *Renew. Sustain. Energy Rev.*, vol. 59, pp. 1298–1306, Jun. 2016, doi: 10.1016/j.rser.2016.01.040.

[76] C. Li, J. Liu, R. Guan, P. Zhang, and Q. Zhang, “Effect of heating and stretching membrane on ionic conductivity of sulfonated poly(phenylene oxide),” *J. Membr. Sci.*, vol. 287, no. 2, pp. 180–186, Jan. 2007, doi: 10.1016/j.memsci.2006.10.015.

[77] K.-D. Kreuer, “Proton Conductivity: Materials and Applications,” *Chem. Mater.*, vol. 8, no. 3, pp. 610–641, Jan. 1996, doi: 10.1021/cm950192a.

[78] K.-D. Kreuer, A. Rabenau, and W. Weppner, “Vehicle Mechanism, A New Model for the Interpretation of the Conductivity of Fast Proton Conductors,” *Angew. Chem. Int. Ed. Engl.*, vol. 21, no. 3, pp. 208–209, Mar. 1982, doi: 10.1002/anie.198202082.

[79] L. Xing *et al.*, “Membrane electrode assemblies for PEM fuel cells: A review of functional graded design and optimization,” *Energy*, vol. 177, pp. 445–464, Jun. 2019, doi: 10.1016/j.energy.2019.04.084.

[80] K. Sopian and W. R. Wan Daud, “Challenges and future developments in proton exchange membrane fuel cells,” *Renew. Energy*, vol. 31, no. 5, pp. 719–727, Apr. 2006, doi: 10.1016/j.renene.2005.09.003.

[81] S. Banerjee and D. E. Curtin, “Nafion® perfluorinated membranes in fuel cells,” *J. Fluor. Chem.*, vol. 125, no. 8, pp. 1211–1216, Aug. 2004, doi: 10.1016/j.jfluchem.2004.05.018.

[82] “3 Polymer International - 2010 - Bai - Recent developments in fuel-processing and proton-exchange membranes for fuel cells (1).pdf.”

[83] Y. Zhou, J. Yang, H. Su, J. Zeng, S. P. Jiang, and W. A. Goddard, “Insight into Proton Transfer in Phosphotungstic Acid Functionalized Mesoporous Silica-Based Proton Exchange Membrane Fuel Cells,” *J. Am. Chem. Soc.*, vol. 136, no. 13, pp. 4954–4964, Apr. 2014, doi: 10.1021/ja411268q.

[84] S. Sambandam and V. Ramani, “SPEEK/functionalized silica composite membranes for polymer electrolyte fuel cells,” *J. Power Sources*, vol. 170, no. 2, pp. 259–267, Jul. 2007, doi: 10.1016/j.jpowsour.2007.04.026.

[85] C.-Y. Yen *et al.*, “Sol–gel derived sulfonated-silica/Nafion® composite membrane for direct methanol fuel cell,” *J. Power Sources*, vol. 173, no. 1, pp. 36–44, Nov. 2007, doi: 10.1016/j.jpowsour.2007.08.017.

[86] T. Tamura and H. Kawakami, “Aligned Electrospun Nanofiber Composite Membranes for Fuel Cell Electrolytes,” *Nano Lett.*, vol. 10, no. 4, pp. 1324–1328, Apr. 2010, doi: 10.1021/nl1007079.

[87] P. S. Kumar *et al.*, “Hierarchical electrospun nanofibers for energy harvesting, production and environmental remediation,” *Energy Env. Sci*, vol. 7, no. 10, pp. 3192–3222, 2014, doi: 10.1039/C4EE00612G.

[88] Q. Liu, J. Zhu, L. Zhang, and Y. Qiu, “Recent advances in energy materials by electrospinning,” *Renew. Sustain. Energy Rev.*, vol. 81, pp. 1825–1858, Jan. 2018, doi: 10.1016/j.rser.2017.05.281.

[89] H. Wang *et al.*, “Modification of Nafion membrane with biofunctional SiO2 nanofiber for proton exchange membrane fuel cells,” *J. Power Sources*, vol. 340, pp. 201–209, Feb. 2017, doi: 10.1016/j.jpowsour.2016.11.072.

[90] J. Choi, R. Wycisk, W. Zhang, P. N. Pintauro, K. M. Lee, and P. T. Mather, “High Conductivity Perfluorosulfonic Acid Nanofiber Composite Fuel-Cell Membranes,” *ChemSusChem*, vol. 3, no. 11, pp. 1245–1248, Nov. 2010, doi: 10.1002/cssc.201000220.

[91] A. N. Ergün, Z. Ö. Kocabaş, M. Baysal, A. Yürüm, and Y. Yürüm, “SYNTHESIS OF MESOPOROUS MCM-41 MATERIALS WITH LOW-POWER MICROWAVE HEATING,” *Chem. Eng. Commun.*, vol. 200, no. 8, pp. 1057–1070, Aug. 2013, doi: 10.1080/00986445.2012.737386.

[92] L. Sierra and J.-L. Guth, “Synthesis of mesoporous silica with tunable pore size from sodium silicate solutions and a polyethylene oxide surfactant,” *Microporous Mesoporous Mater.*, vol. 27, no. 2–3, pp. 243–253, Feb. 1999, doi: 10.1016/S1387-1811(98)00258-3.

[93] N. Rajabalizadeh Mojarrad, B. Iskandarani, A. Taşdemir, A. Yürüm, S. Alkan Gürsel, and B. Yarar Kaplan, “Nanofiber based hybrid sulfonated silica/P(VDF-TrFE) membranes for PEM fuel cells,” *Int. J. Hydrog. Energy*, vol. 46, no. 25, pp. 13583–13593, Apr. 2021, doi: 10.1016/j.ijhydene.2020.08.005.

[94] S. Sadeghi, L. Işıkel Şanlı, E. Güler, and S. Alkan Gürsel, “Enhancing proton conductivity via sub-micron structures in proton conducting membranes originating from sulfonated PVDF powder by radiation-induced grafting,” *Solid State Ion.*, vol. 314, pp. 66–73, Jan. 2018, doi: 10.1016/j.ssi.2017.11.017.

[95] E. Güler, S. Sadeghi, and S. Alkan Gürsel, “Characterization and fuel cell performance of divinylbenzene crosslinked phosphoric acid doped membranes based on 4-vinylpyridine grafting onto poly(ethylene-co-tetrafluoroethylene) films,” *Int. J. Hydrog. Energy*, vol. 43, no. 16, pp. 8088–8099, Apr. 2018, doi: 10.1016/j.ijhydene.2018.03.087.

[96] A. Sivasankaran, D. Sangeetha, and Y.-H. Ahn, “Nanocomposite membranes based on sulfonated polystyrene ethylene butylene polystyrene (SSEBS) and sulfonated SiO 2 for microbial fuel cell application,” *Chem. Eng. J.*, vol. 289, pp. 442–451, Apr. 2016, doi: 10.1016/j.cej.2015.12.095.

[97] M. Linlin, A. K. Mishra, N. H. Kim, and J. H. Lee, “Poly(2,5-benzimidazole)–silica nanocomposite membranes for high temperature proton exchange membrane fuel cell,” *J. Membr. Sci.*, vol. 411–412, pp. 91–98, Sep. 2012, doi: 10.1016/j.memsci.2012.04.018.

[98] J. B. Ballengee and P. N. Pintauro, “Composite Fuel Cell Membranes from Dual-Nanofiber Electrospun Mats,” *Macromolecules*, vol. 44, no. 18, pp. 7307–7314, Sep. 2011, doi: 10.1021/ma201684j.

[99] B. Dong, L. Gwee, D. Salas-de la Cruz, K. I. Winey, and Y. A. Elabd, “Super Proton Conductive High-Purity Nafion Nanofibers,” *Nano Lett.*, vol. 10, no. 9, pp. 3785–3790, Sep. 2010, doi: 10.1021/nl102581w.

[100] E. Ogungbemi, T. Wilberforce, O. Ijaodola, J. Thompson, and A. G. Olabi, “Review of operating condition, design parameters and material properties for proton exchange membrane fuel cells,” *Int. J. Energy Res.*, vol. 45, no. 2, pp. 1227–1245, Feb. 2021, doi: 10.1002/er.5810.

[101] M. A. Raso, T. J. Leo, O. González-Espasandín, and E. Navarro, “New expressions to determine the water diffusion coefficient in the membrane of PEM fuel cells,” *Int. J. Hydrog. Energy*, vol. 41, no. 43, pp. 19766–19770, Nov. 2016, doi: 10.1016/j.ijhydene.2016.05.075.

[102] A. Öztürk and A. Bayrakçeken Yurtcan, “Investigation of synergetic effect of PDMS polymer hydrophobicity and polystyrene-silica particles roughness in the content of microporous layer on water management in PEM fuel cell,” *Appl. Surf. Sci.*, vol. 511, p. 145415, May 2020, doi: 10.1016/j.apsusc.2020.145415.

[103] M. B. Karimi *et al.*, “A comprehensive review on the proton conductivity of proton exchange membranes (PEMs) under anhydrous conditions: Proton conductivity upper bound,” *Int. J. Hydrog. Energy*, vol. 46, no. 69, pp. 34413–34437, Oct. 2021, doi: 10.1016/j.ijhydene.2021.08.015.

[104] L. Santos, D. Powers, R. Wycisk, and P. Pintauro, “Electrospun Hybrid Perfluorosulfonic Acid/Sulfonated Silica Composite Membranes,” *Membranes*, vol. 10, no. 10, p. 250, Sep. 2020, doi: 10.3390/membranes10100250.

[105] Y. P. Ying, S. K. Kamarudin, and M. S. Masdar, “Silica-related membranes in fuel cell applications: An overview,” *Int. J. Hydrog. Energy*, vol. 43, no. 33, pp. 16068–16084, Aug. 2018, doi: 10.1016/j.ijhydene.2018.06.171.

[106] A. Saccà *et al.*, “Influence of doping level in Yttria-Stabilised-Zirconia (YSZ) based-fillers as degradation inhibitors for proton exchange membranes fuel cells (PEMFCs) in drastic conditions,” *Int. J. Hydrog. Energy*, vol. 44, no. 59, pp. 31445–31457, Nov. 2019, doi: 10.1016/j.ijhydene.2019.10.026.

[107] Y. Yagizatli, B. Ulas, A. Cali, A. Sahin, and I. Ar, “Improved fuel cell properties of Nano-TiO2 doped Poly(Vinylidene fluoride) and phosphonated Poly(Vinyl alcohol) composite blend membranes for PEM fuel cells,” *Int. J. Hydrog. Energy*, vol. 45, no. 60, pp. 35130–35138, Dec. 2020, doi: 10.1016/j.ijhydene.2020.02.197.

[108] V. Ramani, H. R. Kunz, and J. M. Fenton, “Metal dioxide supported heteropolyacid/Nafion® composite membranes for elevated temperature/low relative humidity PEFC operation,” *J. Membr. Sci.*, vol. 279, no. 1–2, pp. 506–512, Aug. 2006, doi: 10.1016/j.memsci.2005.12.044.

[109] L. Li and Y. Wang, “Proton conducting composite membranes from sulfonated polyethersulfone Cardo and phosphotungstic acid for fuel cell application,” *J. Power Sources*, vol. 162, no. 1, pp. 541–546, Nov. 2006, doi: 10.1016/j.jpowsour.2006.06.010.

[110] G. Liu, W.-C. Tsen, and S. Wen, “Sulfonated silica coated polyvinylidene fluoride electrospun nanofiber-based composite membranes for direct methanol fuel cells,” *Mater. Des.*, vol. 193, p. 108806, Aug. 2020, doi: 10.1016/j.matdes.2020.108806.

[111] K. Oh, O. Kwon, B. Son, D. H. Lee, and S. Shanmugam, “Nafion-sulfonated silica composite membrane for proton exchange membrane fuel cells under operating low humidity condition,” *J. Membr. Sci.*, vol. 583, pp. 103–109, Aug. 2019, doi: 10.1016/j.memsci.2019.04.031.

[112] H. Kim, S. Prakash, W. E. Mustain, and P. A. Kohl, “Sol–gel based sulfonic acid-functionalized silica proton conductive membrane,” *J. Power Sources*, vol. 193, no. 2, pp. 562–569, Sep. 2009, doi: 10.1016/j.jpowsour.2009.04.040.

[113] V. Maneeratana *et al.*, “Fractal Inorganic−Organic Interfaces in Hybrid Membranes for Efficient Proton Transport,” *Adv. Funct. Mater.*, vol. 23, no. 22, pp. 2872–2880, Jun. 2013, doi: 10.1002/adfm.201202701.

[114] R. Sood *et al.*, “Active electrospun nanofibers as an effective reinforcement for highly conducting and durable proton exchange membranes,” *J. Membr. Sci.*, vol. 622, p. 119037, Mar. 2021, doi: 10.1016/j.memsci.2020.119037.

[115] R. Sood, S. Cavaliere, D. J. Jones, and J. Rozière, “Electrospun nanofibre composite polymer electrolyte fuel cell and electrolysis membranes,” *Nano Energy*, vol. 26, pp. 729–745, Aug. 2016, doi: 10.1016/j.nanoen.2016.06.027.

[116] K. Vezzù *et al.*, “Electric Response and Conductivity Mechanism of Blended Polyvinylidene Fluoride/Nafion Electrospun Nanofibers,” *J. Am. Chem. Soc.*, vol. 142, no. 2, pp. 801–814, Jan. 2020, doi: 10.1021/jacs.9b09061.

[117] Y. Kim, X. Wu, C. Lee, and J. H. Oh, “Characterization of PI/PVDF-TrFE Composite Nanofiber-Based Triboelectric Nanogenerators Depending on the Type of the Electrospinning System,” *ACS Appl. Mater. Interfaces*, vol. 13, no. 31, pp. 36967–36975, Aug. 2021, doi: 10.1021/acsami.1c04450.

[118] M. Oroujzadeh, S. Mehdipour-Ataei, and M. Esfandeh, “Proton exchange membranes with microphase separated structure from dual electrospun poly(ether ketone) mats: Producing ionic paths in a hydrophobic matrix,” *Chem. Eng. J.*, vol. 269, pp. 212–220, Jun. 2015, doi: 10.1016/j.cej.2015.01.088.

[119] E. Güler, R. Elizen, D. A. Vermaas, M. Saakes, and K. Nijmeijer, “Performance-determining membrane properties in reverse electrodialysis,” *J. Membr. Sci.*, vol. 446, pp. 266–276, Nov. 2013, doi: 10.1016/j.memsci.2013.06.045.

[120] J. Woo Park *et al.*, “Electrospun Nafion/PVDF single-fiber blended membranes for regenerative H2/Br2 fuel cells,” *J. Membr. Sci.*, vol. 541, pp. 85–92, Nov. 2017, doi: 10.1016/j.memsci.2017.06.086.

[121] A. Bharti and R. Natarajan, “Recovery of expensive Pt/C catalysts from the end-of-life membrane electrode assembly of proton exchange membrane fuel cells,” *RSC Adv.*, vol. 10, no. 58, pp. 35057–35061, 2020, doi: 10.1039/D0RA06640K.

[122] L. Ahmadian-Alam, M. Kheirmand, and H. Mahdavi, “Preparation, characterization and properties of PVDF-g-PAMPS/PMMA- co -PAMPS/silica nanoparticle as a new proton exchange nanocomposite membrane,” *Chem. Eng. J.*, vol. 284, pp. 1035–1048, Jan. 2016, doi: 10.1016/j.cej.2015.09.048.

[123] H.-Y. Li and Y.-L. Liu, “Nafion-functionalized electrospun poly(vinylidene fluoride) (PVDF) nanofibers for high performance proton exchange membranes in fuel cells,” *J Mater Chem A*, vol. 2, no. 11, pp. 3783–3793, 2014, doi: 10.1039/C3TA14264G.

[124] T. Hwang, V. Palmre, J. Nam, D.-C. Lee, and K. J. Kim, “A new ionic polymer–metal composite based on Nafion/poly(vinyl alcohol- *co* -ethylene) blends,” *Smart Mater. Struct.*, vol. 24, no. 10, p. 105011, Oct. 2015, doi: 10.1088/0964-1726/24/10/105011.

[125] G. Nawn *et al.*, “Structural analyses of blended Nafion/PVDF electrospun nanofibers,” *Phys. Chem. Chem. Phys.*, vol. 21, no. 20, pp. 10357–10369, 2019, doi: 10.1039/C9CP01891C.

[126] J. Nunes-Pereira *et al.*, “Poly(vinylidene fluoride) and copolymers as porous membranes for tissue engineering applications,” *Polym. Test.*, vol. 44, pp. 234–241, Jul. 2015, doi: 10.1016/j.polymertesting.2015.05.001.

[127] M. Vinothkannan, A. R. Kim, G. Gnana kumar, and D. J. Yoo, “Sulfonated graphene oxide/Nafion composite membranes for high temperature and low humidity proton exchange membrane fuel cells,” *RSC Adv.*, vol. 8, no. 14, pp. 7494–7508, 2018, doi: 10.1039/C7RA12768E.

[128] N. A. Nazir, N. Kim, W. G. Iglesias, A. Jakli, and T. Kyu, “Conductive behavior in relation to domain morphology and phase diagram of Nafion/poly(vinylidene-co-trifluoroethylene) blends,” *Polymer*, vol. 53, no. 1, pp. 196–204, Jan. 2012, doi: 10.1016/j.polymer.2011.11.019.

[129] V. Panwar, K. Cha, J.-O. Park, and S. Park, “High actuation response of PVDF/PVP/PSSA based ionic polymer metal composites actuator,” *Sens. Actuators B Chem.*, vol. 161, no. 1, pp. 460–470, Jan. 2012, doi: 10.1016/j.snb.2011.10.062.

[130] V. Panwar, J.-H. Jeon, G. Anoop, H. J. Lee, I.-K. Oh, and J. Y. Jo, “Low voltage actuator using ionic polymer metal nanocomposites based on a miscible polymer blend,” *J. Mater. Chem. A*, vol. 3, no. 39, pp. 19718–19727, 2015, doi: 10.1039/C5TA05807D.

[131] J. Li *et al.*, “Enhanced Proton Conductivity of Sulfonated Polysulfone Membranes under Low Humidity via the Incorporation of Multifunctional Graphene Oxide,” *ACS Appl. Nano Mater.*, vol. 2, no. 8, pp. 4734–4743, Aug. 2019, doi: 10.1021/acsanm.9b00446.

[132] P. Pei, Z. Wu, Y. Li, X. Jia, D. Chen, and S. Huang, “Improved methods to measure hydrogen crossover current in proton exchange membrane fuel cell,” *Appl. Energy*, vol. 215, pp. 338–347, Apr. 2018, doi: 10.1016/j.apenergy.2018.02.002.

[133] D. M. Yu, S. Yoon, T.-H. Kim, J. Y. Lee, J. Lee, and Y. T. Hong, “Properties of sulfonated poly(arylene ether sulfone)/electrospun nonwoven polyacrylonitrile composite membrane for proton exchange membrane fuel cells,” *J. Membr. Sci.*, vol. 446, pp. 212–219, Nov. 2013, doi: 10.1016/j.memsci.2013.06.028.

[134] D. J. Kim, H. Y. Hwang, and S. Y. Nam, “Characterization of sulfonated poly(arylene ether sulfone) (SPAES)/silica-phosphate sol-gel composite membrane: Effects of the sol-gel composition,” *Macromol. Res.*, vol. 21, no. 11, pp. 1194–1200, Nov. 2013, doi: 10.1007/s13233-013-1162-y.

[135] X. Zhang *et al.*, “Nafion/PTFE Composite Membranes for a High Temperature PEM Fuel Cell Application,” *Ind. Eng. Chem. Res.*, vol. 60, no. 30, pp. 11086–11094, Aug. 2021, doi: 10.1021/acs.iecr.1c01447.

[136] C. Feng, Y. Dong, S. Zhong, D. Chen, G. Zeng, and W. He, “Optimizing the Molecular Weight of Poly(vinylidene Fluoride) for Competitive Perfluorosulfonic Acid Membranes,” *Phys. Status Solidi RRL – Rapid Res. Lett.*, vol. 16, no. 2, p. 2100468, Feb. 2022, doi: 10.1002/pssr.202100468.

[137] Z. Shang, Md. M. Hossain, R. Wycisk, and P. N. Pintauro, “Poly(phenylene sulfonic acid)-expanded polytetrafluoroethylene composite membrane for low relative humidity operation in hydrogen fuel cells,” *J. Power Sources*, vol. 535, p. 231375, Jul. 2022, doi: 10.1016/j.jpowsour.2022.231375.

[138] C. Wang *et al.*, “A clustered sulfonated poly(ether sulfone) based on a new fluorene-based bisphenol monomer,” *J. Mater. Chem.*, vol. 22, no. 48, p. 25093, 2012, doi: 10.1039/c2jm34414a.

[139] K. H. Lee, J. Y. Chu, A. R. Kim, and D. J. Yoo, “Effect of functionalized SiO_2 toward proton conductivity of composite membranes for PEMFC application,” *Int. J. Energy Res.*, vol. 43, no. 10, pp. 5333–5345, Aug. 2019, doi: 10.1002/er.4610.